# TO MOTILITY AND BEYOND! CONSERVED MEMBRANE PROTEINS IN THE DIVISION AND DIFFERENTIATION OF *C. ELEGANS* SPERM

by

Kristin Elise Fenker

A dissertation submitted to the faculty of
The University of Utah
in partial fulfillment of the requirements for the degree of

Doctor of Philosophy

Department of Human Genetics

The University of Utah

May 2018

**The University of Utah Graduate School**

# STATEMENT OF DISSERTATION APPROVAL

The dissertation of **Kristin Elise Fenker**

has been approved by the following supervisory committee members:

| | | |
|---|---|---|
| **Gillian Stanfield** | , Chair | **1-22-18** Date Approved |
| **Markus Babst** | , Member | **1-22-18** Date Approved |
| **Erik Jorgensen** | , Member | **1-22-18** Date Approved |
| **Kristen Kwan** | , Member | **1-22-18** Date Approved |
| **Mark Metzstein** | , Member | **1-22-18** Date Approved |

and by **Lynn Jorde**, Chair/Dean of

the Department/College/School of **Human Genetics**

and by David B. Kieda, Dean of The Graduate School.

# ABSTRACT

A cell's morphology plays an important role in its function. Thus, the size, shape, and structure of cells can be strikingly different across biology. In order to create this variation, cells must divide and differentiate in specific and regulated ways. In this dissertation, I describe work using *C. elegans* sperm to understand the programs controlling development of specialized cells. During development, sperm undergo meiotic division and differentiation to become polarized, motile, and capable of fusing with oocytes. From studying these processes, I identified two genes that are important both for sperm development and in contexts beyond reproductive biology.

The first chapters of this dissertation describe a new function for the conserved t-SNARE *syntaxin 7* (*syx-7*) in cytokinesis, the process that separates cells from one another following nuclear division. Without *syx-7*, sperm complete most steps of division, but the final abscission fails. During cytokinesis in animal cells, an actin ring forms between newly partitioning cells. However, it is not currently understood how vesicle traffic is spatiotemporally coupled to actin during cytokinesis. As *syx-7* sperm progress through division, actin becomes mislocalized, providing one of the first examples of a specific component of vesicle trafficking machinery with an impact on actin localization during cytokinesis. Additionally, a specialized lysosome-like organelle is disrupted in *syx-7* sperm, raising interesting questions about the link between this family of organelles and cell division. If a functional contribution is established, this

would represent a new role for lysosome-like organelles, which, when disrupted, cause several human disorders.

The later chapters of this work focus on the final steps of sperm differentiation: cell polarization and acquisition of motility. Our lab identified a signaling pathway that induces sperm motility in response to an extracellular protease. Here, I describe discovery of *snf-10*, a Solute Carrier 6 (SLC6) family gene, which provides the first link connecting the protease signal to changes in sperm physiology, and ultimately motility. Positive regulation by a protease is a novel finding for a member of the SLC6 family, a group of genes that have numerous roles in human physiology, but have been studied in limited contexts.

TABLE OF CONTENTS

LIST OF FIGURES

# ACKNOWLEDGMENTS

First, I would like to thank my advisor, Gillian Stanfield. It has been a privilege to be part of the Stanfield lab these past years. Gillian could not be a more supportive mentor. Her dedication to her students is clear in her day-to-day attitude running the lab, as well as in the many hours we spent together discussing experiments, practicing talks, and revising manuscripts. She is approachable and incredibly patient, while still holding her trainees to very high standards. I will never take for granted how lucky I was to complete my graduate experience under a mentor who was so dedicated to my training and supportive of my career goals. Working with Gillian, I felt part of a team and my opinion was always considered. I learned countless things from Gillian, and her example of hard work, critical thinking, and passion for science is something that I will carry with me throughout my career.

I would like to thank my committee, Kristen Kwan, Mark Metzstein, Markus Babst, and Erik Jorgensen. Their support and guidance was instrumental to my success as a graduate student, whether it was at official committee meetings, or one-on-one discussions. My committee created a fun and supportive environment, helped me interpret data and address problems more critically, and I always left meetings excited and reenergized about my work. Thank you to Suzie Mansour, who subbed on my prelim committee, and also to the Human Genetics Department faculty, fellow students, and staff for being a great community. The advice I received after RIPs and Journal Clubs

changed the way I present and communicate science in a very positive way. I would also like to thank the University's Developmental Biology Community, including the grant on which I was a trainee. It was very valuable to hear about other trainees' projects and present my own work, and many ideas and experiments that came from these discussions are included in this dissertation. Special thanks to Joe Yost, Kristen Kwan, and Teresa Upton, for running the training grant and facilitating all the opportunities it provided.

I would like to thank the Stanfield lab – past and present – for many types of support over the years. To past members Jody Hansen, Joe Smith, and Angela Snow, thank you for training me in worm methods and your support as I started my graduate school journey. Thank you to present members Daniela Chavez, Bri Fisher, Julie Brand, and Amanda Wong, for making lab an enjoyable place to work each day. Your ideas, feedback, moral support, and friendship were critical to my success. I cannot imagine a stronger team of women. Special thanks to Daniela, who I met the first week of graduate school. Daniela has supported me every day for seven years, and always pushed me to explain myself more clearly and ask deeper questions. Her contributions are evident throughout my work and she truly helped me become a stronger scientist. Also special thanks to Julie Brand, for all her help genotyping, brood-counting, antibody staining, and for bringing her uplifting positive attitude to lab each day.

I would like to thank the role models I had growing up, especially Jane Wells and Nancy Jimenez, whose examples encouraged me to be creative and interested in science. Thank you also to Rebekah Egbert, an incredibly inspirational mentor, science communicator, and good friend.

Finally, I would like to give a huge thank you to my friends and family, for the constant support and encouragement. Particularly Reba and Shildes McCaslin (you know why), friends from back east, and those who have made Salt Lake feel like home. Thank you to my siblings – Erin, Mark, Clarissa, John, Bethany, Rebecca, and Jon – for putting up with me, all the laughs and encouragement, and for the entertaining nieces and nephews. Thank you to my in-laws, Bonnie and Irv Taylor, for your love and support, life advice, and your constant interest in science and what I was up to in lab. Thank you to my parents, Karen and Tom Fenker, for being two of the most selfless people I have ever met, especially when it comes to your children. Thank you for raising me to work hard, take on life's challenges, pursue creativity, and be myself. Lastly, thank you to my husband Josh, for keeping me grounded, being completely unpredictable, always making me laugh, and being an unconditionally supportive partner in life.

# CHAPTER 1

## INTRODUCTION

Cell division is an essential part of life. It is necessary to produce sperm and egg cells that come together to create a zygote, and is further required to produce new cells as the zygote undergoes growth and development. In older animals, cell division remains critical as it promotes maintenance and repair of tissue. Because of the lifelong impact on an organism's development and health, defects in cell division cause a wide range of defects and disorders. These range from cancer and neurological conditions, to birth defects and infertility (Sagona and Stenmark, 2010; Normand and King, 2010; Lacroix and Maddox, 2012; Basit et al., 2016; Harding et al., 2016).

Although cell types vary greatly in terms of size, shape, and organization, when it comes time to divide, they share the need to appropriately organize and separate their contents into daughter cells. At the basic level, a cell comprises DNA, cytoplasm, and the organelles necessary for its specialized function, all enclosed by the plasma membrane. A number of events are carefully orchestrated to ensure proper inheritance of these components, and in turn the production of healthy daughter cells. One example is the replication and segregation of DNA, which is achieved through either mitosis or meiosis. Regulated organelle inheritance is also a key event, and the processes governing this inheritance are specialized according to the type of organelle (Jongsma et al., 2015).

Additional regulation is in place to specify if cell division is symmetric or asymmetric. Asymmetric cytokinesis is important as it contributes to cellular diversity by generating cells of a distinct fate or size, for example during stem cell division (Berika et al., 2014) or oogenesis (Liu, 2012).

Throughout cell division, membrane dynamics are also key for success. For a cell to undergo DNA replication and segregation, the nuclear envelope must break down and later reform (LaJoie and Ullman, 2017). Some organelles such as the Golgi are fragmented during division and reassembled in daughter cells (Thyberg and Moskalewski, 1998). Additionally, the plasma membrane must adjust to accommodate the changes in volume as cells divide, ingress at the division plane, and undergo abscission to form new cells that each have their own continuous membrane (Imoto et al., 2011; Chen et al., 2012; Horgan and McCaffrey, 2012). Organelle and vesicle membranes are also quite dynamic within dividing cells, as trafficking events package and deliver machinery for ingression of the furrow, abscission, and other necessary processes (Straight and Field, 2000; Prekeris and Gould, 2008; McKay and Burgess, 2011).

Our knowledge regarding how cell division is orchestrated is constantly expanding, but there are still many interesting questions to address, which hold implications both for human health as well as our fundamental understanding of biology (Pollard, 2017). Much of my graduate work focuses on cytokinesis, the final process by which new cells separate from one another at the culmination of division. Using the nematode worm *C. elegans*, I studied how membrane trafficking promotes the final separation of sperm following meiotic division. This introduction summarizes the current

understanding of cytokinesis with particular emphasis on the mechanisms that guide the process during sperm meiosis, which is most relevant for understanding my work.

## Cytokinesis – A General Overview

Cytokinesis is the process by which two cells separate from one another, following either mitosis or meiosis. The basic underlying mechanisms of cytokinesis – from the general operating principles to the protein machinery used to achieve them – are conserved from yeast to humans (Eggert et al., 2006). At the start of division, a contractile actomosin ring forms just underneath the cortex of the dividing cell (Schroeder, 1972). Constriction of the ring invaginates the plasma membrane, and a cleavage furrow forms creating a barrier between the two new cells, until they are connected only by a thin cytoplasmic region, called the intracellular bridge (Dionne et al., 2015). Finally, abscission machinery assembles within the intercellular bridge to seal off two new membrane compartments, thus completing separation of daughter cells (Chen et al., 2012; Horgan and McCaffrey, 2012). An intricate and complex network of components directs the events required for cytokinesis, allowing them to occur in a manner that is both spatially and temporally precise. Our understanding of this network is constantly expanding, and in fact, a recent review states that how cytoskeletal changes are controlled in a cohesive manner alongside dynamic membrane compartments is one of the most interesting questions in the field of cell division (Straight and Field, 2000).

## Cytokinesis Requires Membrane Traffic

Cytokinesis requires membrane traffic and targeted vesicle fusion at every stage of the process (McKay and Burgess, 2011). The importance of membrane traffic was first identified in studies using brefeldin A to inhibit anterograde transport via the secretory pathway in embryos from *C. elegans* and *Drosophilia*. In both cases, brefeldin A treatment led to regression of the intracellular bridge (Skop et al., 2001; Farkas et al., 2003). Additionally, when Skop et al. isolated midbodies from Chinese hamster ovary cells and identified the proteins present using tandem liquid chromatography and tandem mass spectrometry, they found 33% of the 160 proteins identified fell into the category of membrane trafficking or secretion (2004). This was for only one stage of cytokinesis, and further work has shown that trafficking is also important for contractile ring formation (Riggs et al., 2007), furrow ingression (Pelissier et al., 2003; Riggs et al., 2003; Ai and Skop, 2009), and abscission (Low et al., 2003).

Several studies have highlighted the importance of SNARE (N-ethylmaleimide-sensitive fusion protein (NSF)-attachment protein receptors) proteins, such as the syntaxins, in vesicle docking and fusion throughout cytokinesis. SNAREs are a key component of vesicle trafficking machinery, as the interaction of v-SNAREs on transport vesicles and t-SNAREs on the target membrane brings the two into close proximity and likely drives fusion (Chen and Scheller, 2001; Pelham, 2001). The first syntaxin discovered to function during cytokinesis was KNOLLE in *Arabidopsis*. KNOLLE is a cytokinesis specific syntaxin required for membrane assembly at the cell midline, the means by which plants accomplish cytokinesis (Lukowitz et al., 1996; Lauber et al., 1997). Shortly after KNOLLE's discovery, Conner and Wessel discovered cytokinesis

was inhibited in the sea urchin *Lytechinus variegatus* when syntaxin was inhibited by either drug treatment or antibody injections (1999), and Jantsch-Plunger and Glotzer demonstrated through RNAi depletion experiments that syntaxins were also required for cytokinesis in *C. elegans* embryos (1999). Many more examples have since been identified in numerous cell types and organisms including yeast, *C. elegans*, *Drosophila*, and mammals (Loncar and Singer, 1995; Low et al., 2003; Nakamura et al., 2005; Song et al., 2009; Neto et al., 2013).

In the above examples of SNAREs involved in cytokinesis, each experiment resulted in defects in different stages of cytokinesis. While by no means the only protein family involved, SNAREs clearly fulfill an important role in vesicle docking and fusion throughout the process. So far, they are known to function both in early stages such as formation, ingression, and maintenance of the furrow (Jantsch-Plunger and Glotzer, 1999; Giansanti et al., 2006), and in later stages such as nuclear envelope reformation and abscission (Jantsch-Plunger and Glotzer, 1999; Neto et al., 2013). How the function of SNAREs varies by organism and cell type is beginning to be understood. However, one aspect that remains unclear is how vesicle fusion is spatiotemporally coupled to the actomyosin ring during cytokinesis (Pollard, 2017).

## Vesicle Traffic During Sperm Meiosis

Cytokinesis is a very robust and highly conserved process, and studies have found there is a large amount of overlap in the molecular machinery used, regardless of whether a cell is undergoing meiotic or mitotic division (reviewed in Eggert et al., 2006; Belloni et al., 2012). This emphasizes that much of what we learn from the study of sperm

cytokinesis can be applied more generally. However, sperm are special too. For example, when sperm undergo meiosis, two divisions must occur in a fairly short amount of time. Additionally, there is no transcription or translation in sperm once meiosis begins (Ward, 1983), so machinery for the two consecutive divisions must be recycled or repurposed. Finally, during sperm meiosis, the first division is often followed by an incomplete cytokinesis (Ward, 1983; Hime et al., 1996; Robinson and Cooley, 1996; Greenbaum et al., 2011), and developing sperm are connected to one another by thin cytoplasmic bridges. Previous work suggests meiotic cytokinesis may have unique requirements for vesicle trafficking, perhaps to meet some of these specific features of division during sperm development. *Drosophila* spermatocytes, for example, have either additional or slightly different requirements for cytokinesis as compared to mitotic cells. Mutations affecting the trafficking-related genes *fwd, gio, fws,* and *Arf6* impair cytokinesis in sperm, but not in neuroblasts or S2 cells (Somma et al., 2002; Farkas et al., 2003; Eggert et al., 2004; Giansanti et al., 2006; Dyer et al., 2007; Giansanti et al., 2007; Belloni et al., 2012). This suggests these genes fulfill a role either not required by mitotic cells, or that mitotic cells can accomplish the same goal using different machinery.

Two SNAREs have been identified that are important for sperm cytokinesis. The first, *Stx2,* is involved in both meiotic and mitotic cytokinesis, although this is through apparently different roles. In somatic cytokinesis, *Stx2* is essential for abscission of the intracellular bridge (Low et al., 2003). The role of *Stx2* in sperm was identified through a mutagenesis screen in mice, as males deficient in *Stx2* exhibit infertility (Akiyama et al., 2008; Fujiwara et al., 2013). Deletion alleles of *Stx2* cause an arrest in sperm development and instead of haploid spermatids, mutant males produce multinucleated

sperm cells. Because sperm from mice deficient in sulfoglycolipids exhibit a similar, multinucleated phenotype (Fujimoto et al., 2000; Zhang et al., 2005), and sulfoglycolipid localization to the intracellular bridge is disrupted in *Stx2* mutants, the authors hypothesized that STX2 is involved in transport of sulfoglycolipids and thus maintenance of intracellular bridges between dividing sperm. The other syntaxin identified to function in sperm is *dSyx5* in *Drosophila*. While a complete loss of *dSyx5* is lethal, a hypomorphic allele results in male sterility due to multinucleated germ cells produced from incomplete cytokinesis (Xu et al., 2002). For *dSyx5*, the authors show transport from the Golgi may be disrupted, although how this directly impacts cytokinesis remains unclear. There is no clear role for *dSyx5* in cytokinesis for mitotic cells, unless a division defect is causing the lethality. However, in somatic cells, *dSyx5* is required for reassembly of the Golgi after division (Rabouille et al., 1998).

Overall, it appears both *Stx2* and *dSyx5* could be making specialized contributions to sperm cytokinesis, even though they have other roles as well. One interesting question about SNAREs is how their function is modulated to act at specific stages or in specific cell types. Many SNARE isoforms have been identified, and one idea is that controlled membrane fusion may come at least in part through cooperation between unique sets of SNAREs and interacting proteins with specific cellular distributions (Rothman and Warren, 1994).

## Cell Division During *C. elegans* Sperm Development

*C. elegans* sperm development is a system well suited for the study of cytokinesis. To produce four haploid spermatids, a primary spermatocyte must undergo two

sequential rounds of meiotic division, each accompanied by a cytokinesis (Ward et al., 1981). As in other organisms, this process is accompanied by cytoskeletal restructuring, redistribution of cytoplasm, and regulated organelle inheritance, all tightly coordinated with each other and with dramatic membrane remodeling (Roberts et al., 1986; L'Hernault, 2006).

Sperm initially form in syncytium along a cytoplasmic core and cellularize when they enter meiosis (L'Hernault, 2006). These 4N primary spermatocytes divide to become 2N secondary spermatocytes. The cytokinesis that accompanies meiosis I can be either complete or incomplete, and sperm often remain connected by a thin cytoplasmic bridge (Ward et al., 1981). Following the nuclear division of meiosis II, haploid spermatids form surrounding a central cytoplasmic core called the residual body, from which they eventually separate (Ward et al., 1981). Separated spermatids contain only the necessary cellular components for basic function, motility, and fertilization, most notably a haploid nucleus, mitochondria, major sperm protein, and lysosome-like membranous organelles. Cellular components the spermatids no longer need are left behind in the residual body, including most voltage-gated ion channels, tubulin, actin, and ribosomes (Nelson et al., 1982; Roberts et al., 1986; Machaca et al., 1996).

*C. elegans* is a male/hermaphrodite species. In both males and hermaphrodites, sperm develop in a similar manner until they transition from spermatids to motile spermatozoa, during a process termed sperm activation. In hermaphrodites, newly produced spermatids are pushed into the sperm storage organ where they activate and are stored until they fertilize oocytes (Ward and Carrel, 1979). In males, sperm are stored as nonactivated spermatids. It is not until they are transferred to a hermaphrodite through

mating that they are exposed to a protease activator and become motile (Smith and Stanfield, 2011). Unlike mammalian sperm, *C. elegans* sperm lack a flagella and instead use a pseudopod to crawl (Ward and Carrel, 1979).

## Thesis Summary

In this dissertation, I present my work using *C. elegans* sperm development to study cell division and differentiation. Chapters 2 and 3 discuss the identification and characterization of *syntaxin 7 (syx-7)*, a gene that promotes cytokinesis in sperm following the nuclear division of meiosis II. This is the first time a role in cell division has been identified for the well-conserved gene, and in Chapter 2, I present details of the cytokinesis defects in the mutant. Loss of *syx-7* affects actin localization during sperm development, suggesting a mechanism for why cytokinesis fails and providing one of the first examples of vesicle fusion functioning upstream of actin localization during cytokinesis. In Chapter 3, I present data demonstrating both the formation and function of lysosome-like membranous organelles are disrupted in *syx-7* mutants, and discuss the idea that lysosome-like organelles could broadly contribute to cell division. For Chapters 3, 4, and 5, I move to a process that occurs after meiotic division in sperm development: the activation of sperm motility. These chapters focus on SNF-10, a sperm membrane protein required for motility to be triggered via a protease signaling pathway. Chapter 3 describes discovery of SNF-10 and its role in initiating sperm motility in response to a protease signal in seminal fluid. Chapter 4 is a detailed discussion of the experiments and discoveries presented in Chapter 3, and Chapter 5 contains further experiments designed to address the mechanism of SNF-10's function.

References

Ai, E., Skop, A.R., 2009. Endosomal recycling regulation during cytokinesis. Commun. Integr. Biol. 2, 444-447.

Akiyama, K., Akimaru, S., Asano, Y., Khalaj, M., Kiyosu, C., Oudi, A., Takahashi, S., Katayama, K., Tsuji, T., Noguchi, J., Kunieda, T., 2008. A new ENU-induced mutant mouse with defective spermatogenesis caused by a nonsense mutation of the syntaxin 2/epimorphin (Stx2/Epim) gene. J. Reprod. Dev. 54, 122-128.

Basit, S., Al-Harbi, K.M., Alhijji, S.A., Albalawi, A.M., Alharby, E., Eldardear, A., Samman, M.I., 2016. CIT, a gene involved in neurogenic cytokinesis, is mutated in human primary microcephaly. Hum. Genet. 135, 1199-1207.

Belloni, G., Sechi, S., Riparbelli, M.G., Fuller, M.T., Callaini, G., Giansanti, M.G., 2012. Mutations in Cog7 affect Golgi structure, meiotic cytokinesis and sperm development during *Drosophila* spermatogenesis. J. Cell Sci. 125, 5441-5452.

Berika, M., Elgayyar, M.E., El-Hashash, A.H., 2014. Asymmetric cell division of stem cells in the lung and other systems. Front. Cell Dev. Biol. 2, 33.

Chen, C.T., Hehnly, H., Doxsey, S.J., 2012. Orchestrating vesicle transport, ESCRTs and kinase surveillance during abscission. Nat. Rev. Mol. Cell Biol. 13, 483-488.

Chen, Y.A., Scheller, R.H., 2001. SNARE-mediated membrane fusion. Nat. Rev. Mol. Cell Biol. 2, 98-106.

Conner, S.D., Wessel, G.M., 1999. Syntaxin is required for cell division. Mol. Biol. Cell 10, 2735-2743.

Dionne, L., Wang, X.-J., Prekeris, R., 2015. Midbody: from cellular junk to regulator of cell polarity and cell fate. Curr. Opin. Cell Biol. 35, 51-58.

Dyer, N., Rebollo, E., Dominguez, P., Elkhatib, N., Chavrier, P., Daviet, L., Gonzalez, C., Gonzalez-Gaitan, M., 2007. Spermatocyte cytokinesis requires rapid membrane addition mediated by ARF6 on central spindle recycling endosomes. Development 134, 4437-4447.

Eggert, U.S., Kiger, A.A., Richter, C., Perlman, Z.E., Perrimon, N., Mitchison, T.J., Field, C.M., 2004. Parallel chemical genetic and genome-wide RNAi screens identify cytokinesis inhibitors and targets. PLoS Biol. 2, e379.

Eggert, U.S., Mitchison, T.J., Field, C.M., 2006. Animal cytokinesis: from parts list to mechanisms. Annu. Rev. Biochem. 75, 543-566.

Farkas, R.M., Giansanti, M.G., Gatti, M., Fuller, M.T., 2003. The *Drosophila* Cog5 homologue is required for cytokinesis, cell elongation, and assembly of specialized Golgi architecture during spermatogenesis. Mol. Biol. Cell 14, 190-200.

Fujimoto, H., Tadano-Aritomi, K., Tokumasu, A., Ito, K., Hikita, T., Suzuki, K., Ishizuka, I., 2000. Requirement of seminolipid in spermatogenesis revealed by UDP-galactose: Ceramide galactosyltransferase-deficient mice. J. Biol. Chem. 275, 22623-22626.

Fujiwara, Y., Ogonuki, N., Inoue, K., Ogura, A., Handel, M., Noguchi, J., Kunieda, T., 2013. t-SNARE syntaxin2 (STX2) is implicated in intracellular transport of sulfoglycolipids during meiotic prophase in mouse spermatogenesis. Biol. Reprod. 88, 141-141.

Giansanti, M., Belloni, G., Gatti, M., 2007. Rab11 is required for membrane trafficking and actomyosin ring constriction in meiotic cytokinesis of *Drosophila* males. Mol. Biol. Cell 18, 5034-5047.

Giansanti, M.G., Bonaccorsi, S., Kurek, R., Farkas, R.M., Dimitri, P., Fuller, M.T., Gatti, M., 2006. The class I PITP giotto is required for *Drosophila* cytokinesis. Curr. Biol. 16, 195-201.

Greenbaum, M.P., Iwamori, T., Buchold, G.M., Matzuk, M.M., 2011. Germ cell intercellular bridges. Cold Spring Harb Perspect. Biol. 3, a005850.

Harding, B.N., Moccia, A., Drunat, S., Soukarieh, O., Tubeuf, H., Chitty, L.S., Verloes, A., Gressens, P., El Ghouzzi, V., Joriot, S., Di Cunto, F., Martins, A., Passemard, S., Bielas, S.L., 2016. Mutations in citron kinase cause recessive microlissencephaly with multinucleated neurons. Am. J. Hum. Genet. 99, 511-520.

Hime, G.R., Brill, J.A., Fuller, M.T., 1996. Assembly of ring canals in the male germ line from structural components of the contractile ring. J. Cell Sci. 109 ( Pt 12), 2779-2788.

Horgan, C.P., McCaffrey, M.W., 2012. Endosomal trafficking in animal cytokinesis. Front. Biosci. (Schol Ed) 4, 547-555.

Imoto, Y., Yoshida, Y., Yagisawa, F., Kuroiwa, H., Kuroiwa, T., 2011. The cell cycle, including the mitotic cycle and organelle division cycles, as revealed by cytological observations. J. Electron Microsc. 60 Suppl 1, 36.

Jantsch-Plunger, V., Glotzer, M., 1999. Depletion of syntaxins in the early *Caenorhabditis elegans* embryo reveals a role for membrane fusion events in cytokinesis. Curr. Biol. 9, 738-745.

Jongsma, M., Berlin, I., Neefjes, J., 2015. On the move: organelle dynamics during mitosis. Trends Cell Biol. 25, 112-124.

L'Hernault, S., 2006. Spermatogenesis. WormBook, ed.

Lacroix, B., Maddox, A.S., 2012. Cytokinesis, ploidy and aneuploidy. J. Pathol. 226, 338-351.

LaJoie, D., Ullman, K.S., 2017. Coordinated events of nuclear assembly. Curr. Opin. Cell Biol. 46, 39-45.

Lauber, M.H., Waizenegger, I., Steinmann, T., Schwarz, H., Mayer, U., Hwang, I., Lukowitz, W., Jurgens, G., 1997. The *Arabidopsis* KNOLLE protein is a cytokinesis-specific syntaxin. J. Cell Biol. 139, 1485-1493.

Liu, X.J., 2012. Polar body emission. Cytoskeleton (Hoboken) 69, 670-685.

Loncar, D., Singer, S.J., 1995. Cell membrane formation during the cellularization of the syncytial blastoderm of *Drosophila*. Proc. Natl. Acad. Sci. 92, 2199-2203.

Low, S., Li, X., Miura, M., Kudo, N., Quiñones, B., Weimbs, T., 2003. Syntaxin 2 and endobrevin are required for the terminal step of cytokinesis in mammalian cells. Dev. Cell 4, 753-759.

Lukowitz, W., Mayer, U., Jurgens, G., 1996. Cytokinesis in the *Arabidopsis* embryo involves the syntaxin-related KNOLLE gene product. Cell 84, 61-71.

Machaca, K., DeFelice, L., L'Hernault, S., 1996. A novel chloride channel localizes to *C. elegans* spermatids and chloride channel blockers induce spermatid differentiation. Dev. Biol. 176, 1-16.

McKay, H.F., Burgess, D.R., 2011. ‘Life is a highway’: membrane trafficking during cytokinesis. Traffic 12, 247-251.

Nakamura, T., Kashiwazaki, J., Shimoda, C., 2005. A fission yeast SNAP-25 homologue, SpSec9, is essential for cytokinesis and sporulation. Cell. Struct. Funct. 30, 15-24.

Nelson, G., Roberts, T., Ward, S., 1982. *C. elegans* spermatozoan locomotion: amoeboid movement with almost no actin. J. Cell Biol. 92, 212-131.

Neto, H., Kaupisch, A., Collins, L.L., Gould, G.W., 2013. Syntaxin 16 is a master recruitment factor for cytokinesis. Mol. Biol. Cell 24, 3663-3674.

Normand, G., King, R.W., 2010. Understanding cytokinesis failure. Adv. Exp. Med. Biol. 676, 27-55.

Pelham, H.R., 2001. SNAREs and the specificity of membrane fusion. Trends Cell Biol. 11, 99-101.

Pelissier, A., Chauvin, J.P., Lecuit, T., 2003. Trafficking through Rab11 endosomes is required for cellularization during *Drosophila* embryogenesis. Curr. Biol. 13, 1848-1857.

Pollard, T.D., 2017. Nine unanswered questions about cytokinesis. J. Cell Biol. 216.

Prekeris, R., Gould, G.W., 2008. Breaking up is hard to do – membrane traffic in cytokinesis. J. Cell Sci. 121, 1569-1576.

Rabouille, C., Kondo, H., Newman, R., Hui, N., Freemont, P., Warren, G., 1998. Syntaxin 5 is a common component of the NSF- and p97-mediated reassembly pathways of Golgi cisternae from mitotic Golgi fragments in vitro. Cell 92, 603-610.

Riggs, B., Fasulo, B., Royou, A., Mische, S., Cao, J., Hays, T.S., Sullivan, W., 2007. The concentration of Nuf, a Rab11 effector, at the microtubule-organizing center is cell cycle regulated, dynein-dependent, and coincides with furrow formation. Mol. Biol. Cell 18, 3313-3322.

Riggs, B., Rothwell, W., Mische, S., Hickson, G.R., Matheson, J., Hays, T.S., Gould, G.W., Sullivan, W., 2003. Actin cytoskeleton remodeling during early *Drosophila* furrow formation requires recycling endosomal components Nuclear-fallout and Rab11. J. Cell Biol. 163, 143-154.

Roberts, T.M., Pavalko, F.M., Ward, S., 1986. Membrane and cytoplasmic proteins are transported in the same organelle complex during nematode spermatogenesis. J. Cell Biol. 102, 1787-1796.

Robinson, D.N., Cooley, L., 1996. Stable intercellular bridges in development: the cytoskeleton lining the tunnel. Trends Cell Biol. 6, 474-479.

Rothman, J.E., Warren, G., 1994. Implications of the SNARE hypothesis for intracellular membrane topology and dynamics. Curr. Biol. 4, 220-233.

Sagona, A.P., Stenmark, H., 2010. Cytokinesis and cancer. FEBS Lett 584, 2652-2661.

Schroeder, T.E., 1972. The contractile ring. II. Determining its brief existence, volumetric changes, and vital role in cleaving *Arbacia* eggs. J. Cell Biol. 53, 419-434.

Skop, A.R., Bergmann, D., Mohler, W.A., White, J.G., 2001. Completion of cytokinesis in *C. elegans* requires a brefeldin A-sensitive membrane accumulation at the cleavage furrow apex. Curr. Biol. 11, 735-746.

Skop, A.R., Liu, H., Yates, J., 3rd, Meyer, B.J., Heald, R., 2004. Dissection of the mammalian midbody proteome reveals conserved cytokinesis mechanisms. Science 305, 61-66.

Smith, J., Stanfield, G., 2011. TRY-5 is a sperm-activating protease in *C. elegans* seminal fluid. PLoS Genetics 7.

Somma, M.P., Fasulo, B., Cenci, G., Cundari, E., Gatti, M., 2002. Molecular dissection of cytokinesis by RNA interference in *Drosophila* cultured cells. Mol. Biol. Cell 13, 2448-2460.

Song, S.J., Kim, S.J., Song, M.S., Lim, D.S., 2009. Aurora B-mediated phosphorylation of RASSF1A maintains proper cytokinesis by recruiting Syntaxin16 to the midzone and midbody. Cancer Res. 69, 8540-8544.

Straight, A.F., Field, C.M., 2000. Microtubules, membranes and cytokinesis. Curr. Biol. 10.

Thyberg, J., Moskalewski, S., 1998. Partitioning of cytoplasmic organelles during mitosis with special reference to the Golgi complex. Microsc. Res. Tech. 40, 354-368.

Ward, S., Argon, Y., Nelson, G., 1981. Sperm morphogenesis in wild-type and fertilization-defective mutants of *C. elegans*. J. Cell Biol.

Ward, S., Carrel, J., 1979. Fertilization and sperm competition in the nematode *C. elegans*. Dev. Biol. 73, 304-321.

Ward, S., Hogan, E., Nelson, G., 1983. The initiation of spermiogenesis in the nematode *C. elegans*. Dev. Biol. 98, 70-79.

Xu, H., Brill, J.A., Hsien, J., McBride, R., Boulianne, G.L., Trimble, W.S., 2002. Syntaxin 5 is required for cytokinesis and spermatid differentiation in *Drosophila*. Dev. Biol. 251, 294-306.

Zhang, Y., Hayashi, Y., Cheng, X., Watanabe, T., Wang, X., Taniguchi, N., Honke, K., 2005. Testis-specific sulfoglycolipid, seminolipid, is essential for germ cell function in spermatogenesis. Glycobiology 15, 649-654.

# CHAPTER 2

# *SYNTAXIN 7* PROMOTES ACTIN LOCALIZATION AND CYTOKINESIS DURING SPERM MEIOSIS

Currently under review as-Fenker, K.E., Nikolova, L.S., and Stanfield, G.M. *syntaxin 7* promotes actin localization and cytokinesis during sperm meiosis.
Molecular Biology of the Cell, submitted Jan. 2017.

## Abstract

Cytokinesis requires an intricate interplay between the cytoskeleton and cellular membranes. However, it remains unclear how vesicle traffic is spatiotemporally coupled to actin assembly and disassembly, and how this is regulated to accomplish the variety of cell division patterns that occur in different cell types. Using *C. elegans* sperm, we identified a novel function for the conserved gene *syntaxin 7* (mammalian *Stx12/13*) in promoting actin localization during the second meiotic division. Without *syx-7*, sperm complete most steps of division, including karyokinesis and partitioning of cellular components. However, as they near abscission, F-actin becomes mislocalized and sperm fail to separate from one another. While there are a variety of examples of the dependence of membrane trafficking on cytoskeletal structures, fewer examples have been identified of the converse situation, in which actin function during cell division is dependent on vesicle trafficking machinery. This work suggests distinctive trafficking machinery might modulate cellular division when specific requirements must be met, such as during meiosis. It also provides one of the first examples of vesicle trafficking functioning upstream of actin localization during cytokinesis.


## Introduction

Successful cell division is contingent on a number of carefully orchestrated events. These include replication and segregation of DNA, remodeling of the cytoskeleton and other cellular structures, and partitioning of organelles and other cytoplasmic components into daughter cells. Key to the success of cell division is a dramatic remodeling of cellular membranes. This is particularly evident during

cytokinesis, the final stage of cell division that culminates in the physical separation of daughter cells (McKay and Burgess, 2011). Here, membrane changes are required for formation of the ingression furrow, contractile ring, and midbody, and for abscission to occur (McKay and Burgess, 2011; Neto et al., 2011). Defects in cytokinesis contribute to a wide range of diseases and developmental disorders, from cancer and neurological conditions to birth defects and infertility (Normand and King, 2010; Sagona and Stenmark, 2010; Lacroix and Maddox, 2012; Basit et al., 2016; Harding et al., 2016).

Cytokinesis in animal cells involves several stages whose coordination is critical for proper division. First, the microtubule cytoskeleton positions the division site (Rappaport, 1986). Then, an actomyosin contractile ring forms underneath the cortex of the dividing cell to support invagination of the plasma membrane and formation of the cleavage furrow (Schroeder, 1972). This forms a barrier between the new cells, which eventually remain connected only by a thin cytoplasmic region, the intracellular bridge. Finally, the cortical actin cytoskeleton is disassembled and abscission machinery within the intracellular bridge seals off the two new membrane compartments, completing separation of daughter cells (Chen et al., 2012; Horgan and McCaffrey, 2012). Thus, during cytokinesis, precise coordination between the cytoskeleton and cellular membranes is needed to ensure successful division. One important aspect of cytokinesis that remains unclear is how vesicle fusion is spatiotemporally coupled to actin during cytokinesis, for both contractile ring formation as well as later actin disassembly, which is required for abscission to occur (Cheffings et al., 2016).

While the processes involved in mitotic and meiotic cytokinesis largely overlap and much of the same molecular machinery is used (Eggert et al., 2006; Belloni et al.,

2012), meiotic division during sperm development has additional unique requirements. For example, in many animals, cells must undergo two consecutive divisions in rapid succession. Additionally, the first meiotic division in sperm is often followed by a partial cytokinesis and developing sperm remain connected to one another through a cytoplasmic bridge (Lindsley, 1980; Ward et al., 1981). Furthermore, sperm undergo little transcription or translation during division (Sassone-Corsi, 2002). This means sperm cells not only must produce any required gene products prior to initiating meiosis, but they also must also have mechanisms in place to ensure the machinery is used at the right time and place. Previous work suggests meiotic division may rely on vesicle trafficking components to achieve these specialized requirements, as trafficking proteins have been identified that are required for meiosis but not for mitosis (reviewed in Giansanti et al., 2014).

The SNARE (Soluble N-ethylmaleimide-sensitive fusion protein attachment protein receptor) family of proteins are core components of vesicle trafficking machinery. SNAREs function in nearly all membrane fusion events that occur within cells (Han et al., 2017). SNAREs on different membrane compartments come together via their coiled-coil SNARE motifs, bringing membranes into close proximity and likely driving fusion (Chen and Scheller, 2001; Pelham, 2001). During cytokinesis, SNAREs function to traffic machinery required for contractile ring formation, furrow ingression, and abscission (reviewed in Neto et al., 2011). Two t-SNAREs have been shown to function in sperm cytokinesis: Syntaxin 2 (*Stx2*) in mice (Fujiwara et al., 2013), and syntaxin 5 (*dSyx5*) in *Drosophila* (Xu et al., 2002). Mutations in these genes cause a similar gross phenotype as they result in the formation of large terminal sperm cells with multiple

nuclei, although it is not completely understood what aspect of vesicle trafficking is affected.

We are studying sperm from the nematode *C. elegans* to understand the process of cytokinesis. As *C. elegans* sperm develop, each primary spermatocyte undergoes two rounds of meiotic division to generate four haploid spermatids (Ward et al., 1981). As in other organisms, this is accompanied by cytoskeletal restructuring, distribution of cytoplasm, and regulated organelle inheritance (Roberts et al., 1986; L'Hernault, 2006). Using this system, we identified a new function for the gene *syntaxin 7*, the *C. elegans* ortholog of mammalian t-SNARE syntaxin 12/13 (*Stx12/13*). *Stx12/13* has been previously demonstrated to function during homotypic fusion of early endosomes (Brandhorst et al., 2006), recycling of surface proteins (Prekeris et al., 1998), and the biogenesis of lysosome-related organelles such as melanosomes and platelet granules (Huang et al., 1999; Jani et al., 2015).

Here, we demonstrate a novel function for the t-SNARE *syx-7* in sperm development. In *syx-7* sperm, meiotic cytokinesis is disrupted. While *syx-7* sperm partition many components correctly into dividing spermatids and attempt division, sperm ultimately fail to separate. Interestingly, actin is mislocalized in *syx-7* sperm, suggesting a mechanism for why they fail to complete division after completing so much of the preparatory process. Overall, our results identify a function for SYX-7 in facilitating meiotic division, and add to the growing evidence that specialized vesicle trafficking machinery is important during meiotic cytokinesis. Furthermore, although there is ample evidence for a cytoskeletal requirement for vesicle trafficking, this work

provides one of the first examples of a vesicle trafficking requirement for actin function during cytokinesis.

## Results

### Generation of *syx-7* alleles

We hypothesized that due to the unique requirements of sperm cell division, specific SNAREs would be involved in the process. Therefore, to test the role of the t-SNARE *syx-7* in fertility, we used CRISPR/Cas9 to generate deletions within the *syx-7* coding region. In addition to its SNARE domain, SYX-7 contains two other domains common to SNARE proteins: an N-terminal regulatory domain ($H_{abc}$) and a C-terminal transmembrane anchor (Figure 2.1A, Figure 2S.1). We designed short guide RNAs (sgRNAs) to remove the majority of the coding region of *syx-7* and disrupt these functional domains (Figure 2.1A,B).

Nine alleles were obtained (Figure 2S.2A), and we chose to focus on *jn37* and *jn42* for our detailed studies. *jn37* is a 1312 base pair (bp) deletion, and *jn42* is a 1309 bp deletion with an insertion of 15 bp likely produced by nonhomologous end joining (Kim and Colaiacovo, 2016). Both mutations are likely null alleles of *syx-7*, as each introduces a frameshift just after the exon 2 cut site that results in an early stop, eliminating a large portion of the N-terminal regulatory domain and all of the SNARE domain (Figure 2.1B, 2S.2A). We also obtained two previously-isolated alleles of *syx-7*, *tm1198* and *tm1764* (National BioResource Project:: *C. elegans*). These alleles are deletions of 436 bp and 406 bp, respectively, that remove portions of the N terminus of *syx-7* but leave the SNARE domain in-frame for translation (Figure 2.1B). Sequence analysis of *syx-7*

cDNAs produced from *jn37, jn42, tm1198,* and *tm1764* animals confirmed that these transcripts had the expected structure (data not shown).

### *syx-7* function is required in developing sperm

All of the *syx-7* mutants generated from our CRISPR experiment appeared normal in terms of general appearance and movement, with the exception that the strains produced fewer offspring as compared to wild-type. Therefore, we tested if loss of *syx-7* caused developmental or fertility defects. We found *syx-7* mutant eggs hatched at rates indistinguishable from those of wild-type hermaphrodites, and an equivalent number of offspring survived to the last larval stage (Figure 2.1C). Thus, *syx-7* is not required for viability, but rather for some aspect of fertility.

We observed that hermaphrodites from all of our CRISPR strains, including *syx-7(jn37)* and *syx-7(jn42),* began laying unfertilized oocytes rather than fertilized eggs after approximately 1.5 days of adulthood, indicating that either sperm or oocyte production was abnormal. To better understand this defect, we performed brood counts by tallying the number of progeny generated by self-fertilizing hermaphrodites. For both *syx-7(jn37)* and *syx-7(jn42)* hermaphrodites, brood sizes were significantly reduced as compared to wild-type (Figure 2.1D). These data show *syx-7* is important for fertility. However, when we tested *tm1198* and *tm1164,* these mutants had wild-type levels of fertility (Figure 2.1D), suggesting the N terminus of *syx-7* might be less important than the SNARE domain for function in this context. We also assayed male fertility by crossing *syx-7(jn37), syx-7(jn42),* or wild-type males to *fog-2(q71)* hermaphrodites. *fog-2* mutant hermaphrodites are essentially female, as they lack sperm and can only produce offspring

by acquiring sperm through mating (Schedl and Kimble, 1988). We found that *syx-7* mutant males sired a severely reduced number of progeny as compared to wild-type males (Figure 2.2A). That both *syx-7* hermaphrodites and males exhibited reduced fertility indicates that sperm defects are at least partially responsible for *syx-7* fertility defects.

We next tested if loss of *syx-7* also affects development or function of oocytes. If sperm were defective but oocytes were normal, fertility should be rescued by providing functional sperm. We crossed *syx-7* and wild-type control hermaphrodites to males containing a GFP transgene, *mIs11*, which allowed us to distinguish between cross (GFP-positive) progeny and self (GFP-negative) progeny. We found that mated wild-type and *syx-7* hermaphrodites produced similar numbers of cross progeny in this assay (Figure 2.2B), indicating *syx-7* mutants produce healthy oocytes and are capable of normal fertility if wild-type sperm are provided. Thus, defective sperm are solely responsible for the reduced fertility of *syx-7* animals.

To test if *syx-7* function is required autonomously in sperm, we generated transgenic animals with *syx-7* under the control of the *peel-1* promoter, which drives expression specifically in male germline cells undergoing spermatogenesis (Seidel et al., 2011). We found *Ppeel-1::syx-7* fully rescued the Syx-7 fertility defect and restored broods to wild-type levels (Figure 2.2C). We also introduced a 3.4 kb fragment encompassing the *syx-7* locus into *syx-7(jn37)* animals, and observed significant rescue of the fertility defect in transgenic hermaphrodites (Figure S2.2B). We conclude that *syx-7* functions specifically in sperm to promote fertility.

**_syx-7_ mutants have defects in spermatogenesis**

To determine the nature of the defects in *syx-7* sperm, we used DIC microscopy to examine *syx-7(jn37)* and *syx-7(jn42)* mutant males. The *C. elegans* male gonad is an elongated structure that contains a distal-to-proximal gradient of progressively more differentiated sperm. A broad zone of prespermatogenic, syncitial germ cells is followed by a small region where spermatocytes first cellularize and then undergo meiosis. Each spermatocyte divides to form four haploid spermatids, which bud from the residual bodies, structures where excess cytoplasm and unneeded cellular components are discarded. After division, spermatids move into a proximally-located seminal vesicle, in which they are stored (Figure 2.2D). When dissected from the animal, round spermatids are observed to contain a centrally placed nucleus surrounded by grainy cytoplasm (Figure 2.2D, Inset). In *syx-7* mutant males, the prespermatogenic and spermatocyte-containing zones of the gonad appeared grossly normal. However, mutant males contained a reduced number of wild-type-looking spermatids. Instead, the majority of the seminal vesicle region was dominated by large cells that were spermatocyte-like in size, but lacked the appearance of either normal spermatocytes or spermatids (Figure 2.2E). These abnormal cells exhibited both grainy and smooth regions within a single cell, and nuclei were difficult to discern (Figure 2.2E, Inset). This phenotype was highly penetrant; these cells were present in all *syx-7(jn37)* and *syx-7(jn42)* mutant animals analyzed for this study.

While our DIC imaging revealed there are severe defects in *syx-7* spermatid formation, we wanted to examine the sperm at higher resolution to better understand how cellular structures are affected. Therefore, we performed electron microscopy to examine

sperm within adult males. In wild-type males, individual spermatids were packed very closely into the sperm storage region (Figure 2.2F). We observed condensed nuclei, mitochondria, and membranous organelles within spermatids, as previously described (Figure 2.2F) (Wolf et al., 1978; Ward et al., 1981). Membranous organelles are sperm-specific organelles related to lysosomes, with a double-layered membrane that stains darkly when observed by EM (Nelson et al., 1980). As in our DIC imaging experiment, electron micrographs of *syx-7* mutants revealed sperm that were much larger than wild-type spermatids (Figure 2.2G). The large cells contained both light, spermatid-like and dark, residual body-like regions of cytoplasm, likely corresponding to the grainy and smooth regions revealed by DIC (Figure 2.2E, 2.2G). In some cases, the compartments were partially enclosed by membranes and were within the size range of wild-type spermatids. The compartments contained mitochondria and a nucleus, as well as small vesicles that were not present in wild-type cells (Figure 2.2G). Membranous organelles were not evident in the large *syx-7* sperm, although the few relatively normal-looking spermatids produced in the mutant did contain abnormal structures that showed similarities to membranous organelles (data not shown). Not all of the large cells contained compartments or distinct organelles (data not shown), suggesting a breakdown of cellular components in *syx-7* terminal cells. Based on these data, we conclude *syx-7* is important for the formation of spermatids.

### *syx-7* promotes spermatid separation during meiosis

To define the defects in spermatogenesis in *syx-7* mutants, we used DIC microscopy to observe sperm of dissected males developing in vitro (Figure 2.3A-N').

For *C. elegans*, spermatocytes dissected from the male gonad can undergo spermatogenesis and even give rise to haploid spermatids in the absence of any supporting tissues (Ward et al., 1981). The cellular pathway for sperm differentiation is shown in Figure 2.3A. Wild-type sperm begin meiosis and replicate their genome when they cellularize. During meiosis I, these primary spermatocytes (4N) (Figure 2.3B,B') divide to become secondary spermatocytes (2N), which in most cases remain connected by a thin cytoplasmic bridge (Figure 2.3C,C'). During meiosis II, each spermatocyte gives rise to four haploid spermatids. For cells that show incomplete separation, four spermatids simultaneously bud from a single residual body ("four-bud spermatocytes"; Figure 2.3D,D'). In other cases, where secondary spermatocytes completely separate from one another during meiosis I, each of the daughters goes on to bud two spermatids from a residual body ("two-bud spermatocytes;" Figure 2.3E,E') (Ward et al., 1981). Although few cells achieve complete separation of spermatids in vitro (Figure 2.3F,F'), they often achieve the fully-budded stage prior to arresting and can maintain this appearance for some time (Ward et al., 1981). We scored a cell as having stable buds if it maintained partitioning for at least 25 minutes, and we often observed them in this state for over 40 minutes. Time durations for each stage as well as the outcome of differentiation for cells observed in vitro are shown in Figure 2.4.

A diagram of *syx-7* sperm differentiation is shown in Figure 2.3G. For *syx-7* sperm, we observed that cells initiated meiosis as primary spermatocytes that were indistinguishable from wild-type (Figure 2.3H,H'). Mutant and wild-type secondary spermatocytes also appeared similar, although *syx-7* cells required more time to reach this developmental stage (9.0 ± 4.2 min for *syx-7* cells, as compared to 2.7 ± 0.7 min for wild-

type; Figure 2.4, Figure 2.3I,I'). Like wild-type, *syx-7* primary spermatocytes were capable of undergoing either incomplete or complete cytokinesis during meiosis I, resulting in four-bud or two-bud spermatocytes at meiosis II (Figure 2.3J-K').

At the budding stage, visible differences between *syx-7* and wild-type sperm were usually evident. While *syx-7* mutant sperm showed a similar pattern of budding spermatids, each with a single, presumably haploid nucleus, they often formed extra membrane blebs from the residual body surface. These blebs were smaller than the budding spermatids and contained no nuclei (Figure 2.3J,J'). Additionally, the budding stage was highly dynamic in *syx-7* sperm. When wild-type cells were observed in vitro, spermatid buds consistently grew until they separated from the residual body, or sometimes were resorbed in a slow and consistent manner (Figure 2.4). Budding-stage *syx-7* sperm showed ongoing shrinking and swelling of both the blebs and spermatid buds.

For *syx-7* cells, spermatids rarely separated from residual bodies. Instead, the majority of developing sperm lost the partitioning they had achieved during budding within 8.6 ± 3.4 min (Figure 2.3L,L'; Figure 2.4) and collapsed back into a single, abnormal cell within 27.4 ± 15.6 min (Figure 2.3M,M'; Figure 2.4). A subset of *syx-7* cells were successful at budding (Figure 2.3N,N'; Figure 2.4), although resulting spermatids were often smaller than those of wild-type (data not shown). Our data indicate *syx-7* functions to promote fertility by contributing to the formation of haploid spermatids. In fact, because *syx-7* budding spermatids are so close to separating before they fail, it appears *syx-7* promotes a very late step of cytokinesis during sperm meiosis.

**SYX-7 becomes restricted to a lysosome-like organelle in budding spermatids**

To examine localization of the SYX-7 protein within the germ line, we used MosSCI (Frokjaer-Jensen et al., 2008; Frokjaer-Jensen et al., 2012) to generate transgenic strains harboring a single-copy, N-terminal *syx-7*-GFP fusion driven by the endogenous *syx-7* promoter. These *Psyx-7::gfp::syx-7* animals had wild-type levels of fertility (data not shown), indicating the fusion protein is functional.

At the primary spermatocyte stage, GFP::SYX-7 was distributed in puncta throughout the sperm cytoplasm (Figure 2.5A,B). At the secondary spermatocyte stage, GFP::SYX-7 remained punctate and distributed throughout the cytoplasm of each dividing cell, but it was notably absent from the division plane between the two spermatocytes (Figure 2.5E,F). As sperm continued to mature, GFP::SYX-7 was partitioned into the budding spermatids, and was excluded from the residual body (Figure 2.5I,J). In budded spermatids, GFP::SYX-7 was restricted to a punctate pattern around the periphery of the sperm, just underneath the plasma membrane (Figure 2.5M,N).

This localization pattern was reminiscent of a sperm-specific lysosome-related organelle called a fibrous body-membranous organelle (FB-MO). FB-MOs form during early spermatogenesis and are partitioned into budding spermatids. After budding, the fibrous bodies and MOs dissociate from one another, and MOs become closely associated with the plasma membrane (Wolf et al., 1978; Roberts et al., 1986). We compared the localization of SYX-7 to that of FB-MOs and MOs. In primary spermatocytes, the majority of both signals were present throughout the cytoplasm, without an obvious pattern of overlap. However, at the cell periphery, we observed a ring of 1CB4 where

GFP::SYX-7 signal was clearly absent (Figure 2.5A-D). In secondary spermatocytes, this pattern persisted, with the additional difference that 1CB4 was present in the GFP::SYX-7-free region along the division plane (Figure 2.5E-H). At budding, both 1CB4 and GFP::SYX-7 were partitioned into spermatids (Figure 2.5I-L), and in haploid spermatids, the two signals were almost entirely coincident with one another (Figure 2.5M-P). From these data, we conclude that SYX-7 localizes throughout spermatocytes, and is excluded from at least a subset of FB-MOs, but it moves to the MOs as sperm divide.

### *syx-7* spermatids undergo cellular partitioning

During spermatid budding, nearly all cellular components undergo a striking process of partitioning into either the spermatids or the residual body. While specific proteins and organelles such as the nuclei, mitochondria, and the MOs are distributed to the spermatids, components that are no longer needed, such as tubulin, actin, and ribosomes, are relegated to the residual body (Figure 2.6A) (Roberts et al., 1986; Ward, 1986). This sorting is required for production of functional spermatozoa (Roberts et al., 1986).

While we had observed that nuclei partition appropriately into budding-stage *syx-7* spermatids (Figure 2.3I-I'), we sought to determine if *syx-7* sperm showed defects in sorting of other cellular components. We dissected budding spermatids from males and visualized various components using a variety of antibodies, live dyes, and fluorescent protein tags. In wild-type cells undergoing partitioning, MOs localized to spermatids and were absent from the residual body (Figure 2.6B,B'). We observed a similar pattern in *syx-7* sperm, although small concentrations of the MO antibody were sometimes visible

along the periphery of the residual body (Figure 2.6C,C'). Major sperm protein, which comprises the sperm cytoskeleton (Ward and Klass, 1982), was present in partitioning spermatids and absent from the residual body for both wild-type and *syx-7* cells (Figure 2.6D-E). We found that both wild-type and *syx-7* mitochondria partitioned into spermatids, although a few were left behind in the residual body of *syx-7* mutants (Figure 2.6F-G'). The localization of tubulin also was very similar in *syx-7* as compared to wild-type sperm; it localized to the residual body and formed concentrations just beneath budding spermatids (Figure 2.6H-I'). In summary, initial partitioning between the spermatids and residual body was largely normal in *syx-7* mutants. This finding is consistent with our observations of dividing cells, which proceeded to an advanced stage of budding prior to collapse.

**SYX-7 is required for actin-mediated separation of haploid sperm**

Because budding *syx-7* sperm appeared poised to divide, it seemed likely that a defect was occurring late in the division process. For example, protein machinery needed to generate forces on the membrane and complete spermatid separation might depend on *syx-7* for proper localization or function. To analyze this, we generated transgenic strains expressing LifeAct::mCherry, which binds F-actin (Riedl et al., 2008), and performed confocal microscopy on dissected sperm.

In the wild-type, LifeAct::mCherry showed a dynamic and reproducible pattern of localization during the two meiotic divisions. At the first cytokinesis, it localized to the division plane, where furrow ingression occurs (Figure 2.7A). At the second cytokinesis, LifeAct::mCherry was restricted to the residual body in both four-bud and two-bud

spermatocytes (n=22), and we often saw concentrations under budding spermatids (Figure 2.7C, Figure 2.7D-D').

In *syx-7* sperm undergoing the first meiotic cytokinesis, LifeAct::mCherry localized to the division plane, with no discernable differences as compared to wild-type (Figure 2.7B-B'). However, at the second cytokinesis, defects became apparent. In four-bud spermatocytes, LifeAct::mCherry was restricted to the residual body cytoplasm in only 12% of *syx-7* cells (n=33), and concentrations were never associated with spermatid buds (Figure 2.7C). Instead, LifeAct::mCherry was often detected in concentrations between spermatids on the periphery of the residual body (Figure 2.7E-E'), in budding spermatids (Figure 2.7F-F'), and in the anucleate blebs that form from the residual body in the mutant (Figure 2.7G-G'). Often, we observed a combination of these abnormal patterns in a single cell.

Notably, the defects observed in *syx-7* four-bud spermatocytes were less severe or absent in two-bud spermatocytes. For these cells, LifeAct::mCherry was restricted appropriately to the residual body in 90% of cases (n=21) (Figure 2.7C,I-I'). Furthermore, we often observed concentrations under budding spermatids, as in wild-type (Figure 2.7C, H-I'). Interestingly, when we quantified the number of nuclei present in terminal *syx-7* sperm, we found 98% of cells contained four nuclei (n=52), and none contained only two nuclei; 100% of wild-type spermatids had one nucleus (n=45) (Figure 2.3F-F', M-M'). Thus, *syx-7* is specifically required in cells partitioning into four spermatids. Functional sperm formed by *syx-7* mutants (Figure 2.3K-K') likely arise from two-bud spermatocytes, where actin localization is largely normal.

Taken together, these data establish a strong link between defects in actin

localization and failure to complete spermatid separation in cells lacking *syx-7*. We conclude that the extended F-actin domain is key to the division defects we observe in *syx-7* sperm, and that failure of *syx-7* sperm to complete cytokinesis is likely due to missing contractile force on the membrane.

**SYX-7 and F-actin occupy discrete cellular domains during division**

To determine if the mechanism of SYX-7 regulation of actin localization could be direct, we obtained confocal images of sperm from strains expressing both *gfp::syx-7* and *LifeAct::mCherry*. We found the two markers exhibited mutually exclusive localization during sperm meiotic divisions. In primary spermatocytes, GFP::SYX-7 localized throughout the sperm cytoplasm, while LifeAct::mCherry localized to the cell cortex (Figure 2.7H-H'). In secondary spermatocytes, LifeAct::mCherry concentrated near the division plane, where GFP::SYX-7 is absent (Figure 2.7I-I'). Finally, at the budding stage, LifeAct::mCherry is restricted to the residual body, while GFP::SYX-7 is partitioned into spermatids (Figure 2.7J-J'''). We conclude GFP::SYX-7 and F-actin rarely, if ever, occupy the same domain during sperm meiotic division.

## Discussion

We have discovered a new role for the conserved t-SNARE SYX-7 in promoting meiotic division in sperm cells. Cells lacking *syx-7* are specifically unable to complete the second cytokinesis of meiosis, even after completing much of the preparation for division. Loss of *syx-7* causes defects in actin localization, suggesting a mechanism for

why cytokinesis fails and providing one of the first examples of vesicle fusion functioning upstream of actin localization during cytokinesis.

*C. elegans* sperm, like other dividing cells, undergo a number of regulated events during cytokinesis that culminate with the physical separation of new cells. One such event is the partitioning of cellular components. While all cells must achieve this, sperm have additional requirements as they must also discard excess organelles, proteins, and cytoplasm during differentiation (Ward, 1986; Cooper, 2011). For example, mammalian sperm shed a cytoplasmic droplet (Cooper, 2011), and *C. elegans* sperm bud and separate from a cytoplasmic residual body (Ward et al., 1981). *syx-7* sperm initiate the path to division, as well-defined spermatid buds form around a residual body and most cellular components partition appropriately. However, while wild-type sperm separate from one another following partitioning, sperm without *syx-7* often do not separate. Instead, they lose their partitioning and become large, multinucleated cells. Thus, *syx-7* apparently is not required either for initiating a cleavage furrow, or for partitioning, but rather promotes a later step of division.

What causes cytokinesis to fail in sperm without *syx-7*? By visualizing F-actin throughout sperm cell development, we observed aberrant actin localization in *syx-7* sperm, specifically at the time of spermatid budding and partitioning. When wild-type sperm partition, actin becomes restricted to the residual body and is not visible in spermatid buds. As sperm approach division, actin is also visible as a concentration just underneath each bud. In the *syx-7* mutant, actin is rarely restricted to the residual body, and it fails to form concentrations underneath spermatid buds. Conceivably either of these defects could impair spermatid separation. Actin disassembly is required for

abscission to occur (Tully et al., 2009); therefore, the extended actin domain may represent a failure of this key event. For instance, the persistent actin could be physically blocking entry of abscission machinery to the required sites, or residual actin cables within sperm buds could ectopically tether them to the residual body and thus prevent separation. Alternatively, a lack of actin-mediated force generation at the division plane could hinder abscission. In our time-lapse imaging, we observed actin move into furrows as sperm began to bud, then quickly regress as sperm began to collapse. One explanation might be that without *syx-7,* actin-driven constriction cannot be maintained at the bud neck to allow abscission to occur.

Our data suggest the relationship between SYX-7 and actin is either indirect or highly transient, as the localization of the two proteins is nearly mutually exclusive throughout development (Figure 2.7J-L’’’). We postulate SYX-7 acts upstream of actin localization through effects on an actin regulatory protein. Intriguingly, our studies of SYX-7’s localization show GFP::SYX-7 moves from a general cytoplasmic distribution to the lysosome-like membranous organelles as sperm complete their second cytokinesis. One possibility is that SYX-7 could function to target vesicles containing an actin regulatory protein to the membranous organelles for sequestration. For example, it might remove a factor that promotes actin assembly, thus allowing abscission to occur. It could also sequester a factor that prevents formation of actin concentration beneath spermatids, removing it at the proper time to promote separation.

Our studies of *syx-7,* combined with the work of others, suggests the second meiotic cytokinesis of sperm development requires special molecular processes as compared to other cell divisions. There are four other known *C. elegans* mutants (*spe-4,*

*spe-5*, *spe-26*, and *spe-39*) that, like *syx-7*, are associated with division defects at meiosis II (L'Hernault and Arduengo, 1992; Varkey et al., 1995; Machaca and L'Hernault, 1997; Arduengo et al., 1998; Zhu and L'Hernault, 2003; Gleason et al., 2012), although these mutants all have defects that make them distinct form *syx-7* and actin is not always disrupted. One potentially significant difference between the first and second meiotic division is that *syx-7* is not necessary for targeting actin to the proper domain at the first division. Furthermore, actin localization appears largely normal in *syx-7* mutant sperm that undergo a complete cytokinesis at the first meiotic division and therefore have two buds at the second division. Because abnormal *syx-7* sperm nearly always have four nuclei, two-bud spermatocytes likely represent some if not all of the population of sperm that complete development and allow for some fertility in the absence of *syx-7*. There is no transcription or translation in dividing sperm, so how division is coordinated to accomplish the specialized requirements of the two stages of meiosis when all the factors involved are already in the cell is intriguing.

The underlying mechanisms of contractile ring function, including assembly, attachment to the plasma membrane, and contraction, remain key unknowns in understanding cytokinesis. Here, we have shown actin localization during division can be dependent on conserved vesicle trafficking machinery, and that a SNARE protein functions upstream of actin localization in a specific cellular context. The human ortholog of *syx-7* is expressed in the testis and many other tissues (Human Protein Atlas), so *syx-7* might function during mammalian sperm development or to promote asymmetric divisions in other cell types. Further analysis of SYX-7's function and its interacting partners should reveal how the contractile ring functions during cell division, as well as

how it can be specialized to meet specific cellular goals, such as those of meiotic division.

## Methods

### Nematode growth and strains

*C. elegans* used in this study were derived from Bristol N2 and were grown at 20°C on nematode growth medium (NGM) seeded with the *E. coli* strain OP50 (Brenner, 1974).

The presence of males was achieved by either heat-shock (Sulston and Hodgkin, 1988) or the presence of the *him-5(e1490)* allele (Hodgkin et al., 1979). Both of these methods increase the frequency of nondisjunction of the X chromosome, but do not impact the aspects of sperm development that were the focus of this study. When *him-5(e1490*) was used to generate males, it also was present in matched controls.

### Generation of *syx-7* alleles by CRISPR

Targeting sequences $(N)_{19}$NGG were designed to direct Cas9 to exon 2 and exon 5 of *syx-7,* using the Zhang Lab CRISPR Design Tool (http://crispr.mit.edu). The desired sequences were inserted into pDD162 (Peft-3::Cas9 + Empty sgRNA) using the Q5 Site-Directed Mutagenesis Kit (NEB), as in Dickinson et al. (2013).

An injection mix containing 50 ng/µL of each *syx-7* sgRNA and 20 ng/µL of the Co-CRISPR reagents pJA42 (*rol-6* sgRNA) and AF-JA-53 (*rol-6(su1006)* repair template) was microinjected into the gonads of young adult hermaphrodites (Arribere et al., 2014). Roller F1s were moved to individual plates 3-4 days after injection, allowed

to lay eggs for 3 days, and then screened by PCR using primers 5'-TGAGACAGCCAGTCAGCTTC-3' and 5'-CATTGGATTAACCCTCTACCTGG-3', which flank the expected deletion region. Nonroller progeny from deletion-positive F1 plates were selected to isolate strains homozygous for CRISPR/Cas9-induced deletions.

**cDNA analysis**

To isolate RNA, a process based on the method described in Ly et al. (2015) was used. Briefly, five worms per sample were rinsed in RNAse-free water, then added to a small volume of lysis buffer (5mM Tris, pH 8, 0.5% Triton X-100, 0.5% Tween-20, 0.25mM EDTA, 1 mg/ml Proteinase K). Samples were incubated at 65°C for 10 min to lyse worms, then 85°C for 1 min to deactivate Proteinase K. The Maxima H Minus First Strand cDNA Synthesis Kit (Thermo Scientific) was used for genomic DNA elimination and first-strand synthesis according to kit instructions, using the *syx-7* specific primer 5'-TTACTTAGCCAGGTAGAGGG-3'. After PCR amplification using primers 5'-ATGGATTTCAATCGAGATGC-3' and 5'-TTACTTAGCCAGGTAGAGGG-3, cDNAs were cloned into pCR4Blunt-TOPO vector (Thermo Fisher) and sequenced.

**Generation of transgenic strains**

For *syx-7* genomic rescue, a 3.4 kb fragment surrounding the *syx-7* locus was amplified using primers 5'-CGAACGTCAGATTAGCGATG-3' and 5'-GAAGCAGTGAGATGTGAGAGCT-3'. A mix containing 50 ng/µl each of the *syx-7* fragment and *Psur-5::gfp* plasmid (Yochem et al., 1998) was injected into *syx-7(jn37);*

*him-5(e1490)* hermaphrodites. Transgenic F1 hermaphrodites were selected based on GFP expression and brood sizes were quantified for F2 hermaphrodites.

Mos-mediated single copy insertion (MosSCI) alleles generated for this study were:

*jnSi207[Psyx-7::syx-7::3'syx-7]*, *jnSi274[Psyx-7::mCherry::H2B::3'syx-7]*, *jnSi259[Psyx-7::gfp::syx-7::3'unc-54]*, *jnSi204[Ppeel-1::syx-7::3'unc-54]*, and *jnSi267[Ppeel-1::Lifeact::mCherry::3'unc-54]*. Strains were made as in Frokjaer-Jensen et al. (2008) and Frokjaer-Jensen et al. (2012). Gateway cloning (Life Technologies) was used to generate expression constructs in either the pCFJ150 or pCFJ212 vector, and constructs were injected into *ttTi5605; unc-119(ed3)* or *cxTi10816; unc-119(ed3)* hermaphrodites. The Gateway Slot 2 entry vector containing *LifeAct::mCherry* was a gift from the Plastino lab. The strain *meIs16[Ppie-1::mCherry::his-58, Cb-unc-119(+)]; ruIs57[GFP::tubulin, Cb-unc-119(+)]* was a gift from M. Schvarzstein.

**Assays for fertility and lethality**

To measure hermaphrodite self fertility, L4 hermaphrodites were placed individually on plates and transferred daily for 4-5 days, until eggs were no longer produced. To measure male fertility, L4 males were placed with *fog-2(q71)* L4 hermaphrodites in 1:1 crosses. After 48 hr, males were removed and hermaphrodites were transferred daily until eggs were no longer produced. All progeny were counted after reaching at least the L4 stage, and broods from hermaphrodites that died before reaching 4 days of age were excluded from analysis. For all assays involving fertility, control

strains were assayed in parallel on media from the same production batch. Each experiment was repeated at least three times, with 17-30 animals per genotype.

To assay oocyte viability, *mIs11[Pmyo-2::gfp, Ppes-10::GFP, gut::gfp]; him-5(e1490)* L4 males were placed with L4 hermaphrodites for 48 hr. Males were removed and hermaphrodites were transferred daily until eggs were no longer produced. Cross (GFP-positive) and self (GFP-negative) progeny were counted as above.

Embryonic and developmental lethality was measured by placing batches of five 24 hr post L4 hermaphrodites on 3-5 plates. After 3 hr, hermaphrodites were removed and eggs were counted. Remaining unhatched (dead) eggs were counted at 24 hr, and live progeny were counted after reaching at least the L4 stage.

**Imaging**

For all experiments where sperm were visualized on slides, 24-48 hr virgin post L4 males were dissected into a small drop of Sperm Medium (5 mM HEPES pH 7.4, 50 mM NaCl, 25 mM KCl, 5 mM $CaCl_2$, 1 mM $MgSO_4$, and 10 mM dextrose) (Nelson et al., 1980). To visualize cell membranes, the vital dye FM1-43 (Thermo Fisher) was sometimes included in dissection media at a concentration of 5 µg/mL. MitoTracker Red CMXRos (Chen et al., 2000) (Thermo Fisher) was used to label males at 1 µg/ml in NGM as described in (Stanfield and Villeneuve, 2006), prior to dissection into Sperm Medium and live imaging. To analyze sperm developing in vitro, time-lapse imaging was performed as in (Ward et al., 1981). Images were collected every 1, 3, or 4 min for at least 39 min.

Immunocytochemistry was performed as in Gleason (Gleason et al., 2012). Sperm were dissected onto Colorfrost Plus slides (Fisher), and subjected to a freeze-crack procedure, followed by a 20 min immersion in 100% methanol at -20°C. Washes were performed in PBS pH 7.2 with 0.1% Tween 20 (PBSTw). Blocking (45 min to 1 hr) and antibody incubations were performed in PBSTw with 2% BSA. Primary antibody incubations were done overnight at 4°C, and secondary antibody incubations were done for 2 hr at room temperature. Primary antibodies used were rabbit anti-GFP at 1:1000 (Abcam #AB290); 1CB4 anti-MO at 1:500 or 1:1000 (Arduengo et al., 1998; Okamoto and Thomson, 1985); mouse anti-MSP mAb4A5(G7) and mAb4D5(N2) each at 1:5000 (Kosinski et al., 2005). Secondary antibodies were Alexa Fluor 568 and 488 goat anti-rabbit IgG, and Alexa Fluor 568 and 488 goat anti-mouse IgG (Life Technologies). Secondary antibodies were used at 1:1000.

**Electron microscopy**

EM methods were modified from Ernstrom (Ernstrom et al., 2012). Worms were frozen using high pressure freezing (BAL-TEC HPM 010), with viscous *E. coli* paste as a cryoprotectant. After freezing, specimens were transferred into a cryovial containing fixative (1% OsO4, 1% glutaraldehyde, and 1% water in acetone). Freeze substitution was carried out in a Leica EM AFS with the following program: -90˚C for 48 hr, +5/hr to -25˚C, -25 degrees for 14 hr, +10/hr to room temperature. When the program ended, specimens were rinsed six times with acetone and infiltrated with Epon-Araldite resin in a stepwise fashion (50% resin:acetone for 5 hr, followed by 70% resin:acetone for 8 hr, 90% resin:acetone for 8 hr, and finally 3 changes of 100% resin for 8 hr). Polymerization

was performed at 60˚C for 48 hr. 70 nm sections were stained with saturated uranyl acetate in water for 20 min, and imaging was performed using a JOEL JEM-1400 microscope.

## Acknowledgments

We thank D. Chavez, M. Babst, E. Jorgensen, K. Kwan, and M. Metzstein, as well as faculty and fellow trainees on the Developmental Biology Training Grant for helpful discussions; E. Hujber and T. Vu for electron microscopy advice; D. Greenstein, S. L'Hernault, M. Schvarzstein, and J. Plastino for reagents; and the University of Utah Cell Imaging and Electron Microscopy Core Facilities. This work was supported by NIH R01GM118860 to GMS, and 5T32HD007491 to KEF.

## References

Arduengo P, Appleberry O, Chuang P, L'Hernault S (1998). The presenilin protein family member SPE-4 localizes to an ER/Golgi derived organelle and is required for proper cytoplasmic partitioning during *C. elegans* spermatogenesis. J Cell Sci 111, 3645-3654.

Arribere JA, Bell RT, Fu BX, Artiles KL, Hartman PS, Fire AZ (2014). Efficient marker-free recovery of custom genetic modifications with CRISPR/Cas9 in *Caenorhabditis elegans*. Genetics 198, 837-846.

Basit S, Al-Harbi KM, Alhijji SA, Albalawi AM, Alharby E, Eldardear A, Samman MI (2016). CIT, a gene involved in neurogenic cytokinesis, is mutated in human primary microcephaly. Hum Genet 135, 1199-1207.

Belloni GS, Sechi S, Riparbelli MG, Fuller MT, Callaini G, Giansanti MG (2012). Mutations in Cog7 affect Golgi structure, meiotic cytokinesis and sperm development during *Drosophila* spermatogenesis. J Cell Sci 125, 5441-5452.

Brandhorst D, Zwilling D, Rizzoli SO, Lippert U, Lang T, Jahn R (2006). Homotypic fusion of early endosomes: SNAREs do not determine fusion specificity. Proc Natl Acad Sci 103, 2701-2706.

Brenner S. (1974). The genetics of *Caenorhabditis elegans*. Genetics 77, 71-94.

Cheffings TH, Burroughs NJ, Balasubramanian MK (2016). Actomyosin ring formation and tension generation in eukaryotic cytokinesis. Curr Biol 26, 719-737.

Chen CT, Hehnly H, Doxsey SJ (2012). Orchestrating vesicle transport, ESCRTs and kinase surveillance during abscission. Nat Rev Mol Cell Biol 13, 483-488.

Chen, F, Hersh BM, Conradt B, Zhou Z, Riemer D, Gruenbaum Y, Horvitz HR (2000). Translocation of *C. elegans* CED-4 to nuclear membranes during programmed cell death. Science 287, 1485-1489.

Chen YA, Scheller RH (2001). SNARE-mediated membrane fusion. Nat Rev Mol Cell Biol 2, 98-106.

Cooper TG (2011). The epididymis, cytoplasmic droplets and male fertility. Asian J Androl 13, 130-138.

Dickinson, DJ, Ward JD, Reiner DJ, Goldstein B. (2013). Engineering the *Caenorhabditis elegans* genome using Cas9-triggered homologous recombination. Nat Methods 10, 1028-1034.

Eggert US, Mitchison TJ, Field CM (2006). Animal cytokinesis: from parts list to mechanisms. Annu Rev Biochem 75, 543-566.

Ernstrom GG, Weimer R, Pawar DL, Watanabe S, Hobson RJ, Greenstein D, Jorgensen EM (2012). V-ATPase V1 sector is required for corpse clearance and neurotransmission in *Caenorhabditis elegans.* Genetics 191, 461-475.

Frokjaer-Jensen C, Davis MW, Ailion M, Jorgensen EM (2012). Improved Mos1-mediated transgenesis in *C. elegans*. Nat Methods 9, 117-118.

Frokjaer-Jensen C, Davis MW, Hopkins CE, Newman BJ, Thummel JM, Olesen SP, Grunnet M, Jorgensen RM (2008). Single-copy insertion of transgenes in *Caenorhabditis elegans*. Nat Genet 40, 1375-1383.

Fujiwara Y, Ogonuki N, Inoue K, Ogura A, Handel M, Noguchi J, Kunieda T (2013). t-SNARE syntaxin2 (STX2) is implicated in intracellular transport of sulfoglycolipids during meiotic prophase in mouse spermatogenesis. Biol Reprod 88, 141-141.

Giansanti M, Sechi S, Frappaolo A, Belloni G, Piergentili R (2014). Cytokinesis in *Drosophila* male meiosis. Spermatogenesis 2, 185-196.

Gleason E, Hartley P, Henderson M, Hill-Harfe K, Price P, Weimer R, Kroft T, Zhu GD, Cordovado S, L'Hernault S (2012). Developmental genetics of secretory

vesicle acidification during *C. elegans* spermatogenesis. Genetics 191, 477-491.

Goujon M, McWilliam H, Li W, Valentin F, Squizzato S, Paern J, Lopez R (2010). A new bioinformatics analysis tools framework at EMBL-EBI. Nucleic Acids Res 38, 695-699.

Han J, Pluhackova K, Bockmann RA (2017). The multifaceted role of SNARE proteins in membrane fusion. Front Physiol 8, 5.

Harding BN, Moccia A, Drunat S, Soukarieh O, Tubeuf H, Chitty LS, Verloes A, Gressens P, El Ghouzzi V, Joriot S, Di Cunto F, Martins A, Passemard S, Bielas SL. (2016). Mutations in cCitron kinase cause recessive microlissencephaly with multinucleated neurons. Am J Hum Genet 99, 511-520.

Hodgkin, J, Horvitz, HR, Brenner, S. (1979). Nondisjunction mutants of the nematode *C. elegans*. Genetics 91, 67-94.

Horgan CP, McCaffrey MW (2012). Endosomal trafficking in animal cytokinesis. Front Biosci 4, 547-555.

Huang L, Kuo YM, Gitschier J (1999). The pallid gene encodes a novel, syntaxin 13-interacting protein involved in platelet storage pool deficiency. Nat Genet 23, 329-332.

Jani, R, Purushothaman L, Rani S, Bergam P, Setty S. (2015). STX13 regulates cargo delivery from recycling endosomes during melanosome biogenesis. J Cell Sci 128, 3263-3276.

Kim HM, Colaiacovo MP (2016). CRISPR-Cas9-guided genome engineering in *C. elegans*. Curr Protoc Mol Biol 115, 31-37.

Kosinski M, McDonald K, Schwartz J, Yamamoto I, Greenstein D (2005). *C. elegans* sperm bud vesicles to deliver a meiotic maturation signal to distant oocytes. Development 132, 3357-3369.

L'Hernault, SW (2006). Spermatogenesis, The *C. elegans* Research Community, WormBook doi/10.1895/wormbook.1.85.1, http://www.wormbook.org

L'Hernault, SW, Arduengo PM (1992). Mutation of a putative sperm membrane protein in *Caenorhabditis elegans* prevents sperm differentiation but not its associated meiotic divisions. J Cell Biol 119, 55-68.

Lacroix B, Maddox AS (2012). Cytokinesis, ploidy and aneuploidy. J Pathol 226, 338-351.

Lindsley D, Tokuyasu KT (1980). Spermatogenesis. In: Genetics and Biology of *Drosophila*, ed. M. Ashburner, T.R. Wright, New York: Academic Press, 225-294.

Ly, K, Reid SJ, Snell RG (2015). Rapid RNA analysis of individual *Caenorhabditis elegans*. MethodsX 2, 59-63.

Machaca K, L'Hernault S (1997). The *Caenorhabditis elegans spe-5* gene is required for morphogenesis of a sperm-specific organelle and is associated with an inherent cold-sensitive phenotype. Genetics 146, 567-581.

Marchler-Bauer, A, Bo Y, Han L, He J, Lanczycki CJ, Lu S, Chitsaz F, Derbyshire MK, Geer RC, Gonzales NR, Gwadz M, Hurwitz DI, Lu F, Marchler GH, Song JS, Thanki N, Wang Z, Yamashita RA, Zhang D, Zheng C, Geer LY, Bryant SH (2017). CDD/SPARCLE: functional classification of proteins via subfamily domain architectures. Nucleic Acids Res 45, D200-D203.

Marchler-Bauer, A, Derbyshire MK, Gonzales NR, Lu S, Chitsaz F, Geer LY, Geer RV, He J, Gwadz M, Hurwitz DI, Lanczycki CJ, Lu F, Marchler GH, Song JS, Thanki N, Wang Z, Yamashita RA, Zhang D, Zheng C, Bryant SH (2015). CDD: NCBI's conserved domain database. Nucleic Acids Res 43, D222-226.

Marchler-Bauer A, Lu S, Anderson JB, Chitsaz F, Derbyshire MK, DeWeese-Scott C, Fong JH, Geer LY, Geer RC, Gonzales NR, Gwadz M, Hurwitz DI, Jackson JD, Ke Z, Lanczycki CJ, Lu F, Marchler GH, Mullokandov M, Omelchenko MV, Robertson CL, Song JS, Thanki N, Yamashita RA, Zhang D, Zhang N, Zheng C, Bryant SH (2011). CDD: a conserved domain database for the functional annotation of proteins. Nucleic Acids Res 39, D225-229.

McKay HF, Burgess DR. (2011). ‘Life is a highway’: membrane trafficking during cytokinesis. Traffic 12, 247-251.

Nelson G, Roberts T, Ward S (1980). Vesicle fusion, pseudopod extension and amoeboid motility are induced in nematode spermatids by the ionophore monensin. Cell 19, 457-464.

Neto H, Collins LL Gould GW (2011). Vesicle trafficking and membrane remodelling in cytokinesis. Biochem J 437, 13-24.

Normand, G, King RW (2010). Understanding cytokinesis failure. Adv Exp Med Biol 676, 27-55.

Pelham, HR (2001). SNAREs and the specificity of membrane fusion. Trends Cell Biol 11, 99-101.

Prekeris, R, Klumperman J, Chen YA, Scheller RH (1998). Syntaxin 13 mediates cycling of plasma membrane proteins via tubulovesicular recycling endosomes. J Cell

Biol. 143, 957-971.

Rappaport, R (1986). Establishment of the mechanism of cytokinesis in animal cells. Int Rev Cytol 105, 245-281.

Riedl, J, Crevenna AH, Kessenbrock K, Yu JH, Neukirchen D, Bista M, Bradke F, Jenne D, Holak TA, Werb Z, Sixt M, Wedlich-Soldner R (2008). Lifeact: a versatile marker to visualize F-actin. Nat Methods 5, 605-607.

Roberts, TM, Pavalko FM, Ward S (1986). Membrane and cytoplasmic proteins are transported in the same organelle complex during nematode spermatogenesis. J Cell Biol 102, 1787-1796.

Roelens, B, Schvarzstein M, Villeneuve AM (2015). Manipulation of karyotype in *Caenorhabditis elegans* reveals multiple inputs driving pairwise chromosome synapsis during meiosis. Genetics 201, 1363-1379.

Sagona AP, Stenmark H (2010). Cytokinesis and cancer. FEBS Lett 584, 2652-2661.

Sassone-Corsi, P (2002). Unique chromatin remodeling and transcriptional regulation in spermatogenesis. Science 296, 2176-2178.

Schedl, T, Kimble J (1988). *fog-2*, a germ-line-specific sex determination gene required for hermaphrodite spermatogenesis in *Caenorhabditis elegans*. Genetics 119, 43-61.

Schroeder, TE (1972). The contractile ring. II. Determining its brief existence, volumetric changes, and vital role in cleaving *Arbacia* eggs. J Cell Biol 53, 419-434.

Seidel, HS, Ailion M, Li J, van Oudenaarden A, Rockman MV, Kruglyak L. (2011). A novel sperm-delivered toxin causes late-stage embryo lethality and transmission ratio distortion in *C. elegans*. PLoS Biol. 9, e1001115.

SieversF, Wilm A, Dineen D, Gibson TJ, Karplus K, Li W, Lopez R, McWilliam H, Remmert M, Soding J, Thompson JD, Higgins DG (2011). Fast, scalable generation of high-quality protein multiple sequence alignments using Clustal Omega. Mol Syst Biol 7, 539.

Stanfield G, Villeneuve A (2006). Regulation of sperm activation by SWM-1 is required for reproductive success of *C. elegans* males. Curr Biol 16, 252-263.

Sulston, J. and Hodgkin, J. (1988). Methods. In: The Nematode *C. elegans*, ed. W.B. Wood, New York: Cold Spring Harbor Press, 587-606.

Tully, GH, Nishihama R, Pringle JR, Morgan DO (2009). The anaphase-

promoting complex promotes actomyosin-ring disassembly during cytokinesis in yeast. Mol Biol Cell 20, 1201-1212.

Varkey, JP, Muhlrad PJ, Minniti AN, Do B, Ward S (1995). The *Caenorhabditis elegans spe-26* gene is necessary to form spermatids and encodes a protein similar to the actin-associated proteins kelch and scruin. Genes Dev 9, 1074-1086.

Ward S (1986). The asymmetric localization of gene products during the development of *Caenorhabditis elegans* spermatozoa. In: Gametogenesis and the Early Embryo, ed. J. Gall, New York: A.R. Liss, 55–75.

Ward S, Argon Y, Nelson G (1981). Sperm morphogenesis in wild-type and fertilization-defective mutants of *C. elegans*. J Cell Biol.

Ward S, Klass M (1982). The location of the major protein in *Caenorhabditis elegans* sperm and spermatocytes. Dev Biol 92, 203-208.

Wolf N, Hirsh D, McIntosh J (1978). Spermatogenesis in males of the free-living nematode, *C. elegans*. J Ultrastruct Res 63, 155-169.

Xu H, Brill JA, Hsien J, McBride R, Boulianne GL, Trimble WS (2002). Syntaxin 5 is required for cytokinesis and spermatid differentiation in *Drosophila*. Dev Biol 251, 294-306.

Yochem J, Gu T, Han M (1998). A new marker for mosaic analysis in *Caenorhabditis elegans* indicates a fusion between *hyp6* and *hyp7*, two major components of the hypodermis. Genetics 149, 1323-1334.

Zhu G, L'Hernault S (2003). The *C. elegans spe-39* gene is required for intracellular membrane reorganization during spermatogenesis. Genetics 165, 145-157.

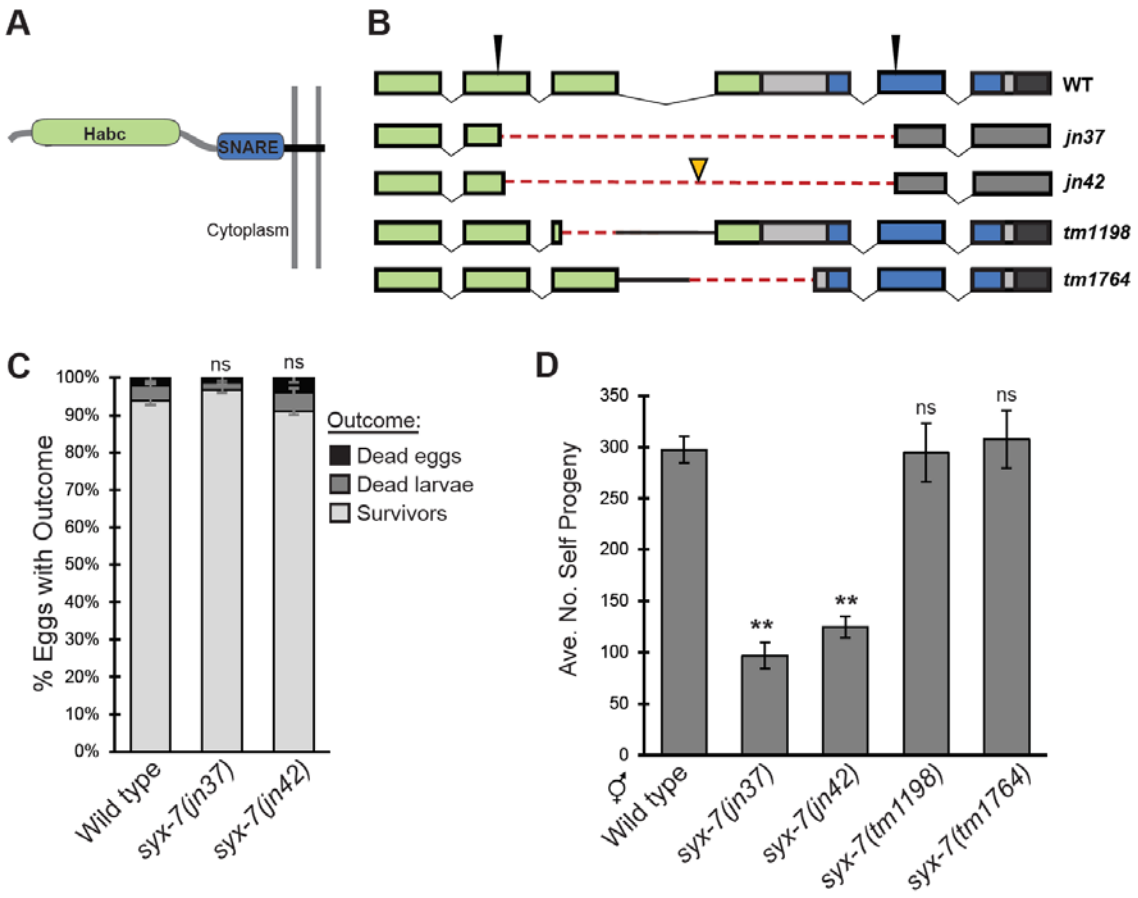


**Figure 2.1. Loss of *syx-7* causes reduced fertility.**
(A) Diagram of SYX-7. Transmembrane domain (black), coiled-coil SNARE domain (blue), and alpha-helical Habc domain (green). (B) Gene model for wild-type *syx-7* and alleles analyzed for this study. Exons (boxes), deleted sequence (dashed red lines), inserted sequence (yellow triangles), Cas9 cut sites (black arrowheads). (C) *syx-7* mutants showed no increase in embryonic or developmental lethality as compared to the wild-type ($p>0.05$, Student's t test). Error bars are standard error of the mean (SEM); n=258-294 eggs. (D) Brood sizes of *syx-7(jn37) and syx-7(jn42)* hermaphrodites were reduced as compared to those of wild-type. Broods of *syx-7(tm1198)* and *syx-7(tm1764)* hermaphrodites were not reduced (**$p<0.001$, Student's t test). Error bars, 95% confidence interval (CI); n=20-22.

**Figure 2.2. *syx-7* functions in sperm to promote spermatogenesis.**
(A) *syx-7* males produce fewer cross progeny as compared to wild-type. Each point represents cross progeny from mating a single male to a spermless *fog-2(q71)* hermaphrodite (**p<0.001, Kolmogorov-Smirnov test). Bars represent medians; n=28-29. (B) *syx-7* hermaphrodites have normal fertility when provided healthy sperm through mating with a wild-type male. Each point represents the total cross-progeny brood from a single hermaphrodite of the indicated genotype (p>0.05, Kolmogorov-Smirnov test). Bars represent medians. (C) Expression of *syx-7* using the sperm-specific *peel-1* promoter restored normal fertility in *syx-7* mutants (p>0.05, Student's t test). Error bars are 95% CI; n=18-20. All comparisons are to wild-type. (D-E) Images of seminal vesicles and dissected sperm (insets) from 48 hr post L4 males. Genotypes shown: (D) wild-type (E) *syx-7(jn37)*. Scale bars: main images, 10 µM; insets, 5 µM. (F-G) Electron micrographs of cells in the seminal vesicles of 24 hr post L4 males. (F) Wild-type spermatids show a stereotypical arrangement with a central nucleus surrounded by mitochondria and with MOs juxtaposed to the plasma membrane; their cytoplasm generally lacks additional structures. (G) The *syx-7* cell contains partially enclosed membrane compartments and membrane-bound vesicles that are not present in wild-type. MOs are not evident in *syx-7* terminal sperm. Scale bar: 1 µM. Nucleus (N), mitochondria (mito), membranous organelles (MO).

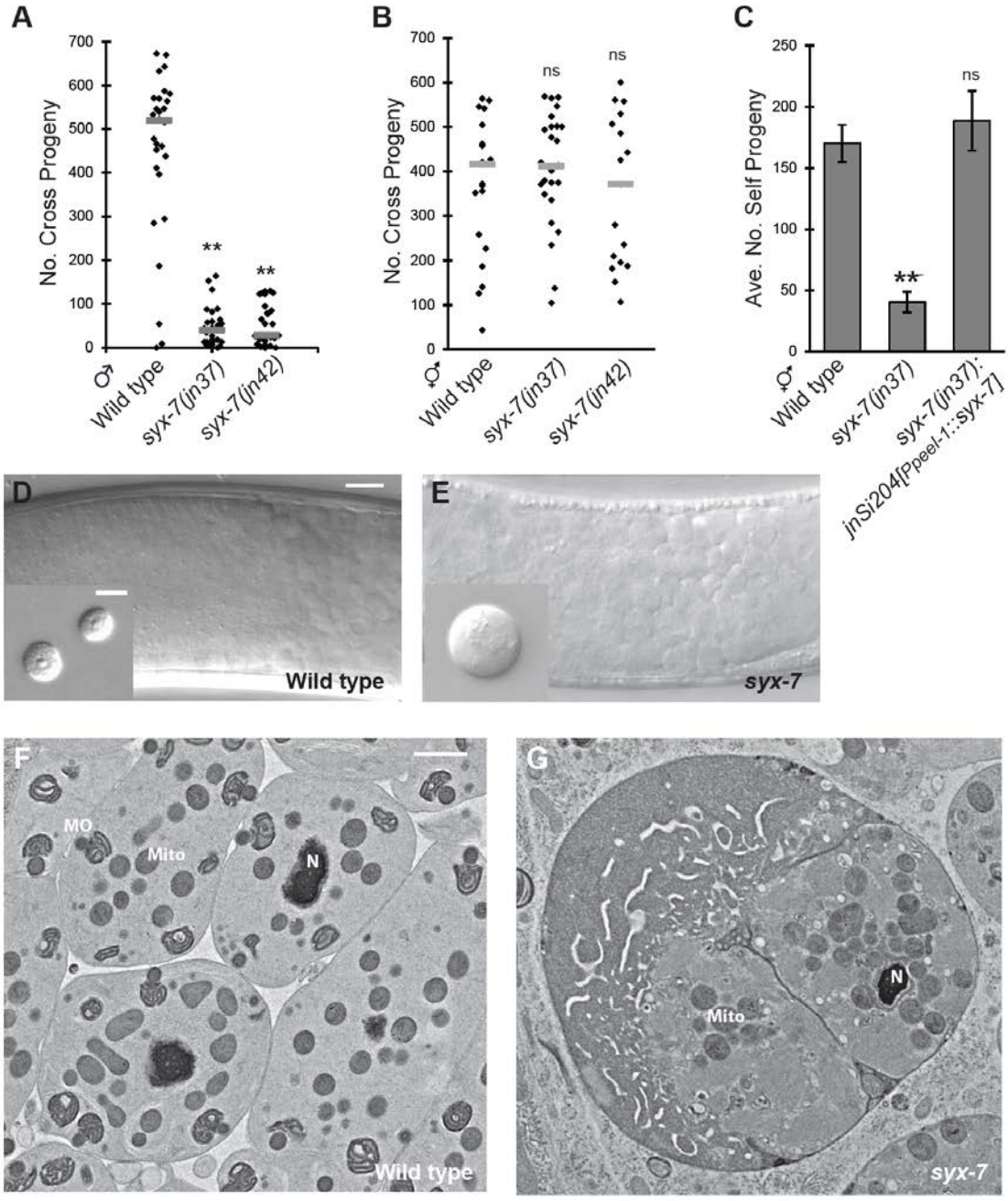
A
No. Cross Progeny
700
600
500
400
300
200
100
0
**
**
♂
Wild type
syx-7(jn37)
syx-7(jn42)
B
No. Cross Progeny
ns
ns
♀
Wild type
syx-7(jn37)
syx-7(jn42)
C
Ave. No. Self Progeny
250
200
150
100
50
0
**
ns
♀
Wild type
syx-7(jn37)
syx-7(jn37);
jnSi204[Ppeel-1::syx-7]
D
Wild type
E
syx-7
F
MO
Mito
N
Wild type
G
N
Mito
syx-7

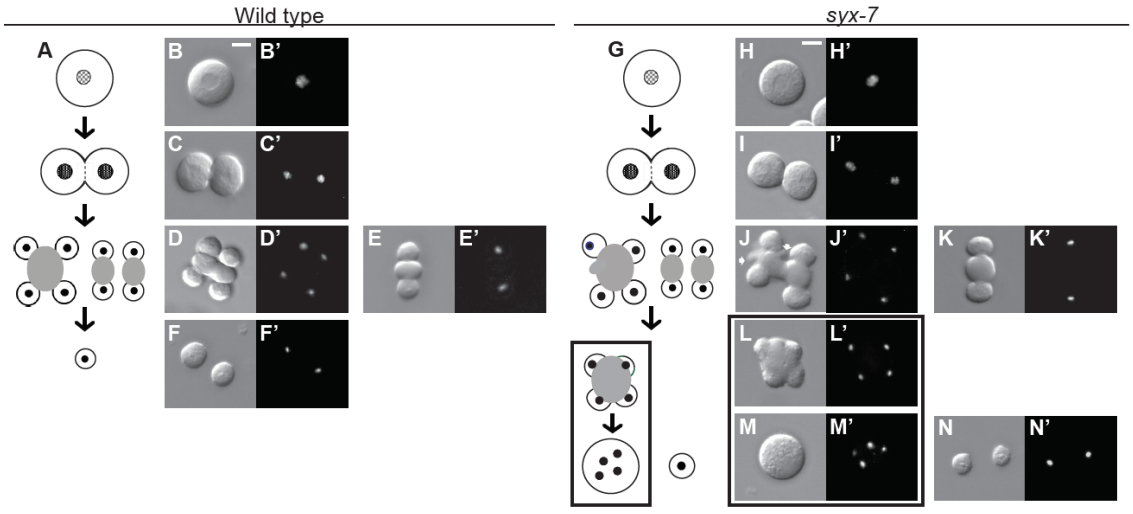


**Figure 2.3. *syx-7* promotes cytokinesis during meiosis II.**
Stages of spermatogenesis observed for wild-type (A-F) and *syx-7* (G-N) males. Paired DIC and fluorescence images of sperm dissected from males expressing *HTAS-1::mCherry*, which marks chromatin and allows visualization of nuclei (D. Chu and GMS, unpublished). (B-B') Wild-type primary spermatocyte. (C-C') Primary spermatocyte undergoing the first meiotic division. (D-D') Secondary four-bud spermatocyte undergoing the second meiotic division. (E-E') Secondary two-bud spermatocyte undergoing the second meiotic division. (F-F') Haploid spermatids. (G-N) Stages of spermatogenesis observed for *syx-7* sperm. In the *syx-7(jn37)* mutant, primary spermatocytes (H-H') and division into secondary spermatocytes (I-I') appeared grossly normal. (J-J') Secondary four-bud spermatocyte undergoing the second meiotic division. Extra blebs (arrows) are visible along the periphery of the residual body. (K-K') Secondary two-bud spermatocyte undergoing the second meiotic division with no noted abnormalities. (L-M) Sperm morphologies observed in *syx-7* but not present in wild-type. (L-L') A four-bud spermatocyte in the process of resorption into the residual body. (M-M') Terminal sperm cell containing 4 nuclei. (N-N') Separated spermatids. Box indicates stages of *syx-7* sperm not seen in wild-type. Scale bars: 5 µM.

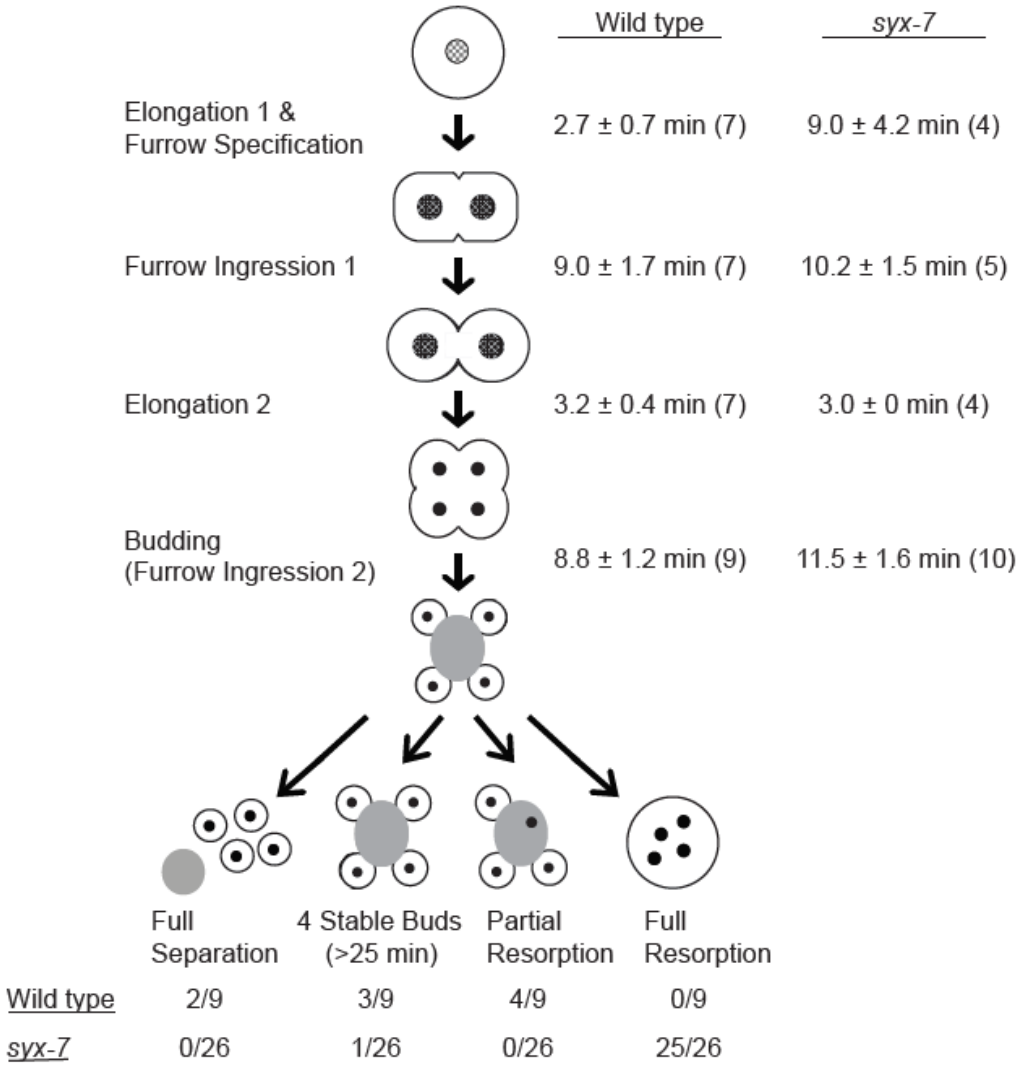


**Figure 2.4. *syx-7* sperm have defects in timing and separation of spermatids during meiosis II.**

Summary of in vitro observations of spermatogenesis for wild-type and *syx-7(jn37)* sperm. Time-lapse images of dissected cells were collected and time series were analyzed for morphological landmarks indicating progression through meiosis. Elongation 1 and Furrow Specification refers to the transition from a round primary spermatocyte to an elongated cell with a visible furrow. Furrow Ingression 1 was considered complete when the cleavage furrow between secondary spermatocytes reached its maximal extent. Elongation 2 was considered complete when secondary spermatocytes were maximally elongated in the directions of both cleavage planes. Cells were considered to be at the budding stage when discrete furrows appeared at budding sites. Timing shown is the average amount of time spent at each stage ± SEM. The number of cells analyzed for each stage is shown in parentheses. Ratios represent the number of cells with the observed outcome over the total number of cells analyzed.

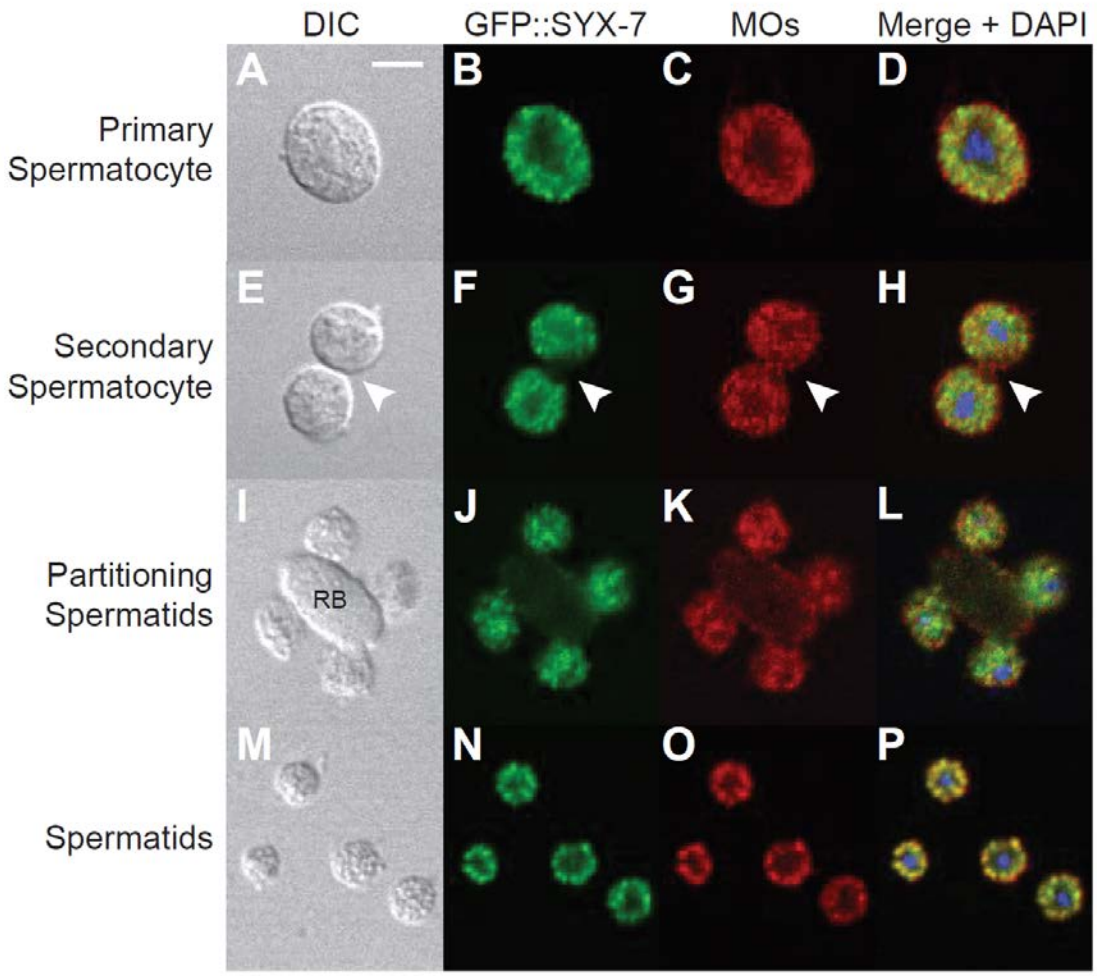


**Figure 2.5. SYX-7 becomes restricted to membranous organelles following spermatid separation.**
(A-P) Antibody-stained sperm dissected from *jnSi259[Psyx-7::GFP::syx-7*] males. Anti-GFP (green), MO marker 1CB4 (red), DAPI (blue). (A-D) Primary spermatocytes had both GFP::SYX-7 and 1CB4 signal throughout the cytoplasm. (E-H) Secondary spermatocytes had cytoplasmic localization of both GFP::SYX-7 and 1CB4, except that GFP::SYX-7 was absent from the thin cytoplasmic connection between the two cells (arrowheads). (I-L) Budding spermatids contained both GFP::SYX-7 and 1CB4, but both markers were mostly absent from the residual body (RB). (M-P) Separated spermatids contained GFP::SYX-7 and 1CB4 in a punctate pattern around the cell periphery, and the two signals colocalized almost entirely at this stage. Scale bar: 5 µM.

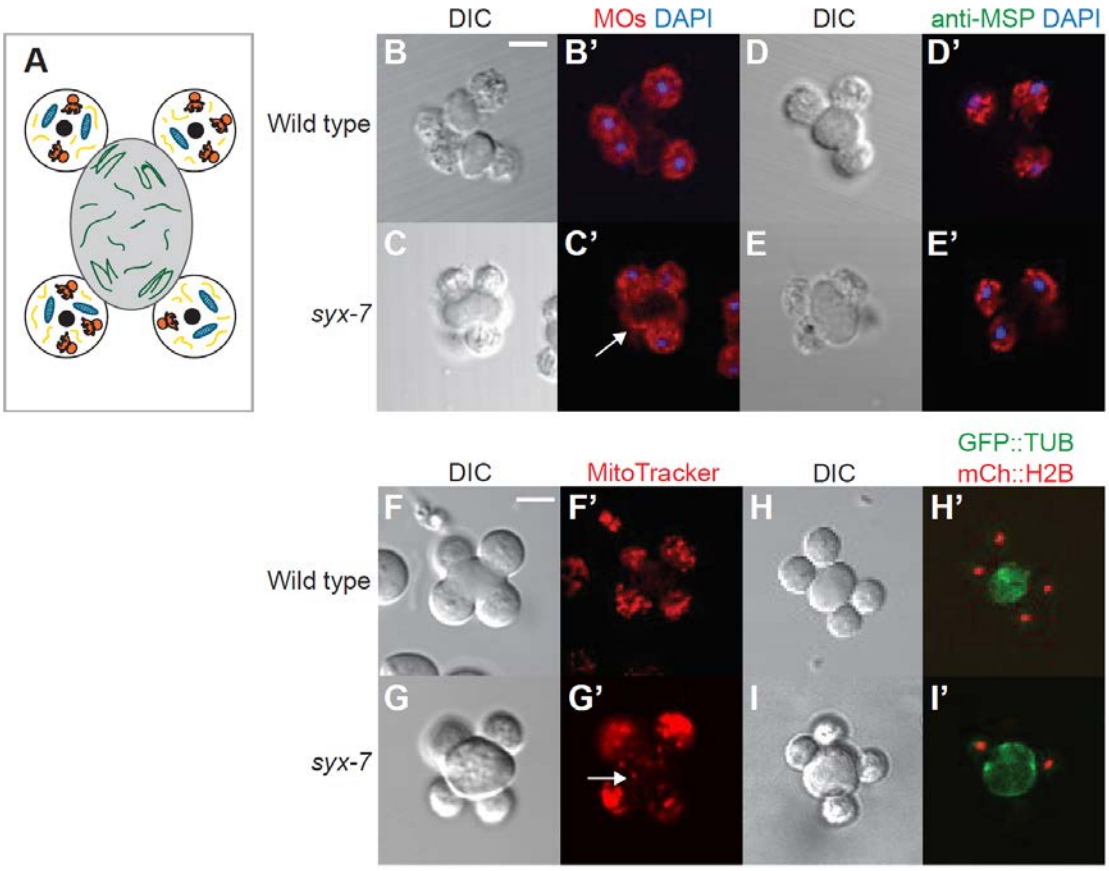


**Figure 2.6. Sperm components are largely partitioned appropriately in budding *syx-7* spermatids.**
(A) Diagram of partitioning during wild-type spermatid budding. Spermatid components: MOs (orange), major sperm protein (yellow), mitochondria (blue), nuclei (black). Residual body components: tubulin (green), actin (not shown). (B-I') Partitioning of MOs, MSP, mitochondria, and tubulin was largely normal in *syx-7* sperm, with the exception of a small number of MOs and mitochondria that were sometimes visible in the residual body. Images show budding-stage spermatids dissected from wild-type and *syx-7(jn37)* males. Cells in B-E' are fixed; F-I' show live images. (B-C') Membranous organelle localization. Cells are labeled with 1CB4 antibody (red) and co-stained with DAPI (blue). One budding spermatid is out of the focal plane. Arrow indicates mislocalized 1CB4 signal on the periphery of the *syx-7* residual body. (D-E') MSP localization. Cells are labeled with monoclonal antibodies mAb4A5(G7) and mAb4D5(N2) (red; (Kosinski et al., 2005), gift of D. Greenstein) and co-stained with DAPI. Note that one of the spermatids (bottom left) completed separation prior to fixation. (F-G') Mitochondria visualized with MitoTracker Red CMXRos (red) Arrow indicates mitochondria within the *syx-7* residual body. (H-I') Cells expressing GFP::tubulin (*meIs16*; green) and mCherry::histone H2B (*ruIs57*; red) (Roelens et al., 2015), gift of M. Schvarzstein). Scale bars: 5 µM.

**Figure 2.7. Actin mislocalizes in budding *syx-7* spermatocytes.**
F-actin localization in dissected spermatocytes during the first and second meiotic cytokinesis, visualized with LifeAct::mCherry (red). (A-B') LifeAct::mCherry localizes to the division plane in both wild-type and *syx-7* spermatocytes at the first meiotic division. (C) Quantification of four-bud and two-bud spermatocytes with the indicated LifeAct::mCherry localization patterns. (n=11-33). (D-D') In wild-type four-bud spermatocytes, actin is restricted to the residual body. (E-G') Aberrant actin localization in four-bud *syx-7* spermatocytes. Actin is not restricted to the residual body and is found in concentrations between spermatids (E-E'), on spermatids (F-F'), and/or in blebs that protrude from the residual body (G-G'). (H-I') Actin localization is restricted to the residual body in wild-type and *syx-7* two-bud spermatocytes. Filled arrowheads, concentrations under forming spermatids; open arrowheads, abnormal localization sites. (J-M''') Images of both GFP::SYX-7 (*jnSi267*; green) and LifeAct::mCherry (*jnSi259*; red) in dissected sperm. SYX-7 and F-actin show very little overlap during sperm division. Scale bars: 5 µm.

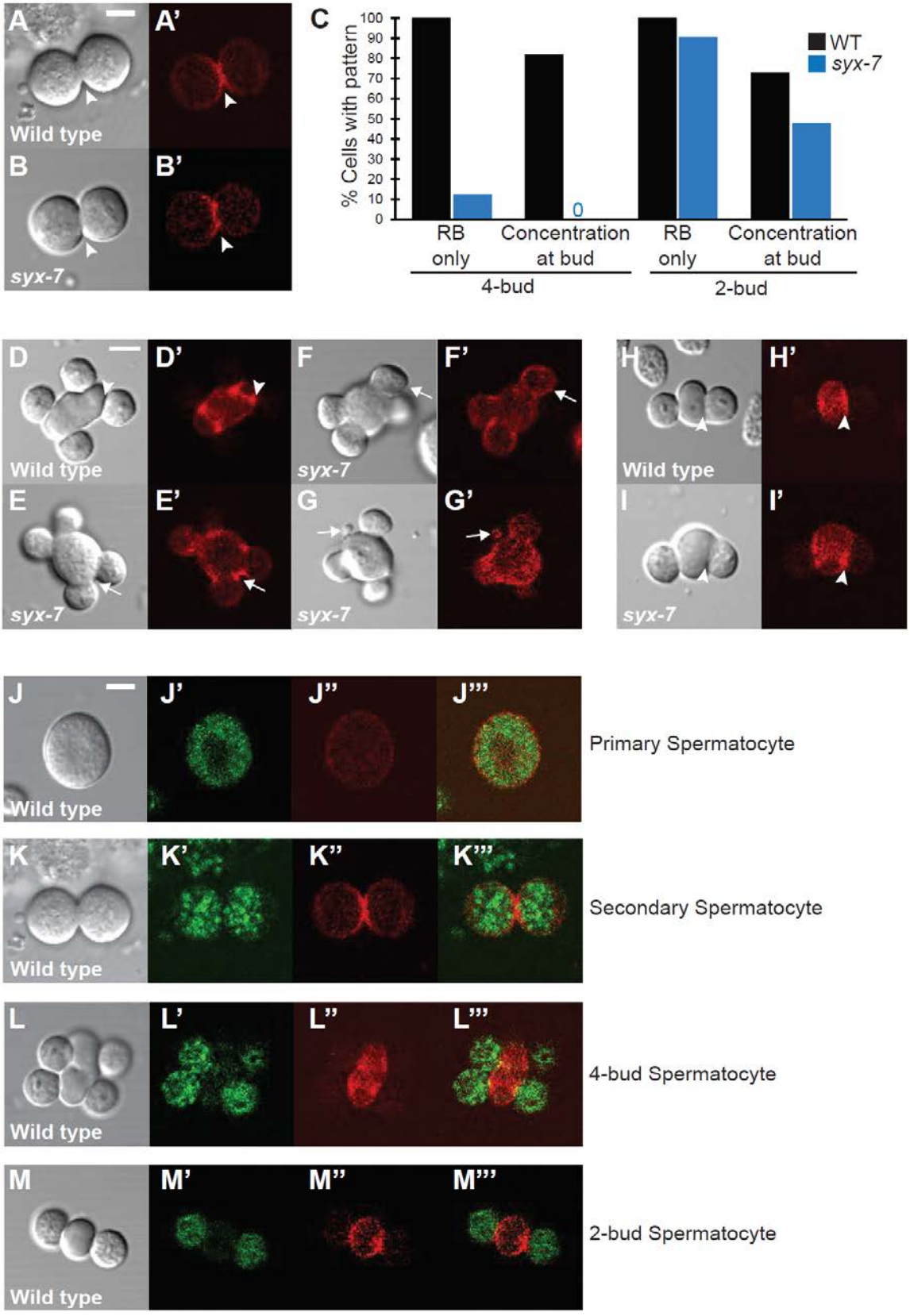
A
A'
Wild type
B
B'
syx-7
C
% Cells with pattern
100
90
80
70
60
50
40
30
20
10
0
WT
syx-7
0
RB only
Concentration at bud
RB only
Concentration at bud
4-bud
2-bud
D
D'
Wild type
E
E'
syx-7
F
F'
syx-7
G
G'
syx-7
H
H'
Wild type
I
I'
syx-7
J
J'
J''
J'''
Wild type
Primary Spermatocyte
K
K'
K''
K'''
Wild type
Secondary Spermatocyte
L
L'
L''
L'''
Wild type
4-bud Spermatocyte
M
M'
M''
M'''
Wild type
2-bud Spermatocyte

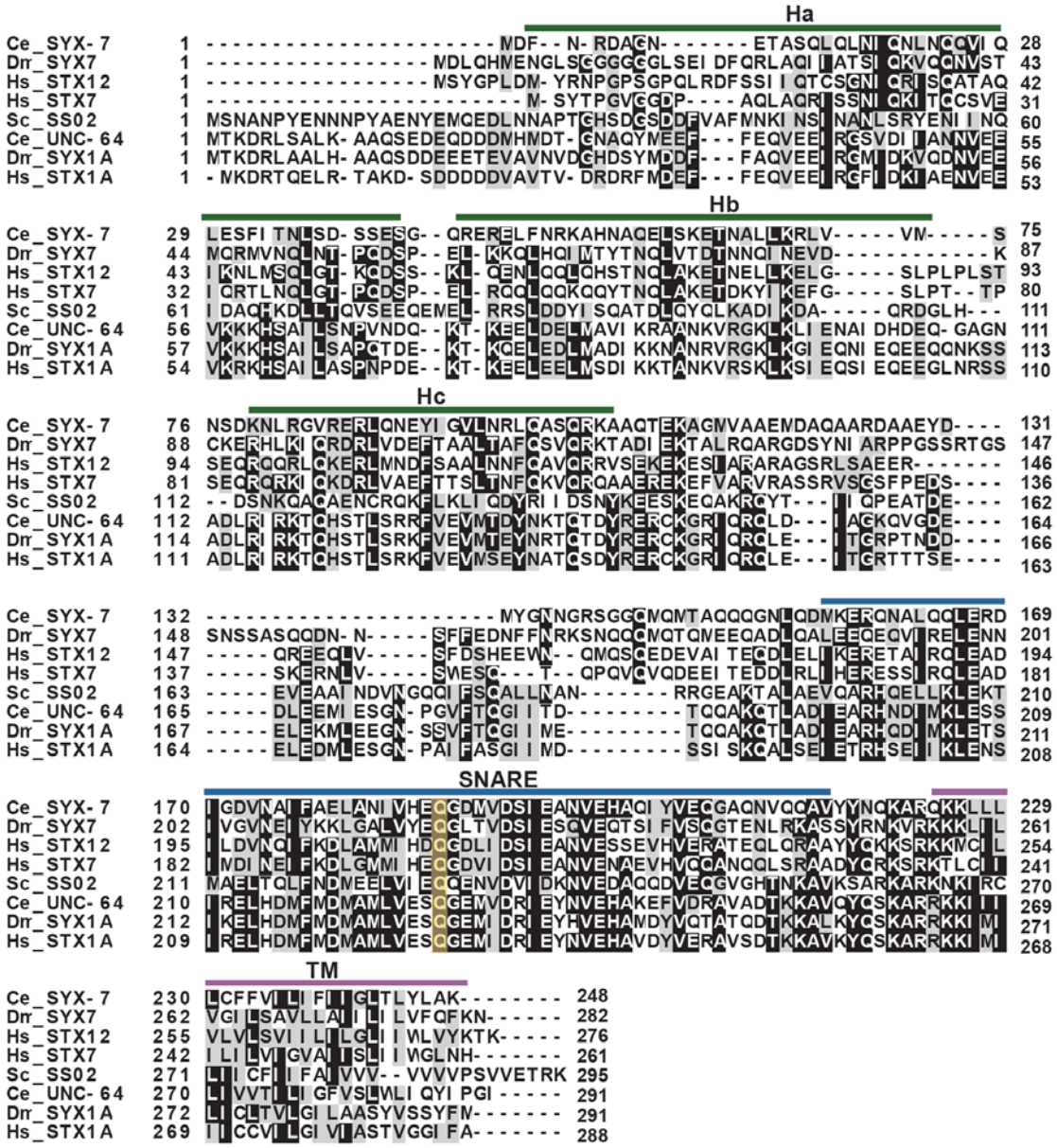


**Figure 2S.1. SYX-7 is a well-conserved t-SNARE that clusters with human STX12.** Alignment of *C. elegans* SYX-7 (accession number O62236) with the most closely related syntaxins from *Drosophila* (SYX7, NP_730632.1) and humans (STX12, Q86Y82; STX7, O15400), as well as well-studied syntaxin 1a from *S. cerevisiae* (SSO2, YMR183C), *C. elegans* (UNC-64, O16000), *Drosophila* (SYX1a, Q24547), and humans (STX1a, Q16623). Alignment was generated using Clustal Omega (Goujon et al., 2010),(Sievers et al., 2011) and BoxShade (https://www.ch.embnet.org/software/BOX_form.html). SYX-7 Habc domain (green) and SNARE domain (blue) predicted by NCBI Conserved Domains Database (Marchler-Bauer et al., 2011), (Marchler-Bauer et al., 2015) (Marchler-Bauer et al., 2017). Transmembrane domain (purple) predicted by TMpred (https://www.ch.embnet.org/software/TMPRED_form.html).

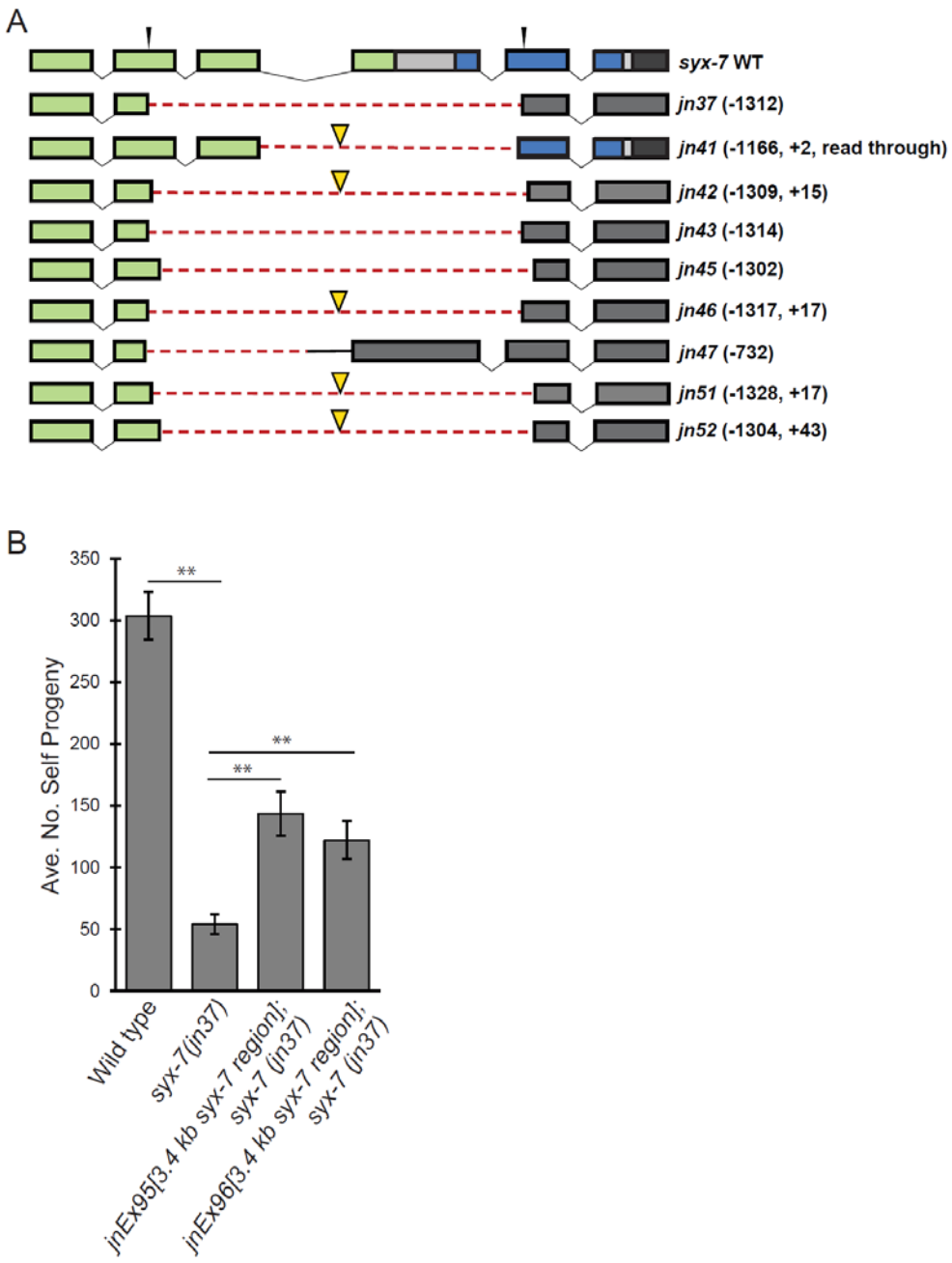


**Figure 2S.2. *syx-7* transgene arrays rescue fertility defects in a deletion mutant of *syx-7*.**
(A) Gene model for wild-type *syx-7* and alleles generated by CRISPR/Cas9 targeting. Boxes (exons), Habc domain (green), SNARE domain (blue), deleted sequence (dashed red lines), inserted sequence (yellow triangles). Cas9 cut sites (arrowheads). (B) Injection of a 3.4 kb genomic fragment encompassing the *syx-7* locus into *syx-7(jn37)* mutant hermaphrodites significantly improved fertility (**p<0.01, Student's t test). Graph shows average total hermaphrodite self brood sizes. Error bars, 95% CI; n=19.

# CHAPTER 3

# LOSS OF *SYX-7* DISRUPTS A SPERM-SPECIFIC, LYSOSOME-LIKE ORGANELLE

## Introduction

Specialized organelles of the secretory and endolysosomal systems are important during sperm development. For example, for sperm to successfully fuse with oocytes, they must first undergo a specialized exocytosis event to deliver proteins required for sperm-oocyte fusion to the cell surface (Berruti and Paiardi, 2011). For mammalian sperm, this is accomplished when the acrosome, a large, acidic organelle related to lysosomes, fuses with the plasma membrane (Cuasnicu et al., 2016). For *C. elegans* sperm, similarly specialized lysosome-like organelles, called fibrous body-membranous organelles (FB-MOs), fuse with the sperm plasma membrane to achieve this goal (Wolf et al., 1978; Gleason et al., 2012). FB-MOs serve other functions during sperm development as well, including a role in asymmetric partitioning and, potentially, in promoting cell division.

The formation of FB-MOs is coordinated with meiotic division (Wolf et al., 1978; Ward et al., 1981). The organelles are first evident in syncytial pachytene spermatocytes, just prior to cellularization (Roberts et al., 1986) (Figure 3.1A). While the FB portion of the organelle contains filamentous major sperm protein (MSP), the sperm motility protein

(Klass and Hirsh, 1981), the MO portion is acidic and vesicle-like (Wolf et al., 1978). However, the two parts form in close association with one another. When primary spermatocytes cellularize, they contain large FBs within MO-derived double-layered membrane envelopes (Roberts et al., 1986) (Figure 3.1B). Stably associated FB-MOs are passed to secondary spermatocytes during the first meiotic division, and are partitioned into spermatids at the second meiotic division (Klass and Hirsh, 1981; Ward and Klass, 1982; Roberts et al., 1986). During spermatid budding, the membrane surrounding the FB retracts and MSP is released (Klass and Hirsh, 1981; Ward and Klass, 1982; Roberts et al., 1986). When spermatids are fully separated from the residual body, they contain MSP dispersed throughout their cytoplasm, as well as MOs that reside just underneath the plasma membrane, poised for fusion as the sperm become motile (Argon and Ward, 1980; Ward and Klass, 1982) (Figure 3.1C).

Recently, I identified a protein that localizes to the MOs during sperm development: SYX-7. SYX-7 is required for fertility, as it promotes the second division of meiosis. The role of SYX-7 in fertility and cell division is explored in Chapter 2 of this dissertation. Briefly, *syx-7* mutant sperm begin the process of division by partitioning many components into dividing spermatids after meiosis II, but cytokinesis fails and most terminal *syx-7* sperm contain 4 nuclei within a common cytoplasm, rather than the single, haploid nucleus found in a wild-type spermatid. Antibody staining for GFP::SYX-7 and MOs revealed the localization of SYX-7 does not primarily overlap with that of the MOs early in sperm development, but GFP::SYX-7 moves to the MOs at later stages.

In this chapter, I further examine the MOs in *syx-7* mutants, and demonstrate that *syx-7* has a role in formation or maintenance of MOs. Abnormal MOs are present in *syx-7*

spermatids, and two different readouts of MO function show loss of *syx-7* decreases, but does not totally abolish, MO function. It remains unclear if the FB-MO defects present in *syx-7* mutants are tied to defects in cell division. However, three other mutants have been identified that affect the formation or function of FB-MOs and also lead to failure of meiotic division (L'Hernault and Arduengo, 1992; Machaca and L'Hernault, 1997; Arduengo et al., 1998; Zhu and L'Hernault, 2003; Zhu et al., 2009; Gleason et al., 2012), suggesting they may function in this context.

## Materials and Methods

### Worm strains and maintenance

Worms were grown on NGM at 20°C and fed with OP50 (Brenner, 1974). Strains used were *him-5(e1490)* and *syx-7(jn37); him-5(e1490). him-5* worms were used as the wild-type to ensure a supply of males for experiments (Hodgkin et al., 1979).

### Electron microscopy

Fixation was performed using a BAL-TEC HPM 010 (BAL-TEC/Leica Microsystems) high-pressure freezing apparatus, then specimens were transferred into fixative (1% OsO4, 1% glutaraldehyde, 1% water, in acetone). Freeze substitution was carried out with the following program: -90˚C for 48h, +5˚C /h to -25˚C, -25˚C for 14 h, +10˚C /h to room temperature. Following freeze substitution, specimens were rinsed 6 times with acetone, then infiltrated with Epon-Araldite resin in a stepwise fashion (50% resin:acetone for 5 h, followed by 70% resin:acetone for 8 h, 90% resin:acetone for 8 h and finally 3 changes of 100% resin for 8 h). Polymerization was performed at 60˚C for

48h. 70 nm thick sections were stained with either saturated uranyl acetate, or lead citrate and uranyl acetate for 20 min prior to imaging.

**LysoSensor stain and MO fusion assays**

To visualize sperm on slides, 24-48 hr virgin post L4 males were dissected into a 7-10 µL drop of Sperm Medium (5 mM HEPES pH 7.4, 50 mM NaCl, 25 mM KCl, 5 mM CaCl2, 1 mM MgSO4, and 10 mM dextrose) (Nelson et al., 1980). Two thin strips of Vaseline were used to elevate the coverslip. Depending on the assay, the Sperm Medium also contained LysoSensor Yellow/Blue DND-160 at 5 µM (Thermo Fisher) (Gleason et al., 2012), or Pronase at 200 µg/ml (Sigma-Aldrich) (Shakes and Ward, 1989) and FM1-43 at 5 µg/mL (Thermo Fisher) (Betz et al., 1996).

## Results

***syx-7* mutant sperm have disrupted membranous organelle ultrastructure**

To determine if FB-MOs or any other cellular structures were abnormal in *syx-7* sperm, we performed transmission electron microscopy on sperm from virgin adult *syx-7* males. In wild-type males, the first FB-MOs observed are in syncytial spermatocytes near the end of the rachis (Figure 3.2A), consistent with previous descriptions (Roberts et al., 1986). Wild-type spermatocytes also contained mitochondria and nuclei that had not yet fully condensed. We were able to visualize few syncytial spermatocytes in the *syx-7* mutant. However, in those we did observe, there were no FB-MO-like structures present, although mitochondria and nuclei were evident (Figure 3.2B). The *syx-7* syncytial

spermatocytes contained large, lightly-stained patches at the cell periphery, which may be MSP that is not enclosed in an FB (Figure 3.2B). While two stages of maturing FB-MOs were evident in wild-type syncytial spermatocytes, with more MSP present in the FBs of spermatocytes near the end of the rachis (Figure 3.2C,D), *syx-7* spermatocytes contained only disorganized patches of filaments that may be free MSP in the spermatocyte cytoplasm (Figure 3.2E). Other structures were well-preserved and appeared normal in the animal (Figure 3.2B,E). Additionally, in dissected and anti-MSP stained *syx-7* spermatocytes, concentrations of MSP were observed that are consistent with the EM data (data not shown). Our sample size for *syx-7* was very low (n=3 spermatocytes from 1 animal), so further EM specimens need to be examined, but these preliminary data indicate MSP is not packaged by the FB-MOs in s*yx-7* mutants.

We next examined spermatids, which are the last stage of sperm found in males, as *C. elegans* male sperm transition to motile spermatozoa only after transfer to a hermaphrodite during mating (Ward and Carrel, 1979). We found that in wild-type males, spermatids were packed very closely into the sperm storage region, and contained condensed nuclei, mitochondria, and MOs that had released the FBs (Figure 3.3A) (n=2 animals). We also examined some of the few spermatids formed by *syx-7* mutants that appeared normal by DIC microscopy (see Chapter 2). In *syx-7* males, spermatids were not as densely packed as in the wild-type, and space was often visible between stored sperm (Figure 3.3D) (n=4 animals). Seminal fluid, which is stored just posterior of the sperm in wild-type males, often moved into the open space between cells in the *syx-7* sperm storage region (data not shown). This is consistent with what occurs in other

mutants that have increased extracellular space in the seminal vesicle (D. Chavez and G. Stanfield, personal communication).

Of the main structures evident in spermatids, only the MOs showed defects in *syx-7* males as compared to the wild-type. Wild-type MOs contain specialized, double-layered membranes that stain darkly by EM (Wolf et al., 1978). The organelle has two lobes: a round head and a body of membrane folds which formerly held MSP (Figure 3.3B). These lobes are separated by an electron-dense collar (Wolf et al., 1978). In wild-type spermatids, membranous organelles localize very close to the plasma membrane (Figure 3.3C), and the two will fuse as sperm gain motility in an event termed sperm activation (Argon and Ward, 1980). In *syx-7* mutant spermatids, MO-like structures were present, but varied greatly in terms of size and structure. Although double membranes were still evident as in wild-type, the organization of the organelle was disrupted in *syx-7* spermatids. A head region was rarely discernable, and the few putative head regions were small in proportion to the body region (Figure 3.3E). The body regions of the MO-like structures in *syx-7* spermatids were disorganized compared to wild-type, often containing large gaps or thickened sections (Figure 3.3E). In many *syx-7* spermatids, fragments of membrane were present that did not appear to be part of larger structures, and often small vesicles were present that we did not see in wild-type sperm (Figure 3.3F). These vesicles stained to a variable degree and thus appear to be heterogenous in nature. While the vesicles are present to some extent in most of the *syx-7* cells we analyzed, there were some cells with very high concentrations of these vesicles (Figure 3.3D). From these data, we conclude the MOs are not forming properly or are not maintained in *syx-7*

mutants. Additionally, the presence of extra membrane fragments and vesicles suggests that *syx-7* may have a role in assembly of the intricate MO membrane structure.

Finally, we analyzed the large terminal sperm in the *syx-7* mutant (n=4 animals). (An additional brief description of these cells can be found in Chapter 2.) *syx-7* terminal sperm are distinguishable as they are much larger than wild-type spermatids and are located just anterior to the few small spermatids formed by the *syx-7* mutant. In some terminal cells, we observed compartments partially separated by membranes (Figure 3.4A). These compartments were roughly the same size as wild-type spermatids and contained mitochondria and a single nucleus (Figure 3.4A). We did not observe MO-like structures in this cell type, although there were small vesicles that were not present in wild-type sperm at any stage. Other *syx-7* terminal cells contained no compartments, and organelles were either not discernible or appeared very sick (Figure 3.4B). This suggests a breakdown of cellular components in *syx-7* terminal cells, although it remains unclear if this cell type ever contained MO-like structures.

**Loss of *syx-7* disrupts MO function during late stages of spermatogenesis**

We used well-defined assays for MO function to further characterize *syx-7* sperm. Like lysosomes, MOs are acidic and can be marked with LysoSensor (Thermo Fisher), a vital dye that fluoresces in acidic environments (Diwu et al., 1999). When we dissected wild-type spermatids into media containing LysoSensor, puncta were visible around the periphery of the cell where the MOs are distributed (Figure 3.5A-A'), as previously described (Gleason et al., 2012). When *syx-7* spermatids were dissected into the same

media, acidic structures were visible, but they formed fewer puncta as compared to wild-type and often formed ring-shaped structures (Figure 3.5B-B') that likely correspond to the abnormal MOs we saw in our electron micrographs (Figure 3.3). These abnormal MOs did not abut the plasma membrane to the same extent as wild-type MOs. We conclude that although MOs are abnormal in *syx-7* mutants, they do acidify to some extent.

To further probe MO function, we took advantage of the fact that in wild-type sperm, MOs stably fuse with the plasma membrane at the onset of motility (Washington and Ward, 2006). To assay such MO fusions, we induced motility in vitro using Pronase in the presence of FM1-43 dye. FM1-43 is a noncell permeable dye that marks the plasma membrane (Betz et al., 1996), and MO fusions are revealed because punctate concentrations of dye appear at the site of membrane fusion (Ward and Miwa, 1978; Washington and Ward, 2006). While wild-type sperm showed many MO fusions, the number of fusions in *syx-7* mutants was drastically reduced (Figure 3.5C-E). Together, these data indicate MO function is reduced in *syx-7* mutants; however, it does not appear to be abolished completely. MO fusion is required for fertilization competence (Ward and Miwa, 1978), and the residual fusion observed in *syx-7* mutants could help explain why these animals are not completely sterile.

### *syx-7* is unlikely to function via a complex with *vti-1* or *syx-6* during sperm development

The presence of numerous small vesicles in *syx-7* but not wild-type sperm (Figure 2.2G, 3.3F, and 2.4A-B) suggested the mutant may have a defect in fusion of these

vesicles to form membranous organelles. The mammalian ortholog of *syx-7*, Stx12/13, functions in a complex with syntaxin 6, the vesicle transport through t-SNARE interaction protein vti1a, and the vesicle-associated membrane protein VAMP4, to mediate homotypic fusion of early endosomes (Brandhorst et al., 2006). The *C. elegans* orthologs of vti1a and syntaxin 6, *vti-1* and *syx-6*, are expressed in sperm (Ma et al., 2014), and I sought to test if this complex functioned during sperm development.

I obtained mutant strains for both *vti-1* and *syx-6* (National BioResource Project:: *C. elegans*). *vti-1(tm6428)* is a 703 base pair deletion that removes a large portion of *vti-1*, beginning in exon 1 and continuing past the 3' end of the gene. *gcc-1 syx-6(tm4733)* is a 420 base pair deletion that removes approximately the first 1.5 exons of *syx-6*, as well as part of the 3'UTR of the neighboring gene, *gcc-1*. The remaining portion of *syx-6* is in frame. I hypothesized that if either *vti-1* or *syx-6* functioned with *syx-7* during sperm development, defects would be present in sperm formation or fertility in these strains, as in *syx-7* mutants. However, when I visualized sperm in 48 hr adult males, neither *vti-1* or *syx-6* mutants were distinguishable from wild-type (Figure 3.6A-C). There were no large, abnormal cells as in a *syx-7* mutant (Figure 3.6D), and no other abnormalities could be detected. Both *vti-1* and *syx-6* mutant hermaphrodites were as fertile as wild-type, and loss of either gene did not exacerbate or rescue the fertility defects of *syx-7* mutants (Figure 3.6E). Thus, it is unlikely *syx-7* functions through a complex with *vti-1* and *syx-6* during sperm development.

## Discussion

Spermatogenesis in *C. elegans* requires the proper morphogenesis of specialized FB-MO secretory vesicles, and there are several functions known or proposed for them. FB-MOs package major sperm protein (MSP), and are involved in its asymmetric partitioning into spermatids (Roberts et al., 1986). Additionally, FB-MOs have been associated multiple times with promoting meiotic division, as sperm cytokinesis is disrupted in several *C. elegans* mutants that affect the biogenesis or function of FB-MOs (L'Hernault and Arduengo, 1992; Machaca and L'Hernault, 1997; Arduengo et al., 1998; Zhu and L'Hernault, 2003; Zhu et al., 2009; Gleason et al., 2012). Finally, MO fusion with the plasma membrane is a required event for sperm to become motile and fertilization competent (Ward and Miwa, 1978).

Our identification of *syx-7* and characterization of defects in *syx-7* mutants strengthen some of these proposed models for FB-MO function, and suggest others are either less likely or more complicated than we currently understand. Our EM data regarding MSP packaging into FBs in the *syx-7* mutant are somewhat incomplete. However, it is clear that terminal *syx-7* sperm contain no structures that resemble FB-MOs, and the MOs present in the few *syx-7* spermatids are highly abnormal. Surprisingly, most of the asymmetric partitioning that occurs during the meiosis II cytokinesis is normal in *syx-7* mutants, even though this is where division fails (see Chapter 2). Even more surprising, is that this includes the partitioning of MSP. In fact, anti-MSP staining revealed no apparent defects in MSP localization at any stage of *syx-7* sperm development, and mutant sperm are able to form MSP-driven pseudopods both in vivo and after Pronase treatment (Chapter 2, Figure 3.5, and data not shown). This suggests

even without fully functional FB-MOs, MSP ends up in the proper location in sufficient quantities to function in pseudopod formation, at least in a subset of sperm. These data highlight the possibility FB-MOs may not be absolutely critical for MSP segregation, as was previously thought.

Whether or not membranous organelle function directly contributes to cell division remains unclear. In addition to *syx-7*, a t-SNARE, loss of the presenilin *spe-4* (L'Hernault and Arduengo, 1992; Arduengo et al., 1998), the vATPase *spe-5* (Machaca and L'Hernault, 1997; Gleason et al., 2012), and the novel HOPS complex interacting factor *spe-39* (Zhu and L'Hernault, 2003; Zhu et al., 2009) all affect FB-MO ultrastructure and lead to cytokinesis defects. Loss of each different gene has its own unique abnormalities in how the FB-MOs are affected, and it is currently unclear how the genes may fit into a pathway(s) that contribute to MO biogenesis or function. It is likely that many more genes exist that contribute to MO physiology, and by continuing to identify them, as with *syx-7*, we will be better able to understand how they function together and clarify if and how FB-MOs function in cell division. While the *vti-1* and *syx-6* mutants I analyzed had grossly normal sperm and wild-type levels of fertility, I have not yet directly assayed MOs in these strains. Therefore, it remains a possibility abnormal MOs could be uncoupled from sperm meiotic division in the *vti-1* or *syx-6* mutants. As an alternative model to MOs functioning directly in cell division, perhaps the presence of abnormal organelles causes sperm to simply fail to pass a checkpoint and arrest division.

Previous work indicated MO fusion with the plasma membrane is a critical event in sperm gaining fertilization competence (Ward and Miwa, 1978). For example, when mutations occur in the dysferlin *fer-1*, MOs do not fuse and animals are completely

sterile (Achanzar and Ward, 1997). One idea for the infertility is that necessary proteins do not localize to the plasma membrane in the absence of MO fusion. *syx-7* animals have some success at fertility, even though MOs are abnormal and fusions are greatly reduced (Figures 3.3 and 3.5). It is possible the few fusions observed in *syx-7* sperm are enough to promote fertility. Alternatively, because MOs are so abnormal in *syx-7* mutants, perhaps proteins that should localize to the MOs are instead rerouted and localize to the plasma membrane, negating the requirement for MO fusion. A third possibility is that other unknown defects in *fer-1* mutants contribute to the complete lack of progeny in the mutant.

Membranous organelles have features of a class of organelles called lysosome-related organelles (LROs). Examples of LROs include melanosomes, dense granules and lytic granules, *Drosophila* eye pigment granules, and *C. elegans* gut granules. Depletion of Stx12/13, the mammalian ortholog of *syx-7*, reroutes proteins required by melanosomes to lysosomes (Jani et al., 2015), indicating there is a role for the protein in LRO function in contexts beyond sperm development. As in our system, direct connections between LROs and cell division are not clear, although in the human disorder Chediak-Higashi Syndrome, melanosomes and other LROs form improperly and uncontrollable white blood cell division is one of the many complications of the disease (Huizing et al., 2008). While questions still exist, our identification of *syx-7* and its effects on membranous organelle biogenesis and cell division demonstrates another link between the two processes. Demonstrating a clear, functional connection between FB-MOs and cell division should be a key goal for future work, as it would identify a new

function for LROs and further the understanding of Chediak-Higashi Syndrome and other lysosomal storage disorders that affect human health.

## Acknowledgements

I would like to thank Linda Nikolova, an EM specialist at the University of Utah's Electron Microscopy Core Laboratory, for her contributions to this work. Linda helped with the high-pressure freezing and subsequent processing of EM samples, including a huge amount of sectioning. I would also like to thank the Jorgensen lab for equipment and advice, particularly Eddie Hujber and Thien Vu for valuable discussions and ideas when Linda and I were troubleshooting fixation methods.

## References

Achanzar, W.E., Ward, S., 1997. A nematode gene required for sperm vesicle fusion. J. Cell Sci. 110 ( Pt 9), 1073-1081.

Arduengo, P., Appleberry, O., Chuang, P., L'Hernault, S., 1998. The presenilin protein family member SPE-4 localizes to an ER/Golgi derived organelle and is required for proper cytoplasmic partitioning during *C. elegans* spermatogenesis. J. Cell Sci. 111, 3645-3654.

Argon, Y., Ward, S., 1980. *C. elegans* fertilization-defective mutants with abnormal sperm. Genetics 96, 413-433.

Berruti, G., Paiardi, C., 2011. Acrosome biogenesis: Revisiting old questions to yield new insights. Spermatogenesis 1, 95-98.

Betz, W.J., Mao, F., Smith, C.B., 1996. Imaging exocytosis and endocytosis. Curr. Opin. Neurobiol. 6, 365-371.

Brandhorst, D., Zwilling, D., Rizzoli, S.O., Lippert, U., Lang, T., Jahn, R., 2006. Homotypic fusion of early endosomes: SNAREs do not determine fusion specificity. Proc. Natl. Acad. Sci. 103, 2701-2706.

Brenner, S., 1974. The genetics of Caenorhabditis elegans. Genetics 77, 71-94.

Cuasnicu, P.S., Da Ros, V.G., Weigel Munoz, M., Cohen, D.J., 2016. Acrosome reaction as a preparation for gamete fusion. Adv. Anat. Embryol. Cell Biol. 220, 159-172.

Diwu, Z., Chen, C.S., Zhang, C., Klaubert, D.H., Haugland, R.P., 1999. A novel acidotropic pH indicator and its potential application in labeling acidic organelles of live cells. Chem. Biol. 6, 411-418.

Gleason, E., Hartley, P., Henderson, M., Hill-Harfe, K., Price, P., Weimer, R., Kroft, T., Zhu, G.-D., Cordovado, S., L'Hernault, S., 2012. Developmental genetics of secretory vesicle acidification during *C. elegans* spermatogenesis. Genetics 191, 477-491.

Hodgkin, J., Horvitz, H.R., Brenner, S., 1979. Nondisjunction mutants of the nematode *Caenorhabditis elegans*. Genetics 91, 67-94.

Huizing, M., Helip-Wooley, A., Westbroek, W., Gunay-Aygun, M., Gahl, W.A., 2008. Disorders of lysosome-related organelle biogenesis: clinical and molecular genetics. Annu. Rev. Genomics Hum. Genet. 9, 359-386.

Jani, R., Purushothaman, L., Rani, S., Bergam, P., Setty, S., 2015. STX13 regulates cargo delivery from recycling endosomes during melanosome biogenesis. J. Cell Sci. 128, 3263-3276.

Klass, M.R., Hirsh, D., 1981. Sperm isolation and biochemical analysis of the major sperm protein from *Caenorhabditis elegans*. Dev. Biol. 84, 299-312.

L'Hernault, S.W., Arduengo, P.M., 1992. Mutation of a putative sperm membrane protein in Caenorhabditis elegans prevents sperm differentiation but not its associated meiotic divisions. J. Cell Biol. 119, 55-68.

Ma, X., Zhu, Y., Li, C., Xue, P., Zhao, Y., Chen, S., Yang, F., Miao, L., 2014. Characterisation of *Caenorhabditis elegans* sperm transcriptome and proteome. BMC Genomics 15, 168.

Machaca, K., L'Hernault, S.W., 1997. The *Caenorhabditis elegans spe-5* gene is required for morphogenesis of a sperm-specific organelle and is associated with an inherent cold-sensitive phenotype. Genetics 146, 567-581.

Nelson, G., Roberts, T., Ward, S., 1980. Vesicle fusion, pseudopod extension and amoeboid motility are induced in nematode spermatids by the ionophore monensin. Cell 19, 457-464.

Roberts, T.M., Pavalko, F.M., Ward, S., 1986. Membrane and cytoplasmic proteins are transported in the same organelle complex during nematode spermatogenesis. J. Cell Biol. 102, 1787-1796.

Shakes, D., Ward, S., 1989. Initiation of spermiogenesis in *C. elegans*: a pharmacological and genetic analysis. Dev. Biol. 134, 189-200.

Ward, S., Argon, Y., Nelson, G., 1981. Sperm morphogenesis in wild-type and fertilization-defective mutants of *C. elegans*. J. Cell Biol.

Ward, S., Carrel, J., 1979. Fertilization and sperm competition in the nematode *C. elegans*. Dev. Biol. 73, 304-321.

Ward, S., Klass, M., 1982. The location of the major protein in *Caenorhabditis elegans* sperm and spermatocytes. Dev. Biol. 92, 203-208.

Ward, S., Miwa, J., 1978. Characterization of temperature-sensitive, fertilization-defective mutants of the nematode *Caenorhabditis elegans*. Genetics 88, 285-303.

Washington, N., Ward, S., 2006. FER-1 regulates Ca2+-mediated membrane fusion during *C. elegans* spermatogenesis. J. Cell Sci. 119, 2552-2562.

Wolf, N., Hirsh, D., McIntosh, J., 1978. Spermatogenesis in males of the free-living nematode, *C. elegans*. J. Ultrastruct. Res. 63, 155-169.

Zhu, G., L'Hernault, S., 2003. The *C.* elegans *spe-39* gene is required for intracellular membrane reorganization during spermatogenesis. Genetics 165, 145-157.

Zhu, G.D., Salazar, G., Zlatic, S.A., Fiza, B., Doucette, M.M., Heilman, C.J., Levey, A.I., Faundez, V., L'Hernault S, W., 2009. SPE-39 family proteins interact with the HOPS complex and function in lysosomal delivery. Mol. Biol. Cell 20, 1223-1240.

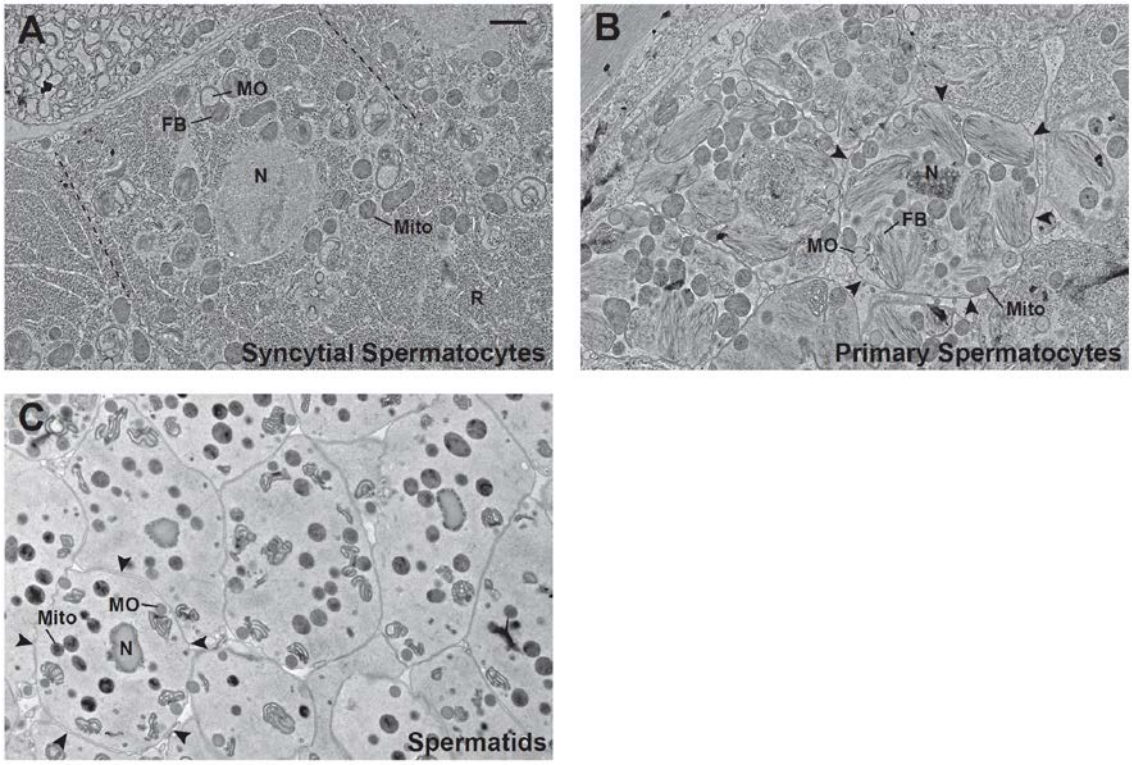


**Figure 3.1. Development of FB-MOs.**
(A-C) Electron micrographs of the sperm development and storage regions of adult, wild-type males. (A) FB-MOs form throughout the cytoplasm of syncytial spermatocytes. Major sperm protein comprises the FB and forms filaments within the MO membrane envelope. (B) FB-MOs reach their largest size in cellularized primary spermatocytes. The FB portion remains associated with the MO head region. (C) Spermatids contain MOs that are no longer associated with FBs. MO heads abut the plasma membrane in preparation for fusion when motility is triggered. All sections in this figure were stained with both uranyl acetate and lead citrate. Nucleus (N), mitochondrion (Mito), rachis (R), fibrous body (FB), membranous organelle (MO). Dashed lines indicate approximate boundary between spermatocytes. Arrowheads indicate boundary of labeled cells. Scale bar: 1 μm.

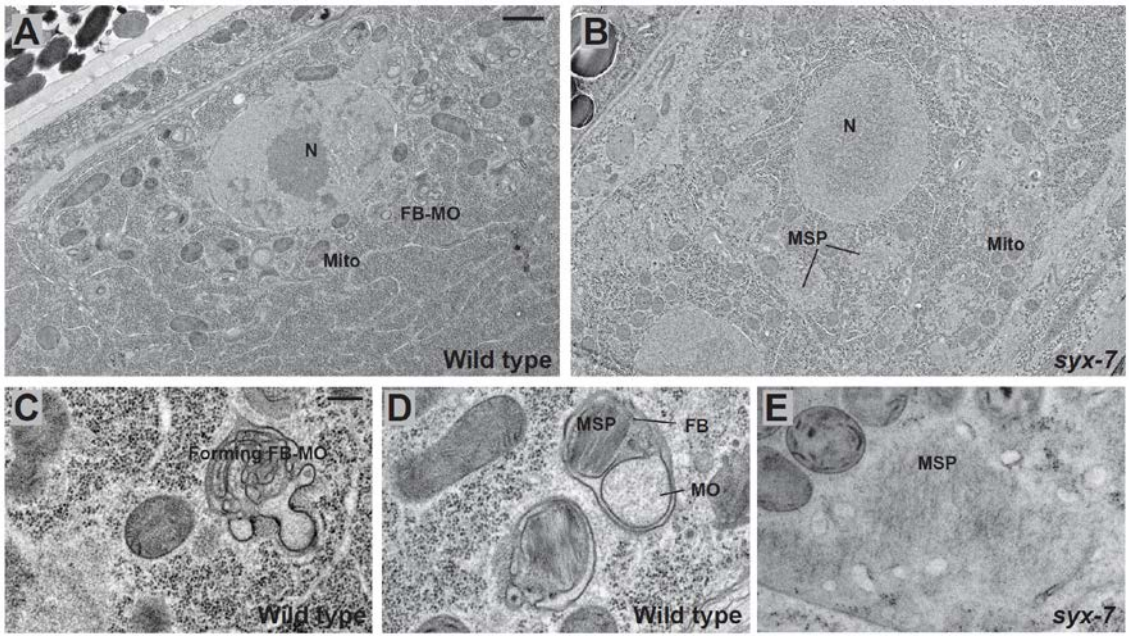


**Figure 3.2. FB-MOs are not evident in syncytial *syx-7* germ cells.**
(A-E) Electron micrographs of sperm during late syncytial development in wild-type or *syx-7(jn37)* males. (A) Wild-type spermatocyte containing an uncondensed nucleus, mitochondria, and forming FB-MOs. (B) *syx-7* spermatocyte containing an uncondensed nucleus and mitochondria, but no discernable FB-MOs. Putative clumps of unpackaged major sperm protein localize near the cell periphery. (C) Forming FB-MO in a young, wild-type syncytial spermatocyte. (D) Forming FB-MO in a wild-type syncytial spermatocyte that is approaching cellularization. Polymerized MSP is packaged into the FB. (E) Putative MSP clump from a *syx-7* syncytial spermatocyte. Note: the wild-type sections shown (A,C,D) were stained using both lead citrate and uranyl acetate, while *syx-7* sections (B,E) were stained with uranyl acetate only. Nucleus (N), fibrous body membranous organelle (FB-MO), mitochondria (Mito), major sperm protein (MSP). Scale bars: 1 µM (top panels), 200 nm (bottom panels).

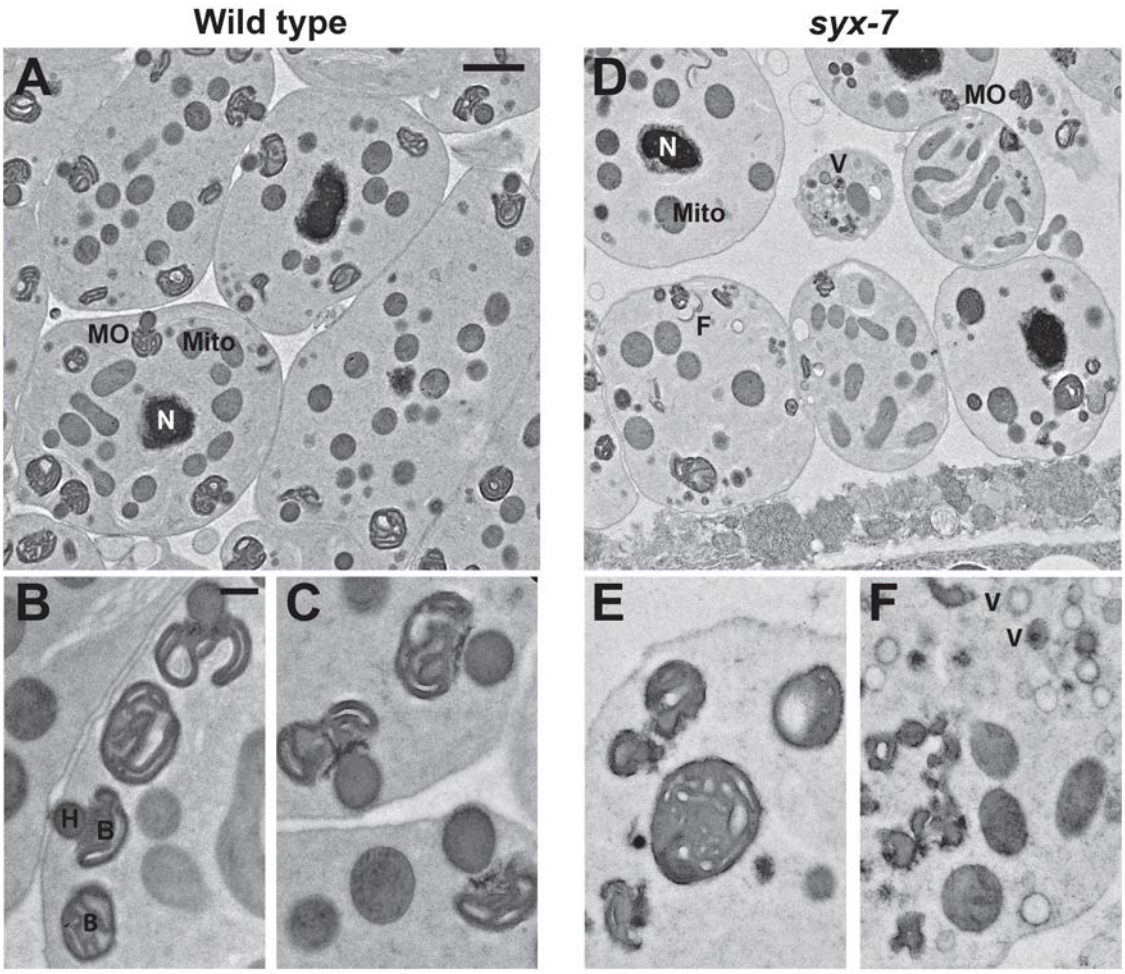


**Figure 3.3. MOs are abnormal in *syx-7* spermatids.**
(A-F). Electron micrographs of the sperm storage region of adult males. (A) MOs in wild-type spermatids. (B) Cross and vertical sections of wild-type MOs. (C) Head regions of wild-type MOs localize just under the plasma membrane of spermatids. (D) MO-like structures, membrane fragments, and small vesicles in *syx-7* spermatids. Vesicles are often concentrated together. (E) Variation of MO-like structures in *syx-7* spermatids. Structures vary in size, and if a head region is discernible, it is usually very small in comparison to the rest of the organelle. (F) Many heterogeneous vesicles are present in *syx-7* spermatids, often concentrated together. All sections in this figure were stained with uranyl acetate only. Nucleus (N), mitochondria (Mito), MOs and MO-like structures in mutant (MO), MO head (H), MO body (B), membrane fragment (F), vesicle (V). Scale bars: 1 µM (top panels), 200 nm (bottom panels).

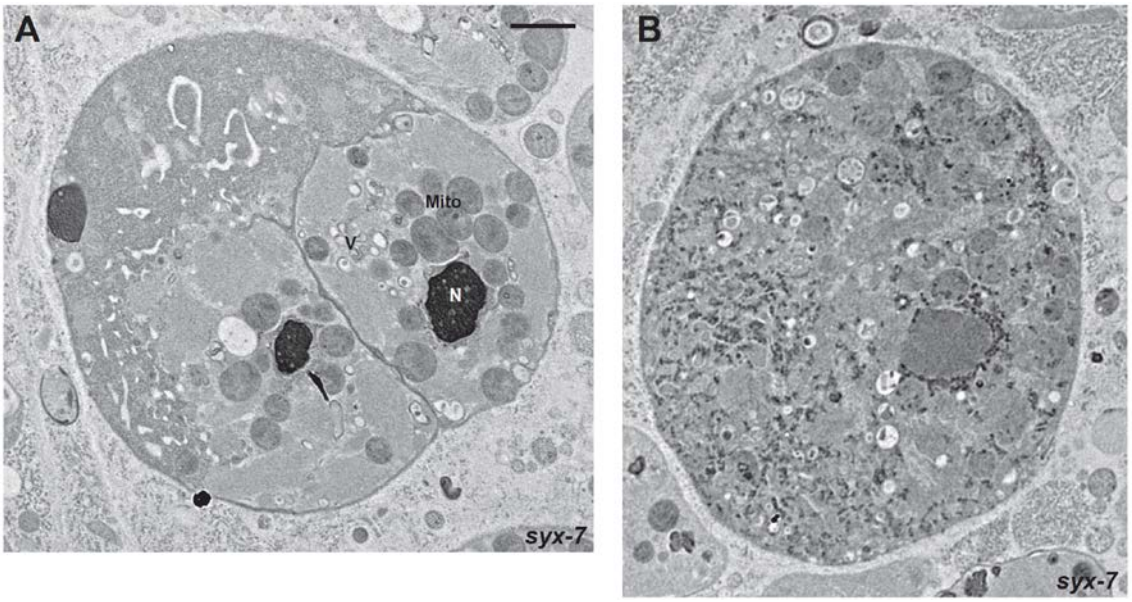


**Figure 3.4. Terminal *syx-7* sperm.**
(A-B). Electron micrographs of terminal *syx-7(jn37)* sperm, from within the sperm storage region of an adult male. (A) Some terminal cells contained spermatid-sized compartments, partially enclosed by membranes. These compartments contained nuclei and mitochondria, as well as vesicles that were not present in any stage of wild-type sperm. (B) Some terminal cells contained no compartments, and organelles appeared to be very sick or breaking down. Both sections in this figure were stained with uranyl acetate only. Nucleus (N), mitochondria (Mito), vesicle (V). Scale bar: 1 µm.

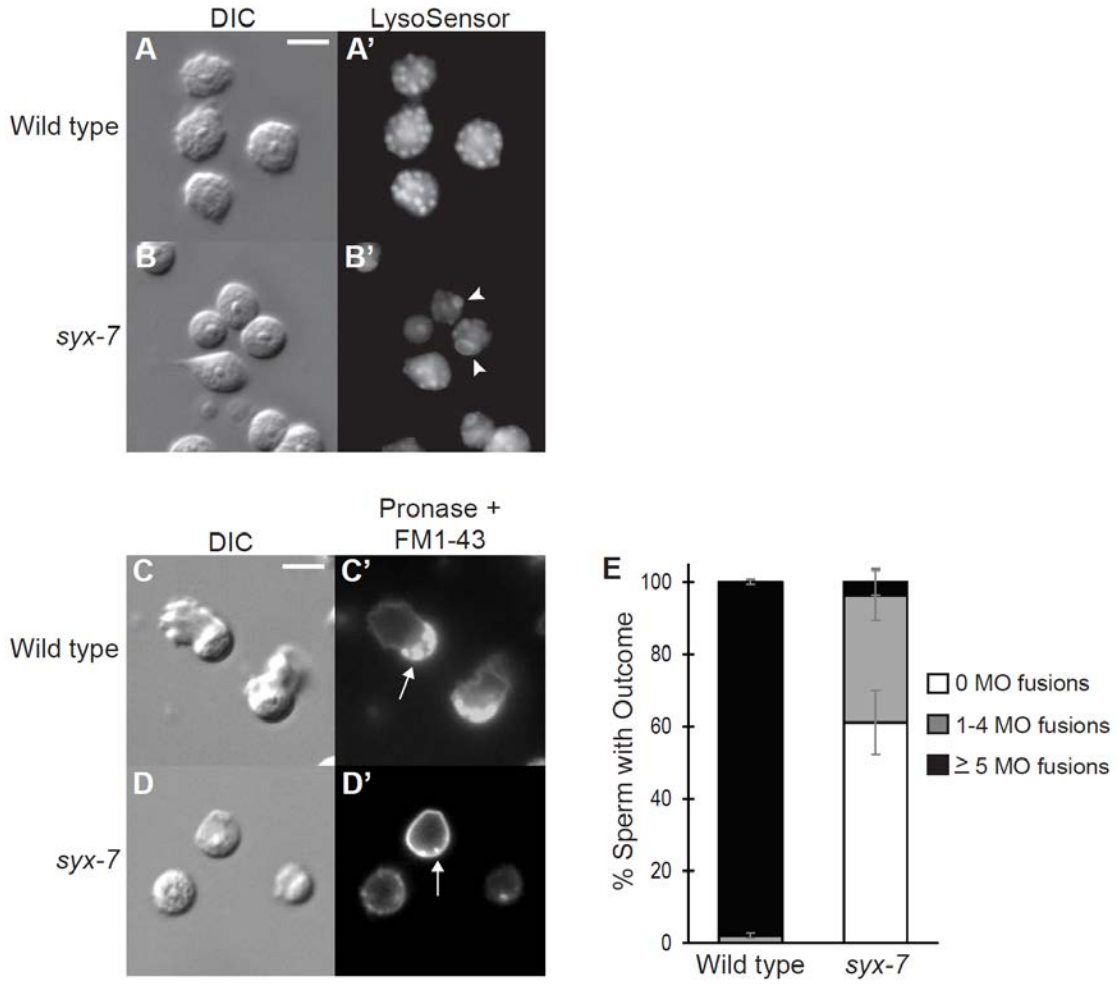


**Figure 3.5. *syx-7* mutants have reduced MO function during late spermatogenesis.** (A-B') Paired DIC and fluorescent images of dissected sperm stained with LysoSensor Yellow/Blue DND-160. (A-A') Wild-type sperm show staining in a punctate pattern near the cell periphery, indicating the presence of acidic MOs. (B-B') LysoSensor staining in *syx-7* sperm reveals acidic structures. Unlike wild-type, these often appear ring-like (arrowheads). (C-D') Paired DIC and fluorescent images of sperm dissected into media containing Pronase and FM1-43. Pronase causes sperm to undergo stable MO fusions and pseudopod extension; FM1-43 is a vital membrane dye that reveals the site of MO fusions. (C-C') Wild-type spermatozoa have many sites of MO fusion per cell (arrow). (D-D') *syx-7(jn37)* spermatozoa have fewer MO fusions compared to wild-type (arrows). Scale bar: 5 µm. (E) Quantification of MO fusion events in wild-type and *syx-7(jn37)* sperm. Error bars are standard error of the mean; n=84-110 cells.

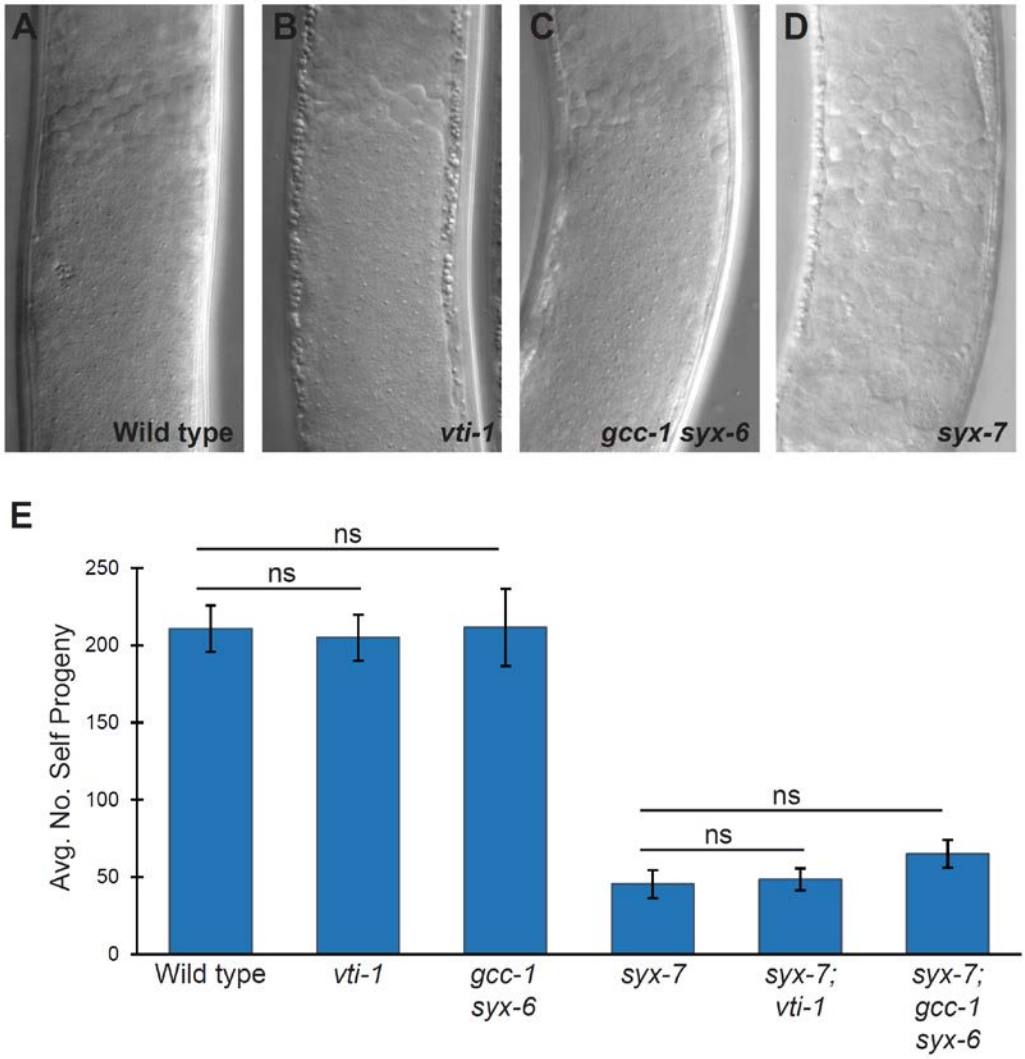


**Figure 3.6. Loss of *vti-1* or *syx-6* does not affect sperm formation or fertility.** (A-D) Images of seminal vesicles from 48 hr post L4 males. Genotypes shown: (A) wild-type (B) *vti-1(tm5428)* (C) *gcc-1 syx-6(tm4733)* (D) *syx-7(jn37).* Sperm from *vti-1* and *gcc-1 syx-6* mutants was indistinguishable from wild-type sperm. (E) Brood sizes of *vti-1* and *gcc-1 syx-6* mutant hermaphrodites were comparable to wild-type broods. Broods of *syx-7; vti-1* and *syx-7; gcc-1 syx-6* mutants were reduced compared to wild-type, but were no different than broods from *syx-7* mutants. (ns $p>0.005$, Student's t test); error bars, 95% confidence interval; n=19-21.

# CHAPTER 4

# SLC6 FAMILY TRANSPORTER SNF-10 IS REQUIRED FOR PROTEASE-MEDIATED ACTIVATION OF SPERM MOTILITY IN *C.ELEGANS*

Originally published as-Fenker, K.E., Hansen, A.A., Chong, C.A., Jud, M.C., Duffy, B.A., Norton, J.P., Hansen, J.M., and Stanfield, G.M. (2014). SLC6 family transporter SNF-10 is required for protease-mediated activation of sperm motility in *C. elegans*. Developmental Biology, *393*(1), 171-182. DOI: 10.1016/j.ydbio.2014.06.001

Developmental Biology 393 (2014) 171–182

Contents lists available at ScienceDirect

Developmental Biology

journal homepage: www.elsevier.com/locate/developmentalbiology

# SLC6 family transporter SNF-10 is required for protease-mediated activation of sperm motility in *C. elegans*

Kristin E. Fenker, Angela A. Hansen, Conrad A. Chong, Molly C. Jud, Brittany A. Duffy, J. Paul Norton, Jody M. Hansen, Gillian M. Stanfield*

*Department of Human Genetics, University of Utah, 15 North 2030 East, Room 6110B, Salt Lake City, UT 84112, USA*

ARTICLE INFO

*Article history:*
Received 21 February 2014
Received in revised form
28 May 2014
Accepted 3 June 2014
Available online 12 June 2014

*Keywords:*
Sperm
Cell motility
Signaling
Reproduction
SLC6 transporter
*C. elegans*

ABSTRACT

Motility of sperm is crucial for their directed migration to the egg. The acquisition and modulation of motility are regulated to ensure that sperm move when and where needed, thereby promoting reproductive success. One specific example of this phenomenon occurs during differentiation of the ameboid sperm of *Caenorhabditis elegans* as they activate from a round spermatid to a mature, crawling spermatozoon. Sperm activation is regulated by redundant pathways to occur at a specific time and place for each sex. Here, we report the identification of the solute carrier 6 (SLC6) transporter protein SNF-10 as a key regulator of *C. elegans* sperm activation in response to male protease activation signals. We find that SNF-10 is present in sperm and is required for activation by the male but not by the hermaphrodite. Loss of both *snf-10* and a hermaphrodite activation factor render sperm completely insensitive to activation. Using *in vitro* assays, we find that *snf-10* mutant sperm show a specific deficit in response to protease treatment but not to other activators. Prior to activation, SNF-10 is present in the plasma membrane, where it represents a strong candidate to receive signals that lead to subcellular morphogenesis. After activation, it shows polarized localization to the cell body region that is dependent on membrane fusions mediated by the dysferlin FER-1. Our discovery of *snf-10* offers insight into the mechanisms differentially employed by the two sexes to accomplish the common goal of producing functional sperm, as well as how the physiology of nematode sperm may be regulated to control motility as it is in mammals.



## Introduction

A key feature of sexual reproduction is the generation of motile sperm cells capable of migrating to and fertilizing an oocyte. Upon transfer to a female, sperm become motile and then must further modulate their motility in response to local cues during transit through the reproductive tract (Bloch Qazi et al., 2003; Suarez, 2008). Thus, as for many other cell types that migrate during development, sperm motility is tightly and dynamically regulated in response to the external environment. However, unlike other cell types, sperm must accomplish these tasks without new protein synthesis. Instead they rely on interactions between soluble factors and cell surface receptors that trigger alterations in cellular physiology, ultimately leading to remodeling of cell structure and/or motility. In mammalian sperm, ion channel activity promotes several crucial steps in remodeling the internal and external properties of the sperm cell to render it competent for directional migration and fertilization; these include capacitation, the acrosome reaction, chemotaxis and acquisition of hyperactivated motility (Darszon et al., 2011; Lishko et al., 2011; Santi et al., 2013; Shukla et al., 2012). Sperm from other species must undergo analogous processes of maturation and are similarly dependent on signals from the extracellular milieu (Darszon et al., 2008; Santella et al., 2012).

In the nematode *Caenorhabditis elegans*, sperm lack flagella and instead move by crawling using a pseudopod (L'Hernault, 2006; Ward and Carrel, 1979). Both motility and fertilization competence are acquired during a process termed activation, during which the pseudopod is generated and proteins important for fertilization are displayed on the cell surface. Both sexes make sperm, and activation is regulated in sex-specific ways to ensure that sperm become motile only when and where it is appropriate. For hermaphrodites, it is advantageous to initiate self sperm motility rapidly after its production, thus ensuring functional sperm are available to fertilize oocytes. For males, sperm motility must be prevented during storage within the gonad; otherwise, when mating occurs, sperm transfer fails (Stanfield and Villeneuve, 2006). However, after transfer to a hermaphrodite, male sperm also need to become motile rapidly to migrate into the reproductive tract and avoid being swept out by

* Corresponding author.
*E-mail address:* gillians@genetics.utah.edu (G.M. Stanfield).

http://dx.doi.org/10.1016/j.ydbio.2014.06.001
0012-1606/

the outward passage of oocytes (Argon and Ward, 1980). Males accomplish this in part by including an activator(s) in seminal fluid, which is mixed with sperm during transfer (Shakes and Ward, 1989; Ward et al., 1983). The two sexes have distinct genetic requirements for sperm activation that facilitate these differential spatial and temporal requirements. In hermaphrodites, a set of sperm-specific proteins, the SPE-8 group, is required for self sperm activation, possibly in response to a zinc signal (L'Hernault et al., 1988; Liu et al., 2013). In males, the seminal fluid serine protease TRY-5 is a strong candidate to initiate activation (Smith and Stanfield, 2011), but sperm factors involved in this male-specific pathway have not been identified. Although male sperm do not normally require *spe-8* group function to activate via the male-specific pathway, they express these genes, and they can activate via the hermaphrodite pathway if the male activator is not present (LaMunyon and Ward, 1994; Smith and Stanfield, 2011). Likewise, if hermaphrodite sperm lack *spe-8* group function, they can "transactivate" in response to the male activator, which is transferred in seminal fluid during mating (Shakes and Ward, 1989). For both sexes, it is unclear how signals are transduced into changes in cellular morphology required for sperm function.

In this study, we report the identification of *snf-10* (*snf*, sodium: neurotransmitter transporter *f*amily) as a key regulator of sperm motility in *C. elegans*. SNF-10 is a member of the SLC6 (solute carrier 6) family of transporters, which couple the import of cargo such as amino acids, osmolytes, or monoamine neurotransmitters to the influx of sodium (Broer and Gether, 2012; Kristensen et al., 2011). SLC6 transporter activity is crucial for cellular function and homeostasis in diverse tissues, from neurons to the mammalian kidney, and mutations in human transporters are implicated in hereditary forms of intellectual disability and aminoaciduria, among other diseases (Pramod et al., 2013). In *Drosophila*, the SLC6 transporter Ntl (Neurotransmitter transporter-like) is required for spermiogenesis (Chatterjee et al., 2011). Here we show that *C. elegans* SNF-10 is required in sperm for activation by protease signals via the male-specific pathway. The localization of SNF-10 is regulated during activation and dependent in part on the dysferlin FER-1, providing a link between signaling and cellular morphogenesis.

## Materials and methods

### *Nematode growth and strains*

Unless indicated otherwise, *C. elegans* nematodes were grown at 20 °C on NGM (nematode growth medium) seeded with *Escherichia coli* strain OP50 (Brenner, 1974). The *him-5(e1490)* (Hodgkin et al., 1979) allele was present in all strains for which males were analyzed, including wild-type controls. Loss of *him-5* does not affect sperm activation, but leads to nondisjunction of the X chromosome, resulting in ~30% male offspring from self-fertilizing hermaphrodites and ensuring the presence of males in a strain. All strains were derived from Bristol N2 with the exception of the strain CB4856 used for mapping. Previously described alleles used in this work were *fer-1(hc1ts)*, *spe-8(hc40, hc53)*, *sem-4(n1378)*, *unc-13(e51)*, *ttTi5605*, *unc-119(ed3, ed9)*, *dpy-18(e364)*, *spe-6(hc163)*, *cxTi10816*, *spe-27(it110)*, *dpy-20(e1282)*, *spe-17(ok2593)*, *dpy-4(e1166)*, *dpy-11(e224)*, *swm-1(me66, me86, me87)*, *him-5(e1490)*, *unc-76(e911)*, *fog-2(q71)*, *nT1[unc(n754) let qIs50]*, *nT1[qIs51]*, *mIs11*.

For analysis of *spe-27; snf-10* double mutant hermaphrodites, Dumpy non-GFP-positive offspring were selected from *spe-27 dpy-20/nT1; snf-10 him-5/nT1[unc(n754) let qIs50]* mothers or control *spe-27 dpy-20/nT1; him-5/nT1[unc(n754) let qIs50]* mothers. For analysis of *spe-27; snf-10* double mutant males, Dumpy non-GFP-positive offspring were selected from crosses between *spe-27 dpy-20/nT1; snf-10 him-5/nT1[qIs51]* parents or control *spe-27 dpy-20/nT1; him-5/nT1[qIs51]* parents. For analysis of *spe-17* sperm expressing SNF-10::mCherry, GFP-negative male offspring were selected from crosses between *jnSi96[Psnf-10::SNF-10:mCh]; unc-119; spe-17/nT1; snf-10 him-5/nT1[qIs51]* parents.

### *Cloning of snf-10*

The allele *jn3* was shown to be linked to the *swm-1 him-5* region of chromosome V by the following data: *swm-1(me86) him-5; jn3* males were crossed to *dpy-11 swm-1(me86) him-5* hermaphrodites, non-Dumpy F1 hermaphrodites were selected and allowed to self-fertilize, and 40/40 F2 Dumpy male offspring were non-Activated. For fine mapping, *dpy-11(e224) swm-1(me86) snf-10(jn3) him-5(e1490) unc-76(e911)* hermaphrodites were crossed to CB4856 males, heterozygous F1 hermaphrodites were allowed to self-fertilize, and F2 Dpy non-Unc and Unc non-Dpy recombinant hermaphrodites were selected. Homozygous recombinants were isolated and scored for single-nucleotide polymorphisms using either restriction digest or sequencing. If the recombination breakpoint was potentially informative, the recombinant strain was crossed to *swm-1(me86) him-5* and *swm-1(me86) snf-10(jn3) him-5* strains to test for complementation with *swm-1* and *snf-10*. We thus iteratively identified a ~49 kb region between the polymorphisms WBVar00001560 and WBVar00001645 that contained *jn3* (Supplementary Fig. 1; Wormbase release WS240).

### *Molecular biology and generation of transgenic strains*

Standard procedures for molecular biology were used. RNA was isolated from mixed-stage *him-5(e1490)* worms using TRIzol (Life Technologies) and RNeasy (Qiagen). RACE (rapid amplification of cDNA ends) was performed using the GeneRacer system (Life Technologies) and RT-PCR was used to generate a full-length cDNA based on sequence data from RACE products.

For rescue experiments involving extrachromosomal arrays, a ~3.9 kb PCR fragment comprising the *snf-10* locus was amplified using the primers 5'-GGGTCCACGAGGTATAGAAGG-3' and 5'-CGGGAATTTCAATCGAGAAG-3'. This fragment was mixed with *Psur-5::gfp* plasmid (Yochem et al., 1998) at 75–100 ng/μl each and injected into *swm-1(me86) snf-10(jn4) him-5(e1490)* hermaphrodites (Mello et al., 1991). Independent lines were founded from individual transgenic F1 hermaphrodites.

Single-copy transgenic strains were generated using MosSCI (Frokjaer-Jensen et al., 2012; Frokjaer-Jensen et al., 2008). *snf-10* constructs were generated in the pCFJ150 vector using Gateway cloning (Life Technologies) and injected into *ttTi5605; unc-119* hermaphrodites. Details of primers used to generate expression constructs are available upon request.

### *Fertility and sperm competition*

To measure hermaphrodite fertility, single L4 hermaphrodites were placed on plates and transferred daily until eggs were no longer produced. To measure male fertility, L4 males were placed with either *spe-8(hc40); dpy-4(e1166)* or *fog-2(q71)* L4 hermaphrodites in 1:1 crosses (i.e., one male was placed with one hermaphrodite) for 48 h; males were then removed and hermaphrodites were transferred daily. *spe-8* hermaphrodites allow for detection of mating in all cases where seminal fluid is transferred, even if sperm are not functional (Shakes and Ward, 1989), and *fog-2(q71)* hermaphrodites lack sperm and thus are essentially female (Schedl and Kimble, 1988). To assay sperm competition, L4 males were placed with L4 *dpy-4(e1166)* hermaphrodites in 1:1 crosses for 24 h, males were removed, and hermaphrodites were transferred to new plates daily until egg laying ceased. For all fertility assays, non-Dumpy cross progeny and/or Dumpy self progeny were counted after reaching at least the L4 stage. Only broods for which hermaphrodites survived for at least four days were

included in analyses. For these and other assays involving measurements of progeny, sperm migration, or mating, assays for control strains were done in parallel, assay data were compared among matched samples to control for variation in factors such as temperature and media quality, and each experiment was repeated 2–4 times.

*Transactivation*

To assay transactivation by males, *fer-1* or *fer-1; snf-10* L4 males raised at 25 °C were placed with L4 *spe-8(hc53); dpy-4(e1166)* hermaphrodites in 1:1 crosses for 48 h at 25 °C. After the mating period, adults were removed, progeny were allowed to develop until at least the L4 stage, and Dumpy self progeny were counted. Only matings lacking non-Dumpy (cross) progeny were included in analysis. To assay the ability of hermaphrodite sperm to transactivate, *swm-1(me87) him-5(e1490); mIs11* males were placed with *spe-27 dpy-20; him-5* or *spe-27 dpy-20; snf-10 him-5* hermaphrodites in 1:1 crosses for 48 h; progeny counts and analyses were performed as for the male assays.

*Sperm migration and mating frequency*

Sperm transfer and migration rates were assayed in 1:1 crosses between MitoTracker-labeled males and *spe-8(hc40); dpy-4(e1166)* hermaphrodites as described in Stanfield (2006). For infertile male strains, mating frequency was assessed by placing MitoTracker (Life Technologies) labeled males with *sem-4 unc-13* or *fog-2* hermaphrodites for 5 h and scoring for sperm transfer as described by Smith and Stanfield (2011).

*Sperm activation assays*

The activation state of individual sperm cells was scored based on the absence or presence of a pseudopod visible by DIC microscopy. To measure the frequency of sperm activation within the male gonad, L4 males were isolated from hermaphrodites and scored 48 h later for the presence of activated or non-activated sperm within the seminal vesicle. Males were considered non-activated if 100% of sperm lacked a pseudopod, fully activated if fewer than 1% of cells lacked a pseudopod, and partially-activated at intermediate frequencies.

Assays of *in vitro* activation were performed essentially as described by Shakes and Ward (1989). Virgin 24–48 h post-L4 males were dissected in Sperm Medium (SM) containing 5 mM HEPES pH7.0 or 7.4, 50 mM NaCl, 25 mM KCl, 5 mM $CaCl_2$, 1 mM $MgSO_4$, and 10 mM dextrose. Additional medium with (SM+) or without (SM−) activator was added to the cells and images were collected every 3–5 min for 24–42 min. For each activator, wild-type controls and controls lacking activator were performed in parallel for each repeat, at least two slides were examined for each condition per experiment, and each experiment was repeated at least three times. Essentially no activation was ever observed on SM- slides. Between 42 and 181 cells were examined on each slide. Concentrations of activators used were: pronase, 200 μg/μL; triethanolamine (TEA), 60 mM; monensin, $5 \times 10^{-7}$ M; 4,4'-diisothiocyano-2,2'-stilbenedisulfonic acid (DIDS), 0.4 mM; $ZnCl_2$, 1 mM.

*Immunocytochemistry*

Sperm from 1–2 day post-L4 virgin males was dissected into SM onto Colorfrost Plus slides (Fisher). Fixation was performed by a freeze-crack procedure followed by immersion in ice-cold methanol for 15 min (Gleason et al., 2012). Washes were performed in PBS pH 7.2 with 0.1% Tween 20 (PBSTw). Blocking (30 min) and antibody incubations (2 h each) were performed in PBSTw with 1% BSA. Antibodies used were: 1CB4 anti-MO monoclonal at 1:500 (Arduengo et al., 1998; Okamoto and Thomson, 1985), rabbit anti-RFP at 1:1000 (Rockland #600-401-379), Alexa Fluor 568 goat anti-rabbit IgG at 1:500 and Alexa Fluor 488 goat anti-mouse IgG at 1:200–1:500 (Life Technologies).

## Results

*The SLC6 family transporter SNF-10 is required for sperm activation in swm-1 mutant males*

Males with a mutation in the protease inhibitor gene *swm-1* show premature sperm activation in the absence of an opportunity to mate. We took advantage of this ectopic sperm activation phenotype of *swm-1* mutant males to perform suppressor screens searching for genes that promote sperm activation caused by protease signaling (Smith and Stanfield, 2011; Stanfield and Villeneuve, 2006 and data not shown). In wild-type males, sperm are stored in the seminal vesicle in the form of non-activated, round spermatids (Fig. 1A). In *swm-1* mutants, male sperm become prematurely activated prior to sperm transfer (Fig. 1B), leading to infertility. We mutagenized strains carrying a mutation in *swm-1* as well as in *him-5* to ensure the presence of males (Hodgkin et al., 1979), screened visually for males containing non-activated sperm, and isolated strains harboring suppressor mutations. One complementation group comprised four strong suppressors (*jn1*, *jn3*, *jn4*, *jn20*), for which nearly all *swm-1; suppressor* double mutant males showed a non-activated, wild-type phenotype (Fig. 1E). All these mutations were recessive and mutant animals exhibited no obvious phenotypic defects apart from suppression of *swm-1* (data not shown).

To identify the gene affected in these suppressor strains, we performed meiotic mapping of the *jn3* suppressor mutation against the polymorphic Hawaiian strain CB4856 and localized *jn3* to a 49 kb region of chromosome V (Material and methods, Supplementary Fig. 1). Within this region, one gene, *snf-10*, had been shown previously to have sperm-enriched expression (Reinke et al., 2004; Reinke et al., 2000). We determined the sequence of *snf-10* in the four non-complementing mutant strains and identified specific lesions in each of them (Fig. 1F). Additionally, we obtained a *snf-10* deletion allele, *hc194* (gift of Harold Smith), and constructed a *snf-10(hc194) swm-1(me87)* double mutant strain to test for suppression of the null Swm-1 sperm activation phenotype. We found that *hc194* males appeared wild-type and showed full suppression of this allele of *swm-1* in assays of both sperm activation and male fertility (Fig. 1C, D, G and H). To confirm that *snf-10* was the affected gene, we introduced *snf-10* transgenes into *swm-1 snf-10* animals and scored sperm activation in males. Males harboring transgenes containing a ~3.9 kb region encompassing the *snf-10* coding sequence showed strong rescue of sperm activation (Material and methods; Fig. 1I). Thus, function of the *snf-10* gene is required for sperm activation resulting from misregulation of protease activity in *C. elegans* males.

*snf-10* encodes a member of the SLC6 family of sodium- and sometimes chloride-dependent transporters (Beuming et al., 2008; Broer and Gether, 2012; Pramod et al., 2013). In mammals, SLC6 transporters are functionally important in a variety of tissues, including the nervous system and kidney, and their loss is implicated in a number of inherited human diseases including Hartnup disease, hyperekplexia, and X-linked intellectual disability. The best-characterized family members reside on the plasma membrane and function to import specific cargo into cells. Different family members transport cargo such as amino acids, neurotransmitters, or osmolytes, and this activity is coupled to symport of sodium ions, as well as chloride in some cases. A high-resolution structure has been determined for a prokaryotic SLC6 leucine transporter, LeuT (Yamashita et al., 2005), which has

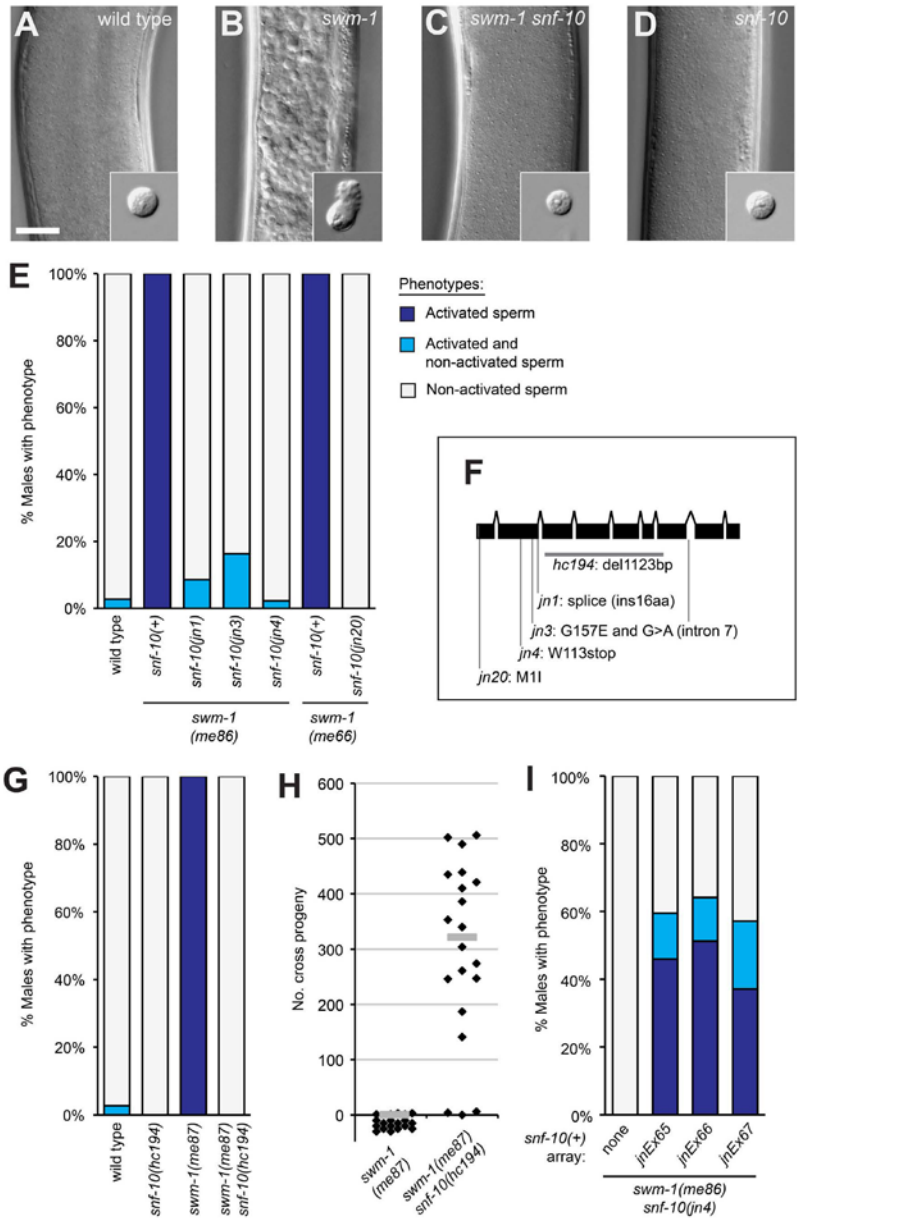


**Fig. 1.** Suppressor mutations prevent early sperm activation and loss of fertility caused by loss of *swm-1* in males. (A–D) Images of seminal vesicles and dissected sperm (insets) from 48 h post-L4 males. Genotypes shown: (A) wild type (B) *swm-1(me87)* (C) *swm-1(me87) snf-10(hc194)*, and (D) *snf-10(hc194)*. All strains also contained *him-5(e1490)*. Scale bar, 20 μm. (E) Quantitation of suppression of *swm-1* sperm activation by mutations in *snf-10*. For this and other whole-worm activation data, column shading indicates the percent of males containing only activated sperm (dark blue), a mixture of spermatids and activated sperm (light blue), or only non-activated sperm (gray). n, 34–74. (F) Gene model diagram for *snf-10* showing the locations of mutant alleles isolated in the screen and the deletion *hc194*. The *jn1* allele alters the splice donor of the second intron and is expected to result in an insertion of 16 amino acids (YLSEPNFSFFQNPQFR) between Arg169 and Thr170. The *jn3* strain harbors two mutations, a missense change and a G to A change within intron 7 that is predicted to be silent. (G) Quantitation of suppression of the sperm activation phenotype of the null *swm-1(me87)* allele by the *snf-10* deletion *hc194*. n, 31–74. (H) Male fertility is restored in a *swm-1 snf-10* double mutant. Each point represents the total cross-progeny (non-Dumpy) brood of a single mated *spe-8; dpy-4* hermaphrodite; bars represent medians. To permit depiction of all data points, some "0" data points are shown below the *X* axis. (I) Rescue of the sperm activation phenotype of *snf-10* in three strains carrying independently-derived extrachromosomal arrays. Categories for stacked column as in Fig. 1E; n, 32–39.

facilitated biochemical analyses of transport and conductance activities of eukaryotic family members (reviewed in Kristensen et al., 2011). Eukaryotic SLC6 proteins contain 12 transmembrane (TM) spanning regions, of which TM1-5 and TM6-10 subdomains show two-fold symmetry across the membrane and together compose the channel. Regions surrounding TM1, TM3, TM6 and TM8 are the most conserved among family members and are involved in substrate and sodium binding, as well as a number of highly conserved gating interactions.

Although clearly a member of the SLC6 family, SNF-10 is divergent by several criteria. SNF-10 is well-conserved in related *Caenorhabditis* nematodes, but we could not identify a clear ortholog from more distant species (data not shown). When compared against all family members, SNF-10 clusters with other SLC6 proteins from *C. elegans* but does not show particularly strong similarity to any specific SLC6 protein from mammals (Boudko, 2012 and data not shown). While the overall sequence of SNF-10 shows closest similarity to glycine transporters (*e.g.*, it shares 58% similarity with human SLC6A5/GlyT2), its substrate-binding residues are not well-conserved with any SLC6 transporter with a known cargo (Supplementary Fig. 2). In addition, residues directly implicated in sodium passage are divergent in SNF-10. Thus, SNF-10 falls within the orphan class of this large transporter family.

### *snf-10 is not required for fertility or sperm competition*

Since *snf-10* is required for the ectopic sperm activation that occurs in *swm-1* mutant males, we reasoned that *snf-10* might be required generally for males and/or hermaphrodites to activate their sperm. Sperm motility is required for fertility, as non-activated sperm cannot maintain their position within the female reproductive tract and are incompetent for fertilization, so we assayed fertility as a proxy to measure activation. To assess male fertility, we measured cross progeny produced by wild-type and *snf-10(hc194)* mutant males in crosses to *spe-8; dpy-4* hermaphrodites. *snf-10* mutant males were highly fertile and showed minor, if any, defects in progeny production (Fig. 2A). Thus, *snf-10* male sperm are transferred, become activated, and fertilize oocytes at essentially normal levels. To assess hermaphrodite fertility, we counted progeny generated by self-fertilizing hermaphrodites. In *C. elegans*, virtually 100% of the self sperm generated during development go on to fertilize an egg, so measurement of self progeny is equivalent to quantitation of functional sperm. We found that *snf-10(hc194)* hermaphrodite brood sizes were only slightly reduced relative to those of wild-type controls, essentially within the variability observed for typical wild-type strains (Fig. 2B and data not shown). Thus, *snf-10* is dispensable for fertility in both males and hermaphrodites, consistent with involvement in the male-specific pathway for sperm activation (Smith and Stanfield, 2011).

While motility is generally required for sperm function, males transfer large numbers of sperm and can be highly fertile even if a subset of cells is defective. However, assays of competition can reveal more subtle defects. We thus took advantage of the male-hermaphrodite mode of reproduction in *C. elegans* to further evaluate *snf-10* sperm function and determine their success in a competitive situation. In wild-type *C. elegans*, male sperm show strong preferential usage as compared to hermaphrodite sperm. After male sperm are transferred, the fraction of offspring sired by male sperm rises rapidly and often reaches close to 100% (LaMunyon and Ward, 1995). If loss of *snf-10* reduced activation, this male precedence effect might be reduced or delayed. To test this possibility, we performed crosses of *snf-10(hc194)* and wild-type males to *dpy-4* recipient hermaphrodites and measured production of both cross and self progeny over time. We found that as compared to the wild type, *snf-10* mutant males showed an equivalent level of early success, as measured by preferential generation of cross progeny (Fig. 2C), indicating that *snf-10* male sperm activate rapidly and then show normal precedence over hermaphrodite self sperm. However, at later time points, cross-progeny production was slightly decreased. Visual inspection of sperm transfer and migration using MitoTracker-labeled males failed to reveal any obvious differences between *snf-10* and wild-type males (data not shown), suggesting that *snf-10* males transfer a normal number of sperm, which activate rapidly and crawl to the spermathecae. It is possible that *snf-10* sperm have reduced long-term viability as compared to the wild type. Regardless of these minor defects, the fertility and competition data indicate that *snf-10* sperm are highly competent to activate, migrate, and fertilize oocytes.

### *snf-10 is not required for the production or transfer of male activator*

A sperm activator is transferred from males to hermaphrodites during mating (Ward and Carrel, 1979). Previous analyses of suppressors of *swm-1* identified TRY-5, a seminal fluid protease that likely functions as the male activator (Smith and Stanfield, 2011). One possibility for *snf-10* function was that it might be required for production and/or transfer of the male activator. As a specific assay for the male activator, males that fail to transfer functional sperm, but do transfer seminal fluid (*e.g.*, a *fer-1* mutant), can be crossed to *spe-8* mutant hermaphrodites, whose sperm are defective for response to hermaphrodite activator, but not the male one. Self progeny, which arise from "transactivation" of hermaphrodite sperm by male seminal fluid, are then counted (Shakes and Ward, 1989). To assay transactivation by *snf-10* males, we crossed *fer-1; snf-10* or *fer-1* control males to *spe-8; dpy-4* hermaphrodites and measured induction of Dumpy self progeny after mating. There was no statistical difference between transactivation levels caused by males mutant for *snf-10* as compared to wild-type (Fig. 2D). In addition, we looked directly at the pattern of TRY-5 expression and localization in animals mutant for *snf-10*. In wild-type animals, TRY-5::GFP is expressed within the male somatic gonad in cells of the seminal vesicle, valve and vas deferens, where it localizes to large vesicle-like structures; this pattern is unchanged in *snf-10* mutant males (Smith and Stanfield, 2011 and data not shown). These data indicate that *snf-10* is not required for production or transfer of male activator but rather functions in a downstream step of activation.

### *snf-10 functions cell-autonomously in sperm to promote sperm activation*

To address how SNF-10 regulates sperm activation, we sought to determine in which cells SNF-10 functions. *snf-10* was previously reported to show sperm-enriched expression in genome-wide expression analyses (Reinke et al., 2004; Reinke et al., 2000). To determine whether SNF-10 indeed functions in sperm, we performed tissue-specific rescue and inactivation experiments. First, we generated animals expressing the SNF-10 protein under the control of the sperm-specific *peel-1* promoter (Seidel et al., 2011) and assayed for rescue of sperm activation in *swm-1(me87) snf-10(hc194)* males. Expression of SNF-10 in sperm fully restored the Swm-1 ectopic sperm activation phenotype, equivalent to expression using the *snf-10* promoter (Fig. 3A). Importantly, *swm-1(+)* animals carrying *snf-10* transgenes contained non-activated sperm, indicating that the activation observed in the *swm-1* mutant background represented rescue of *snf-10* rather than a gain-of-function effect. To confirm that *snf-10* function is required in sperm, we performed germ line-specific RNAi of *snf-10*, using a mutation in *rrf-1* to reduce RNAi efficacy in somatic tissues (Kumsta and Hansen, 2012; Sijen et al., 2001). When fed *snf-10* RNAi bacteria, both *swm-1* and *rrf-1; swm-1* males showed equivalent levels of suppression of the Swm-1 sperm activation phenotype, consistent with strong reduction of *snf-10* function in both genotypes (Supplementary Fig. 3). Thus, activity of *snf-10* in the germ line is both sufficient and necessary to promote sperm activation in males.

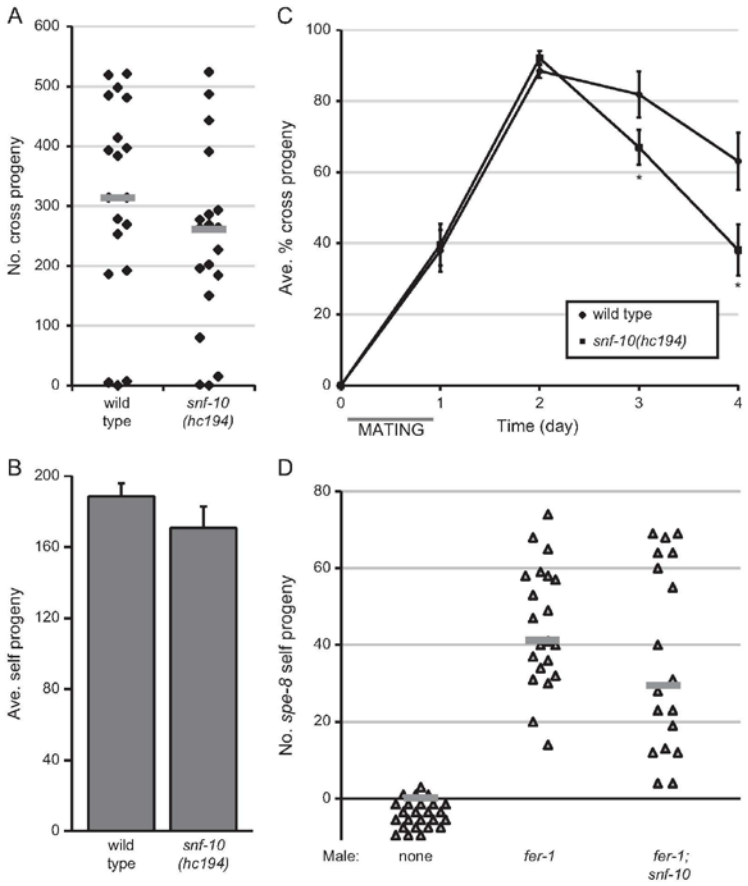


**Fig. 2.** *snf-10* is not required for sperm function or for transfer of male activator. (A) *snf-10* mutant males showed no significant decrease in fertility as compared to the wild type ($P > 0.05$, Kolmogorov–Smirnov test). Each point represents the total cross-progeny brood of a single *spe-8; dpy-4* hermaphrodite; bars represent medians. (B) *snf-10* hermaphrodite brood sizes were indistinguishable from those of the wild type ($P > 0.05$, Student's *t* test; error bars, standard error of the mean). (C) *snf-10* males show a normal competitive advantage in crosses to self-fertile *dpy-4* hermaphrodites at early time points, but long-term success is decreased as compared to wild-type males. Error bars, 95% confidence intervals; $^*P < 0.05$, Kolmogorov–Smirnov test. (D) Transactivation by *snf-10* mutant males. Each point represents self progeny generated by an individual *spe-8; dpy-4* hermaphrodite after crossing to the indicated male strain; bars represent medians. No significant difference between *fer-1* and *fer-1; snf-10* was detected ($P > 0.05$, Kolmogorov–Smirnov test).

### *SNF-10 localizes to the sperm plasma membrane and is polarized to the cell body of mature spermatozoa*

To examine *snf-10* expression and protein localization within the germ line, we generated transgenic animals expressing *snf-10* reporters under the control of the genomic region sufficient for rescue activity. To identify cells expressing *snf-10*, we used transcriptional *Psnf-10::htas-1::mCh* (mCherry) and *Psnf-10::GFP::H2B* (histone H2B) reporters with fluorescent proteins targeted to sperm chromatin (Chu et al., 2006; Merritt et al., 2008). Expression was visible in the male and hermaphrodite germ line in cells undergoing differentiation into spermatocytes as well as at later stages of spermatogenesis (Supplementary Fig. 4 and data not shown). No fluorescence was visible in somatic tissues, in the mitotic or meiotic-prophase regions of the germ line, or in germline cells developing into oocytes.

To determine where in sperm the SNF-10 protein localizes, we examined *Psnf-10::SNF-10::mCh* worms expressing full-length SNF-10 fused to mCherry. Use of either the *snf-10* genomic coding region or a *snf-10* cDNA was sufficient for rescue of the sperm activation phenotype of *swm-1 snf-10* mutant males (Fig. 3A and data not shown), indicating that the fusion protein was functional. *C. elegans* sperm show a stereotypical arrangement of cell structures (L'Hernault, 2006) (shown in Fig. 3B). Non-activated spermatids are spherical and contain a central chromatin mass surrounded by mitochondria; the sperm-specific membranous organelles (MOs) reside adjacent to the

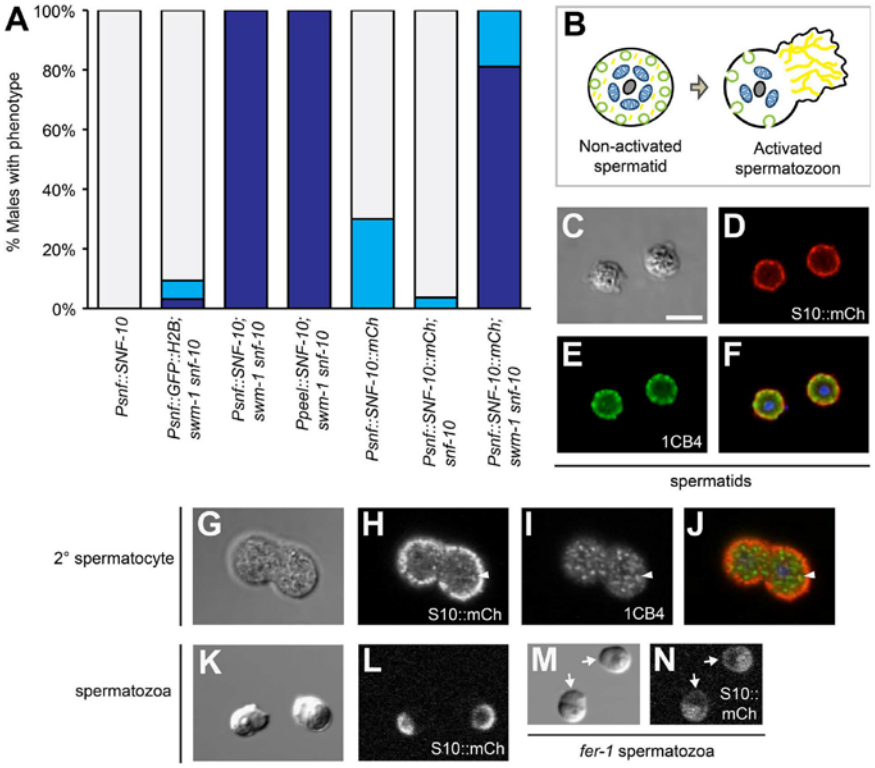


**Fig. 3.** *snf-10* is expressed in and functions in sperm. (A) Rescue of the sperm activation phenotype by *snf-10* transgenes. Either a *snf-10* or sperm-specific *peel-1* promoter can confer rescue, as can expression of SNF-10::mCherry reporter protein. As in Fig. 1E, column shading indicates the percent of males containing only activated sperm (dark blue), a mixture of spermatids and activated sperm (light blue), or only non-activated sperm (gray); n, 30–55. (B) Schematic of spermatid and spermatozoon structure. Gray, chromatin; blue, mitochondria; green, MOs; yellow, MSP cytoskeleton. (C–J) In *jnSi96[Psnf-10::SNF-10::mCh]* spermatids, SNF-10::mCh and 1CB4 are both localized primarily to the cell periphery; some concentrations of mCh and 1CB4 are clearly distinct from one another. In 2° spermatocytes, most mCh is on the cell cortex and fails to colocalize with 1CB4, but some cytoplasmic puncta are visible. Arrowhead indicates a region of overlap between mCh and 1CB4. Images are fixed cells visualized by (C and G) DIC, (D and H) anti-RFP staining, (E and I) 1CB4 staining, and (F and J) a merge of anti-RFP, 1CB4, and DAPI. (K-N) SNF-10::mCh is polarized to the cell body plasma membrane in activated spermatozoa, but distributed throughout the plasma membrane in a *fer-1* mutant. Live sperm were visualized by (K and M) DIC and (L and N) mCherry fluorescence. Arrows indicate SNF-10::mCh in *fer-1* pseudopodia. (A-N) All strains were mutant for *unc-119* and *him-5*, as well as *snf-10(hc194)*, except as indicated in (A). (M and N) Worms were raised at 25 °C, the non-permissive temperature for *fer-1(hc1)*. Scale bar for all images, 5 microns.

plasma membrane. In activated, polarized spermatozoa, the cell body retains the nucleus, mitochondria, and MO fusion sites while the pseudopod contains the network of MSP filaments that power cell movement. We found that in spermatids, SNF-10::mCh was primarily localized to the cell cortex, with brighter concentrations in some regions, as well as in occasional puncta deeper within the cell (Fig. 3C and D; Supplementary Fig. 5A and B and data not shown). Due to the close apposition of MOs and the plasma membrane in spermatids, it is difficult to distinguish between them by conventional fluorescence microscopy, so this cortical localization could indicate the presence of SNF-10 on the plasma membrane, the MOs, or both. Thus we performed additional experiments to distinguish between these cellular compartments. First, we performed coincident imaging of SNF-10::mCh with two different MO markers, the monoclonal antibody 1CB4 (Okamoto and Thomson, 1985) and PEEL-1::GFP (Seidel et al., 2011). We found that while the SNF-10::mCh and 1CB4 signals were very close and potentially overlapping, the areas of high cortical SNF-10 concentration were often distinct from MO puncta (Fig. 3C and F). Similarly, in live cells, SNF-10::mCherry was peripheral to PEEL-1::GFP (Supplementary Fig. 5A–D). Second, we examined SNF-10 localization in situations where MOs are located farther from the plasma membrane. In cells at earlier stages of spermatogenesis, MOs are distributed throughout the cytoplasm, and they move to abut the plasma membrane after the meiotic divisions (L'Hernault, 2006). In secondary spermatocytes and immature spermatids, the majority of SNF-10 was localized to the cell cortex as at later stages, and this pattern was largely distinct from that of 1CB4; occasional cytoplasmic puncta appeared to show overlap (Fig. 3G–J and data not shown). We also examined *spe-17* mutant spermatids, which contain MOs and other organelles asymmetrically mislocalized within the cytoplasm (L'Hernault et al., 1993). In *spe-17* spermatids, SNF-10::mCh was present not only on the cell cortex but also in asymmetric, bright cytoplasmic foci, suggesting that some SNF-10 is indeed present on MOs, though it is also possible that SNF-10 is mislocalized in this

mutant (Supplementary Fig. 5E and F). Taken together, these data suggest that in spermatids, the majority of SNF-10 is present in the plasma membrane, but we cannot exclude the possibility that at least a portion may localize to MOs as well.

In activated spermatozoa, SNF-10::mCh became restricted to the cell body region of the plasma membrane and was absent from the pseudopod (Fig. 3K and L). In many cells, brighter cortical puncta were visible. These concentrations likely corresponded to the sites of fused MOs, as activated sperm retain stable invaginations at these sites that show elevated staining with plasma membrane markers, including dyes such as FM1-43, due to the increased concentration of membrane there (Washington and Ward, 2006 and data not shown). We sought to determine whether SNF-10::mCh localization would be altered in the mutant *fer-1*, in which MOs associate with the plasma membrane but fail to fuse with it during activation (Ward and Miwa, 1978; Washington and Ward, 2006). We found that in activated *fer-1* sperm, SNF-10::mCh was visible not only in cortical and intracellular puncta of the cell body but also on the pseudopod plasma membrane, from which it is normally excluded (Fig. 3M and N). Thus, SNF-10 shows a restricted localization in spermatozoa, which is dependent on either FER-1 or some other protein that is absent from the cell surface when MOs fail to fuse.

### *snf-10 is required for sperm to respond to the male protease activator*

To understand how SNF-10 promotes sperm activation, we next sought to distinguish between a role in the "male" pathway downstream of protease signaling or a role in the "hermaphrodite" pathway, which requires *spe-8* group activity and can be triggered by extracellular zinc (Liu et al., 2013). Loss of the hermaphrodite pathway is sufficient to result in hermaphrodite self sterility, though males are fertile (L'Hernault et al., 1988); the activity of both pathways must be lost to result in male sterility (Smith and Stanfield, 2011). Our *swm-1* suppression screen could identify factors in either pathway, as loss of either leads to reduced activation of male sperm (Stanfield and Villeneuve, 2006 and G.M.S., unpublished results). However, *spe-8* group; *swm-1* double mutants show a characteristic "spiky" morphology associated with partial activation (Shakes and Ward, 1989; Stanfield and Villeneuve, 2006), so our finding that *swm-1 snf-10* double mutants show no sign of activation suggested *snf-10* was in the male pathway. To test this explicitly, we assayed fertility in double mutants lacking the activity of both *snf-10* and either *try-5* or *spe-8* group function. First, we generated *try-5(tm3813) snf-10(hc194)* double mutant males. Their fertility was at least as high as that of either single mutant and indistinguishable from that of wild-type worms (Fig. 4A).

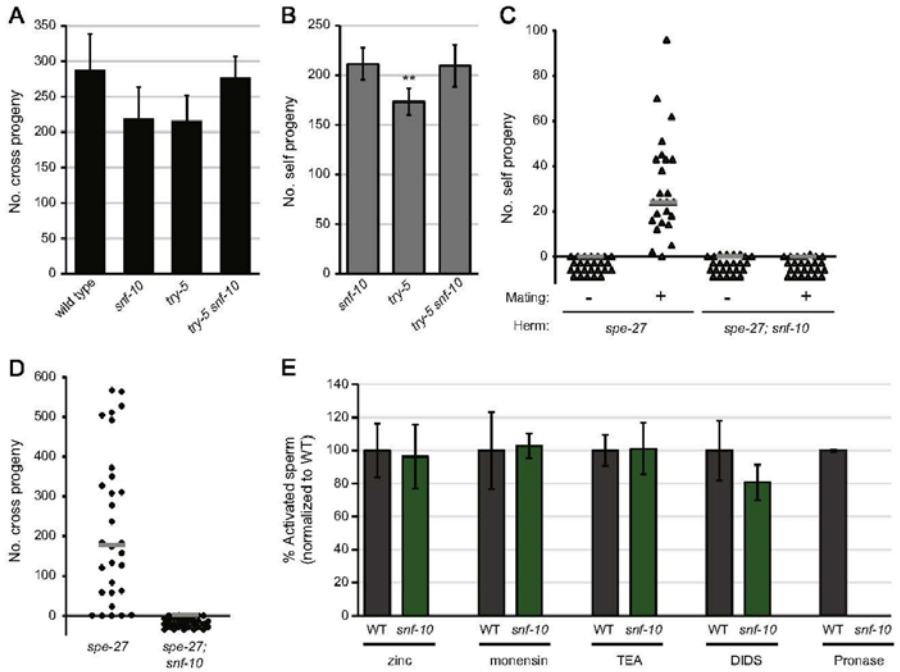


**Fig. 4.** *snf-10* functions in the male sperm activation pathway downstream of the protease activator. (A) *try-5 snf-10* double mutant males show levels of fertility indistinguishable from those of the wild type or single mutants ($P > 0.05$, Kolmogorov–Smirnov test). The indicated males were crossed to *spe-8; dpy-4* hermaphrodites and total offspring were counted. Error bars, 95% confidence intervals. (B) *try-5 snf-10* double mutant hermaphrodites show no reduction in fertility relative to single mutants. Note that the *try-5* strain showed slightly reduced fertility in this experiment ($P < 0.01$, Kolmogorov–Smirnov test). (C) *spe-27; snf-10* double mutant hermaphrodite sperm are unresponsive to transactivation, in contrast to *spe-27* hermaphrodites whose self fertility is rescued after transfer of male seminal fluid. The symbol "−" designates controls in which no males were present (hermaphrodites were allowed to self-fertilize); "+" indicates that *swm-1* males were present (transactivation conditions). (D) *spe-27; snf-10* double mutant males are completely infertile. The indicated males were crossed to *fog-2* hermaphrodites for 48 h and total offspring were counted. (C and D) Bars represent medians. (E) *snf-10* mutant sperm are resistant to *in vitro* activation by Pronase, but respond normally to other activators. Wild-type (WT) or *snf-10(hc194)* spermatids were dissected from males and incubated in activators as indicated. Graph shows percent of activated cells normalized to that observed in wild-type for each experiment. Error bars, 95% confidence intervals.

*try-5 snf-10* hermaphrodites were also fully fertile (Fig. 4B). We then generated animals doubly mutant for both *snf-10* and the *spe-8* group gene *spe-27*. *spe-27(it110); snf-10(hc194)* hermaphrodites were self-sterile, as expected due to the *spe-27* mutation. To assay response to male activator, we performed transactivation assays by crossing these hermaphrodites to *swm-1* mutant males, which are defective for sperm transfer but competent for seminal fluid transfer (Stanfield and Villeneuve, 2006 and data not shown). We found that *spe-27; snf-10* double mutant hermaphrodite sperm were incapable of transactivation (Fig. 4C). In addition, *spe-27; snf-10* males were completely sterile in crosses to *fog-2* "females" (Fig. 4D). We confirmed that *spe-27; snf-10* males were capable of mating and transferring sperm by staining them with MitoTracker dye and assaying transfer of labeled sperm after a 5 h mating period. While the frequency of sperm transfer for *spe-27; snf-10* males was at least as high as that for the control (37/59 or 63% transferred sperm, as compared to 30/56 or 54% for *spe-27*), double mutant sperm were never observed to migrate towards the spermathecae (data not shown), consistent with failure to activate. Thus, loss of both *snf-10* and *spe-8* group activities results in profound sterility in both sexes, suggesting that all pathways to activation are blocked.

To further place *snf-10* in the male pathway for sperm activation, we sought to distinguish between a role in the response of sperm to extracellular signals or a role in more downstream events. While sperm normally activate in response to extracellular cues, mutations in genes involved in spermatogenesis can lead to signal-independent activation (Liau et al., 2013; Muhlrad and Ward, 2002). In particular, certain alleles of the casein kinase 1 gene *spe-6* or other genes in this class suppress the sterility of *spe-8* group mutants and lead to ectopic sperm activation within males. To determine whether *snf-10* is required for this activation, we examined males mutant for both *snf-10* and the activating mutation *spe-6(hc163)*. *spe-6; snf-10* double mutants showed a fully-activated phenotype indistinguishable from that of *spe-6* males (Table 1). Thus, *snf-10* likely functions in the response of sperm to activator.

### *snf-10 is required for in vitro activation by proteases*

The presence of SNF-10 in sperm suggests a role in reception or transduction of the activation signal. Little is known about how extracellular signals result in the morphological changes that occur during activation. However, sperm can be activated *in vitro* by a variety of different compounds that presumably alter cell physiology in ways that mimic or otherwise feed into the normal *in vivo* pathways (Liu et al., 2013; Machaca et al., 1996; Nelson and Ward, 1980; Shakes and Ward, 1989; Ward et al., 1983). To probe the mechanism by which SNF-10 promotes sperm activation, we sought to determine whether its activity was required for response to these activators. Most activators were fully effective on *snf-10(hc194)* mutant sperm (Fig. 4D). Treatment of *snf-10* sperm with zinc, which is thought to activate sperm via the hermaphrodite pathway (Liu et al., 2013), resulted in normal levels of activation as compared to the wild type. We observed similar results with the sodium-selective ionophore monensin and the weak base TEA, both of which lead to alkalinization of sperm cytoplasm (Ward et al., 1983). *snf-10* mutant sperm also activated normally with DIDS (4,4'-diisothiocyano-2,2'-stilbenedisulfonic acid), a chloride channel blocker that has been shown to activate sperm with similar dose dependence as seen for inhibition of a spermatid Clr channel activity (Machaca et al., 1996). Thus, all of these activators apparently bypass SNF-10's function in sperm activation. However, *snf-10(hc194)* mutant sperm failed to activate in Pronase, a mixture of protease activities that are thought to mimic the male activator (Smith and Stanfield, 2011). Wild-type sperm activate rapidly to high levels (often >95%) when incubated in Pronase, but even when *snf-10* cells were subjected to extended treatment (42 min, over twice as long as normally required), almost no activation was observed. Furthermore, Pronase-treated *snf-10* spermatids remained spherical and lacked any signs of spiking or other cytoskeletal extensions. To assess whether MO fusions might still occur in the absence of other morphological rearrangements, we incubated spermatids in the vital membrane dye FM1-43 during Pronase treatment, but observed no fusion events in *snf-10* mutant spermatids (0/268 *snf-10* cells showed one or more fusions after 15 min, as compared to 169/198 wild-type cells). Therefore, the results of both our genetic analysis and *in vitro* assays indicate that SNF-10 functions specifically in the male pathway and is required downstream of TRY-5 for sperm to respond to protease sperm activation signals.

**Table 1**
*snf-10* is not required for activation in *spe-6* animals.

| Genotype[a] | % Act[b] | *n* |
|---|---|---|
| Wild type | 2.8 | 36 |
| *spe-6(hc163)* | 100 | 38 |
| *snf-10(hc194)* | 2.1 | 47 |
| *spe-6(hc163); snf-10(hc194)* | 100 | 38 |

[a] All strains also contained the mutations *dpy-18(e364)* and *him-5(e1490)*.
[b] Percent of 48 h post-L4 males containing activated sperm.

## Discussion

Like flagellate sperm, the ameboid sperm of *C. elegans* and other nematodes require motility to migrate to and fertilize an oocyte. Successful sperm motility requires both execution of a complex differentiation program during cellular development as well as appropriate responses to environmental cues encountered during the migration process. In *C. elegans*, the regulation of sperm motility is further influenced by its male-hermaphrodite mode of reproduction. As a result, *C. elegans* harbors a surprisingly complex network of factors that control the activation of sperm to a motile state. Males and hermaphrodites utilize sex-biased but redundant pathways to ensure that their sperm become motile in the correct time and place to promote reproductive success. In this study, we describe a role for an SLC6 family transporter, SNF-10, in *C. elegans* sperm activation. SNF-10 is required for sperm to respond to protease signaling for activation via the male-specific pathway. However, it is completely dispensable in hermaphrodites as well as in most known physiological activation assays *in vitro*. SNF-10 functions in sperm and localizes to the plasma membrane, placing it in a prime position to transduce signals from extracellular protease activity to effect subcellular morphogenesis.

The SLC6 transporters (also known as NTT for neurotransmitter transporters, NSS for neurotransmitter sodium symporters, or NAT for nutrient amino acid transporters) are members of the larger superfamily of APC (amino acid–polyamine–organocation) transporters (Vangelatos et al., 2009), which comprises several protein families with similar structure but unrelated primary sequence. Characterized SLC6 family transporters couple the import of molecules such as amino acids, monoamine neurotransmitters, or osmolytes to the import of sodium and often chloride ions. However, channel activity uncoupled from cargo movement also has been observed (DeFelice and Goswami, 2007). Much focus has been on the monoamine transporters, taking advantage of pharmacological approaches to analyze transport activity and its regulation by trafficking, post-translational modifications, and interactions with other proteins (Broer and Gether, 2012).

Is SNF-10 an active transporter, and if so then what is its cargo? In keeping with its function in reproduction, SNF-10 is a relatively divergent member of the SLC6 family. Its substrate-binding region is not well conserved, making it difficult to predict specificity. In addition, none of the typical molecules transported by SLC6

proteins are present in the sperm medium used for *in vitro* activation studies, suggesting that such a cargo is not required for activation or is generated *in situ* at the cell surface and works in a paracrine fashion. Given the variety of transport activities exhibited by the family, it is also possible that SNF-10 promotes sperm activation via channel activity rather than transport of larger cargo. The influx of ions is well known to regulate motility of flagellate sperm in a variety of ways (Darszon et al., 2011; Lishko et al., 2011; Santi et al., 2013; Shukla et al., 2012). Less is known about the relationship between cellular ion physiology and motility of nematode sperm, although activation to motility requires specific ions and can be induced by compounds that challenge cellular ion homeostasis (Liu et al., 2013; Machaca et al., 1996; Nelson and Ward, 1980; Shakes and Ward, 1989). Furthermore, pH gradients within the cell may act to regulate dynamics of the pseudopodial MSP cytoskeleton, as shown for the larger sperm of *Ascaris suum* (Italiano et al., 1999; King et al., 1994). Thus, it is likely that ameboid nematode sperm use ion flux as a way to sense and respond to their environment, just as flagellate sperm do. Alternatively, SNF-10 might lack transport activity and instead function in signal transduction, perhaps in a receptor or scaffolding role. Functions for SLC6 family members that may be based on protein-protein interactions rather than any form of transport or channel activity have been identified previously. For example, the *Drosophila* SLC6 protein Bedraggled has been shown to play a role in tissue polarity in the eye (Rawls et al., 2007). Recently, *C. elegans* SNF-12 was shown to function in innate immunity by binding to STA-2, a STAT transcription factor, promoting transcriptional responses to fungal exposure (Dierking et al., 2011). In both of these cases, it is unclear whether any canonical transport activity is involved.

In activated spermatozoa, SNF-10 becomes restricted to the cell body region of the plasma membrane. This localization pattern is so far unique, but a number of other spermatozoan cell surface proteins (SPE-9, SPE-38) are restricted to the pseudopod, while others (FER-1, TRP-3/SPE-41) are found on both the pseudopod and cell body (Chatterjee et al., 2005; Washington and Ward, 2006; Xu and Sternberg, 2003; Zannoni et al., 2003). Little is known about how nematode sperm polarization is regulated, including how specific protein domains are established, but several membrane proteins are sequestered in MOs prior to activation and could be involved in the polarization process. For example, the function of SPE-38 is required for the proper distribution of TRP-3/SPE-41 (Singaravelu et al., 2012). Since SNF-10 does not appear to play a major role in sperm after activation, its polarized localization might arise from earlier interaction with other proteins that remain restricted to the cell body region. Related to this idea, we find that in *fer-1* spermatozoa, SNF-10 is no longer confined to the cell body but rather is distributed throughout the plasma membrane. FER-1 and other dysferlins are involved in membrane fusion in a variety of contexts including muscle repair as well as neurotransmission (Lek et al., 2011). While activated *fer-1* sperm are grossly polarized, specific proteins involved in fertilization are trapped in unfused MOs and thus absent from the sperm surface (Chatterjee et al., 2005; Xu and Sternberg, 2003). Our data suggest that restriction of SNF-10 to the cell body is dependent on interaction with either FER-1 or possibly another protein derived from MOs, since FER-1 is not itself restricted to the same domain as SNF-10 (Lek et al., 2011).

We have found that SNF-10 is primarily present on the plasma membrane in spermatids, but our data also suggest that some SNF-10 could be present on MOs. There is precedent for such a site of action: while most SLC6 proteins are present on the plasma membrane, some other family members are localized to intracellular vesicles (*e.g.*, Parra et al., 2008; Renick et al., 1999). Their function in this location has not been analyzed, though when expressed on the plasma membrane at least one shows a typical sodium-dependent cargo import activity. We speculate that SNF-10 could function to alter cytoplasmic ion or osmolyte homeostasis via the release of pools present in MOs.

How does SNF-10 function downstream of protease activity to promote the morphological changes associated with sperm activation? One simplistic but intriguing model is that SNF-10 is cleaved directly by the serine protease TRY-5 (Fig. 5A). Importantly, such cleavage should induce or alter, but not eliminate, SNF-10's activity. If so, this would define a novel regulatory mechanism for SLC6 family proteins. Several of the monoamine transporters have been shown to be cleaved by calpain-family proteases, but this resulted either in reduced activity or in no functional consequence (*e.g.*, Baliova and Jursky, 2010; Baliova et al., 2009). Overall, little data exists to address if positive or negative regulation of the family by proteolysis could be more widespread. Another possibility is that in spermatids, SNF-10 associates with an inhibitor that is itself cleaved by TRY-5, leading to SNF-10's activity (Fig. 5B). Finally, if SNF-10 functions on the MOs, activation or de-inhibition by TRY-5 would necessarily be indirect (Fig. 5A and B).

Another SLC6 transporter, Ntl, has been shown recently to be required for spermiogenesis in *Drosophila* (Chatterjee et al., 2011). Some mammalian SLC6 transporters show testis expression (Farmer et al., 2000; Hoglund et al., 2005), including the protein SLC6A16, which also shows divergent sequence features as compared to family members expressed in other tissues. However, the mammalian testis-expressed genes have not been analyzed genetically so the nature of

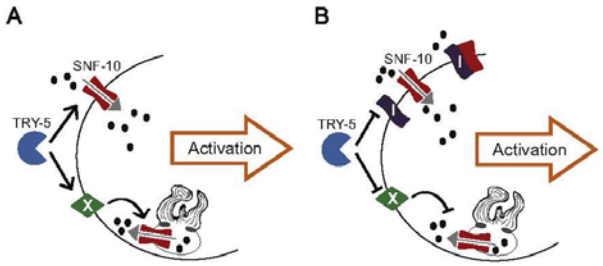


**Fig. 5.** Models for the role of SNF-10 in protease-initiated sperm activation. (A) Model 1: TRY-5 positively regulates SNF-10 activity in spermatids. TRY-5 might act directly on SNF-10 localized to the plasma membrane; it also might cleave an intermediate (X) that promotes SNF-10 activity on the MO membrane. Ultimately, SNF-10 transport and/or channel activity (gray arrow) induces maturation of the spermatid into a motile, active spermatozoon. Black arrows represent positive regulation; black ovals indicate substrates and/or ions to which SNF-10 is permeable. (B) Model 2: TRY-5 cleaves an inhibitor (I) of SNF-10 activity, which prevents SNF-10 activity either directly or through an intermediate (X). With the inhibitor disabled, SNF-10 functions to promote sperm activation. Black bars represent inhibition.

their role in spermatogenesis is unknown. Our identification of SNF-10 as a regulator of sperm activation in *C. elegans* suggests a shared role for SLC6 proteins in sperm physiology and function from invertebrates to mammals.

## Acknowledgments

Some strains were provided by the *Caenorhabditis* Genetics Center (Grant no. P40 OD010440), which is funded by the NIH Office of Research Infrastructure Programs (P40 OD010440). We thank Wormbase; the University of Utah Imaging and Sequencing Core Facilities; M. Ailion and C. Frokjaer-Jensen for reagents; E. Jorgensen and M. Metzstein for helpful discussions; and S. Mansour and C. Murtaugh for comments on the manuscript. This work was supported by NIH R01-GM087705.

## Appendix A. Supporting information

Supplementary data associated with this article can be found in the online version at http://dx.doi.org/10.1016/j.ydbio.2014.06.001.

## References

Arduengo, P.M., Appleberry, O.K., Chuang, P., L'Hernault, S.W., 1998. The presenilin protein family member SPE-4 localizes to an ER/Golgi derived organelle and is required for proper cytoplasmic partitioning during *Caenorhabditis elegans* spermatogenesis. J Cell Sci. 111 (Pt 24), 3645–3654.

Argon, Y., Ward, S., 1980. *Caenorhabditis elegans* fertilization-defective mutants with abnormal sperm. Genetics 96, 413–433.

Baliova, M., Jursky, F., 2010. Calcium dependent modification of distal C-terminal sequences of glycine transporter GlyT1. Neurochem. Int. 57, 254–261.

Baliova, M., Knab, A., Franekova, V., Jursky, F., 2009. Modification of the cytosolic regions of GABA transporter GAT1 by calpain. Neurochem. Int. 55, 288–294.

Beuming, T., Kniazeff, J., Bergmann, M.L., Shi, L., Gracia, L., Raniszewska, K., Newman, A.H., Javitch, J.A., Weinstein, H., Gether, U., Loland, C.J., 2008. The binding sites for cocaine and dopamine in the dopamine transporter overlap. Nat. Neurosci. 11, 780–789.

Bloch Qazi, M.C., Heifetz, Y., Wolfner, M.F., 2003. The developments between gametogenesis and fertilization: ovulation and female sperm storage in *Drosophila melanogaster*. Dev. Biol. 256, 195–211.

Boudko, D.Y., 2012. Molecular basis of essential amino acid transport from studies of insect nutrient amino acid transporters of the SLC6 family (NAT-SLC6). J. Insect Physiol. 58, 433–449.

Brenner, S., 1974. The genetics of *Caenorhabditis elegans*. Genetics 77, 71–94.

Broer, S., Gether, U., 2012. The solute carrier 6 family of transporters. Br. J. Pharmacol. 167, 256–278.

Chatterjee, I., Richmond, A., Putiri, E., Shakes, D.C., Singson, A., 2005. The *Caenorhabditis elegans spe-38* gene encodes a novel four-pass integral membrane protein required for sperm function at fertilization. Development 132, 2795–2808.

Chatterjee, N., Rollins, J., Mahowald, A.P., Bazinet, C., 2011. Neurotransmitter Transporter-Like: a male germline-specific SLC6 transporter required for *Drosophila* spermiogenesis. PLoS One 6, e16275.

Chu, D.S., Liu, H., Nix, P., Wu, T.F., Ralston, E.J., Yates 3rd, J.R., Meyer, B.J., 2006. Sperm chromatin proteomics identifies evolutionarily conserved fertility factors. Nature 443, 101–105.

Darszon, A., Guerrero, A., Galindo, B.E., Nishigaki, T., Wood, C.D., 2008. Sperm-activating peptides in the regulation of ion fluxes, signal transduction and motility. Int. J. Dev. Biol. 52, 595–606.

Darszon, A., Nishigaki, T., Beltran, C., Trevino, C.L., 2011. Calcium channels in the development, maturation, and function of spermatozoa. Physiol. Rev. 91, 1305–1355.

DeFelice, L.J., Goswami, T., 2007. Transporters as channels. Annu. Rev. Physiol. 69, 87–112.

Dierking, K., Polanowska, J., Omi, S., Engelmann, I., Gut, M., Lembo, F., Ewbank, J.J., Pujol, N., 2011. Unusual regulation of a STAT protein by an SLC6 family transporter in *C. elegans* epidermal innate immunity. Cell Host Microbe 9, 425–435.

Farmer, M.K., Robbins, M.J., Medhurst, A.D., Campbell, D.A., Ellington, K., Duckworth, M., Brown, A.M., Middlemiss, D.N., Price, G.W., Pangalos, M.N., 2000. Cloning and characterization of human NTT5 and v7-3: two orphan transporters of the $Na^+/Cl^-$ -dependent neurotransmitter transporter gene family. Genomics 70, 241–252.

Frokjaer-Jensen, C., Davis, M.W., Ailion, M., Jorgensen, E.M., 2012. Improved Mos1-mediated transgenesis in *C. elegans*. Nat. Methods 9, 117–118.

Frokjaer-Jensen, C., Davis, M.W., Hopkins, C.E., Newman, B.J., Thummel, J.M., Olesen, S.P., Grunnet, M., Jorgensen, E.M., 2008. Single-copy insertion of transgenes in *Caenorhabditis elegans*. Nat. Genet. 40, 1375–1383.

Gleason, E.J., Hartley, P.D., Henderson, M., Hill-Harfe, K.L., Price, P.W., Weimer, R.M., Kroft, T.L., Zhu, G.D., Cordovado, S., L'Hernault, S.W., 2012. Developmental genetics of secretory vesicle acidification during *Caenorhabditis elegans* spermatogenesis. Genetics 191, 477–491.

Hodgkin, J., Horvitz, H.R., Brenner, S., 1979. Nondisjunction mutants of the nematode *Caenorhabditis elegans*. Genetics 91, 67–94.

Hoglund, P.J., Adzic, D., Scicluna, S.J., Lindblom, J., Fredriksson, R., 2005. The repertoire of solute carriers of family 6: identification of new human and rodent genes. Biochem. Biophys. Res. Commun. 336, 175–189.

Italiano Jr., J.E., Stewart, M., Roberts, T.M., 1999. Localized depolymerization of the major sperm protein cytoskeleton correlates with the forward movement of the cell body in the amoeboid movement of nematode sperm. J. Cell Biol. 146, 1087–1096.

King, K.L., Stewart, M., Roberts, T.M., 1994. Supramolecular assemblies of the *Ascaris suum* major sperm protein (MSP) associated with amoeboid cell motility. J. Cell Sci. 107 (Pt 10), 2941–2949.

Kristensen, A.S., Andersen, J., Jorgensen, T.N., Sorensen, L., Eriksen, J., Loland, C.J., Stromgaard, K., Gether, U., 2011. SLC6 neurotransmitter transporters: structure, function, and regulation. Pharmacol. Rev. 63, 585–640.

Kumsta, C., Hansen, M., 2012. *C. elegans rrf-1* mutations maintain RNAi efficiency in the soma in addition to the germline. PLoS One 7, e35428.

L'Hernault, S.W., 2006. Spermatogenesis, *WormBook*, ed. The *C. elegans* Research Community. WormBook. doi/10.1895/wormbook.1.85.1. (http://www.wormbook.org).

L'Hernault, S.W., Benian, G.M., Emmons, R.B., 1993. Genetic and molecular characterization of the *Caenorhabditis elegans* spermatogenesis-defective gene *spe-17*. Genetics 134, 769–780.

L'Hernault, S.W., Shakes, D.C., Ward, S., 1988. Developmental genetics of chromosome I spermatogenesis-defective mutants in the nematode *Caenorhabditis elegans*. Genetics 120, 435–452.

LaMunyon, C.W., Ward, S., 1994. Assessing the viability of mutant and manipulated sperm by artificial insemination of *Caenorhabditis elegans*. Genetics 138, 689–692.

LaMunyon, C.W., Ward, S., 1995. Sperm precedence in a hermaphroditic nematode (*Caenorhabditis elegans*) is due to competitive superiority of male sperm. Experientia 51, 817–823.

Lek, A., Evesson, F.J., Sutton, R.B., North, K.N., Cooper, S.T., 2011. Ferlins: regulators of vesicle fusion for auditory neurotransmission, receptor trafficking and membrane repair. Traffic 13, 185–194.

Liau, W.S., Nasri, U., Elmatari, D., Rothman, J., LaMunyon, C.W., 2013. Premature sperm activation and defective spermatogenesis caused by loss of *spe-46* function in *Caenorhabditis elegans*. PLoS One 8, e57266.

Lishko, P.V., Kirichok, Y., Ren, D., Navarro, B., Chung, J.J., Clapham, D.E., 2011. The control of male fertility by spermatozoan ion channels. Annu. Rev. Physiol. 74, 453–475.

Liu, Z., Chen, L., Shang, Y., Huang, P., Miao, L., 2013. The micronutrient element zinc modulates sperm activation through the SPE-8 pathway in *Caenorhabditis elegans*. Development 140, 2103–2107.

Machaca, K., DeFelice, L.J., L'Hernault, S.W., 1996. A novel chloride channel localizes to *Caenorhabditis elegans* spermatids and chloride channel blockers induce spermatid differentiation. Dev. Biol. 176, 1–16.

Mello, C.C., Kramer, J.M., Stinchcomb, D., Ambros, V., 1991. Efficient gene transfer in *C. elegans*: extrachromosomal maintenance and integration of transforming sequences. EMBO J. 10, 3959–3970.

Merritt, C., Rasoloson, D., Ko, D., Seydoux, G., 2008. 3' UTRs are the primary regulators of gene expression in the *C. elegans* germline. Curr. Biol. 18, 1476–1482.

Muhlrad, P.J., Ward, S., 2002. Spermiogenesis initiation in *Caenorhabditis elegans* involves a casein kinase 1 encoded by the *spe-6* gene. Genetics 161, 143–155.

Nelson, G.A., Ward, S., 1980. Vesicle fusion, pseudopod extension and ameboid motility are induced in nematode spermatids by the ionophore monensin. Cell 19, 457–464.

Okamoto, H., Thomson, J.N., 1985. Monoclonal antibodies which distinguish certain classes of neuronal and supporting cells in the nervous tissue of the nematode *Caenorhabditis elegans*. J. Neurosci. 5, 643–653.

Parra, L.A., Baust, T., El Mestikawy, S., Quiroz, M., Hoffman, B., Haflett, J.M., Yao, J.K., Torres, G.E., 2008. The orphan transporter Rxt1/NTT4 (SLC6A17) functions as a synaptic vesicle amino acid transporter selective for proline, glycine, leucine, and alanine. Mol. Pharmacol. 74, 1521–1532.

Pramod, A.B., Foster, J., Carvelli, L., Henry, L.K., 2013. SLC6 transporters: structure, function, regulation, disease association and therapeutics. Mol. Aspects Med. 34, 197–219.

Rawls, A.S., Schultz, S.A., Mitra, R.D., Wolff, T., 2007. Bedraggled, a putative transporter, influences the tissue polarity complex during the R3/R4 fate decision in the *Drosophila* eye. Genetics 177, 313–328.

Reinke, V., Gil, I.S., Ward, S., Kazmer, K., 2004. Genome-wide germline-enriched and sex-biased expression profiles in *Caenorhabditis elegans*. Development 131, 311–323.

Reinke, V., Smith, H.E., Nance, J., Wang, J., Van Doren, C., Begley, R., Jones, S.J., Davis, E.B., Scherer, S., Ward, S., Kim, S.K., 2000. A global profile of germline gene expression in *C. elegans*. Mol Cell. 6, 605–616.

Renick, S.E., Kleven, D.T., Chan, J., Stenius, K., Milner, T.A., Pickel, V.M., Fremeau Jr., R. T., 1999. The mammalian brain high-affinity L-proline transporter is enriched

preferentially in synaptic vesicles in a subpopulation of excitatory nerve terminals in rat forebrain. J. Neurosci. 19, 21–33.
Santella, L., Vasilev, F., Chun, J.T., 2012. Fertilization in echinoderms. Biochem. Biophys. Res. Commun. 425, 588–594.
Santi, C.M., Orta, G., Salkoff, L., Visconti, P.E., Darszon, A., Trevino, C.L., 2013. K+ and Cl− channels and transporters in sperm function. Curr. Top. Dev. Biol. 102, 385–421.
Schedl, T., Kimble, J., 1988. *fog-2*, a germ-line-specific sex determination gene required for hermaphrodite spermatogenesis in *Caenorhabditis elegans*. Genetics 119, 43–61.
Seidel, H.S., Ailion, M., Li, J., van Oudenaarden, A., Rockman, M.V., Kruglyak, L., 2011. A novel sperm-delivered toxin causes late-stage embryo lethality and transmission ratio distortion in *C. elegans*. PLoS Biol. 9, e1001115.
Shakes, D.C., Ward, S., 1989. Initiation of spermiogenesis in *C. elegans*: a pharmacological and genetic analysis. Dev. Biol. 134, 189–200.
Shukla, K.K., Mahdi, A.A., Rajender, S., 2012. Ion channels in sperm physiology and male fertility and infertility. J. Androl. 33, 777–788.
Sijen, T., Fleenor, J., Simmer, F., Thijssen, K.L., Parrish, S., Timmons, L., Plasterk, R.H., Fire, A., 2001. On the role of RNA amplification in dsRNA-triggered gene silencing. Cell 107, 465–476.
Singaravelu, G., Chatterjee, I., Rahimi, S., Druzhinina, M.K., Kang, L., Xu, X.Z., Singson, A., 2012. The sperm surface localization of the TRP-3/SPE-41 Ca2+-permeable channel depends on SPE-38 function in *Caenorhabditis elegans*. Dev. Biol. 365, 376–383.
Smith, J.R., Stanfield, G.M., 2011. TRY-5 is a sperm-activating protease in *Caenorhabditis elegans* seminal fluid. PLoS Genet. 7, e1002375.
Stanfield, G.M., Villeneuve, A.M., 2006. Regulation of sperm activation by SWM-1 is required for reproductive success of *C. elegans* males. Curr. Biol. 16, 252–263.
Suarez, S.S., 2008. Regulation of sperm storage and movement in the mammalian oviduct. Int. J. Dev. Biol. 52, 455–462.
Vangelatos, I., Vlachakis, D., Sophianopoulou, V., Diallinas, G., 2009. Modelling and mutational evidence identify the substrate binding site and functional elements in APC amino acid transporters. Mol. Membr. Biol. 26, 356–370.
Ward, S., Carrel, J.S., 1979. Fertilization and sperm competition in the nematode *Caenorhabditis elegans*. Dev. Biol. 73, 304–321.
Ward, S., Hogan, E., Nelson, G.A., 1983. The initiation of spermiogenesis in the nematode *Caenorhabditis elegans*. Dev. Biol. 98, 70–79.
Ward, S., Miwa, J., 1978. Characterization of temperature-sensitive, fertilization-defective mutants of the nematode *Caenorhabditis elegans*. Genetics 88, 285–303.
Washington, N.L., Ward, S., 2006. FER-1 regulates $Ca^{2+}$-mediated membrane fusion during *C. elegans* spermatogenesis. J. Cell Sci. 119, 2552–2562.
Xu, X.Z., Sternberg, P.W., 2003. A *C. elegans* sperm TRP protein required for sperm-egg interactions during fertilization. Cell 114, 285–297.
Yamashita, A., Singh, S.K., Kawate, T., Jin, Y., Gouaux, E., 2005. Crystal structure of a bacterial homologue of Na+/Cl− -dependent neurotransmitter transporters. Nature 437, 215–223.
Yochem, J., Gu, T., Han, M., 1998. A new marker for mosaic analysis in *Caenorhabditis elegans* indicates a fusion between hyp6 and hyp7, two major components of the hypodermis. Genetics 149, 1323–1334.
Zannoni, S., L'Hernault, S.W., Singson, A.W., 2003. Dynamic localization of SPE-9 in sperm: a protein required for sperm-oocyte interactions in *Caenorhabditis elegans*. BMC Dev. Biol. 3, 10.

Supplementary Materials

**Supplementary Methods, Figure Legends, and References**

**RNAi**

To prepare RNAi plates, bacterial strains containing dsRNA plasmids (Kamath et al., 2003) were grown overnight in LB with 10 µg/mL tetracycline and 50 µg/mL ampicillin, concentrated by centrifugation, and spotted onto NGM agar containing 1mM IPTG and 75 µg/mL ampicillin (Ahringer, 2006). Gravid hermaphrodites were placed on RNAi plates and allowed to lay eggs overnight at 15°C. Progeny were allowed to develop at 15°C until reaching the L4 stage. To score sperm activation, male progeny were then transferred to fresh RNAi plates which had been allowed to induce overnight, incubated for 72 hr, and examined by DIC. To score *unc-22,* animals were examined directly without transfer.

**Generation of transcriptional fusion reporter constructs and transgenes**

To allow for determination of cell identities, we generated animals harboring transgenes containing the *snf-10* promoter region driving expression of fluorescent proteins fused to either histone H2B (Merritt et al., 2008) or the sperm-specific small nuclear basic protein HTAS-1(Chu et al., 2006). Transgene plasmids were constructed using Multisite Gateway Three-Fragment Vector Construction kit entry vectors (Life Technologies). The 1044 bp region immediately upstream of the *snf-10* coding region was amplified using the primers 5'-GGGGACAACTTTGTATAGAAAAGTTGGGGTCCACGAGGTATAGAAGG-3' and 5'-GGGGACTGCTTTTTTGTACAAACTTGTTCACTGTTTTTATAAAACC-3' and

cloned into pDONR P4-P1R, generating the plasmid pAAH004. The 568 bp region immediately downstream of *snf-10* was amplified using the primers 5'-GGGGACAACTTTGTATAATAAAGTTGCGGGAATTTCAATCGAGAAG-3' and 5'-GGGGACAGCTTTCTTGTACAAAGTGGTAATGAATTATTCTACTTTTAT-3' and cloned into pDONR P2R-P3, generating the plasmid pAAH007. The *htas-1* coding region was amplified using the primers 5'-GGGGACAAGTTTGTACAAAAAAGCAGGCTTGATGGCTCGTCTCAAACAAAGACC-3' (primer htasL) and 5'-TCTTCTTCACCCTTTGAGACCATAGAATTATTTTCTTTGTCATC-3', mixed with an *mCherry* fragment generated from plasmid pCFJ33 (Frokjaer-Jensen et al., 2008) using the primers 5'-ATGGTCTCAAAGGGTGAAGAAG-3' and 5'-GGGGACCACTTTGTACAAGAAAGCTGGGTCTACTTATACAATTCATCCATGCC-3' (primer mChR), and an *htas-1::mCherry* fusion fragment was generated using the primers htasL and mChR (Hobert, 2002). Finally, recombination of *htas-1::mCherry* into pDONR221 generated the plasmid pENTRL1L2_htas-1mCh. The Psnf-10::GFP::H2B::3'snf-10 expression plasmid pAAH014 was then constructed by recombination of pAAH004, pCM1.35 (Merritt et al., 2008), and pAAH007 into pCFJ150 (Frokjaer-Jensen et al., 2008). The Psnf-10::htas-1::mCherry::3'snf-10 expression plasmid pAAH013 was constructed by recombination of pAAH004, pENTRL1L2_htas-1mCh, and pAAH007 into pCFJ150. Transgenes were inserted into the *ttTi5605 II* insertion site using MosSCI as in Frokjaer-Jensen (2008, 2012).

**Supplementary Figures**

**Supplementary Fig. 1. Mapping *snf-10*.** Schematic of the *dpy-11-unc-76* region of chromosome V showing CB4856 polymorphisms used for localizing *snf-10(jn3)* to a ~50 kb region (Wormbase, 2014).

**Supplementary Fig. 2. SNF-10 is a divergent SLC6 transporter.** Alignment of sequence regions of transmembrane (TM) domains 1, 3, 6, and 8 for *C. elegans* SNF-10 (accession number O45915) and SLC6 family members *A. aeolicus* LeuT (NP_214423), *Drosophila* CG5549 (Q9W1J0), human GlyT2/SLC6A5 (AAK12641.1), and human NTT5/SLC6A16 (Q9GZN6). Alignment was generated using Clustal Omega (Goujon et al., 2010; Sievers et al., 2011). Yellow indicates transmembrane domains for LeuT as reported previously in Yamashita (2005) and as predicted for SNF-10 by TMpred (Hofmann and Stoffel, 1993). Colors indicate residues involved in intracellular gating (Loland et al., 2004; Loland et al., 2002; Yamashita et al., 2005), extracellular gating (Cao et al., 1998; Kristensen et al., 2011; Pantanowitz et al., 1993; Yamashita et al., 2005), and binding of sodium and substrate (Yamashita et al., 2005).

**Supplementary Fig. 3. *snf-10* activity is required in the germ line.** Germline-restricted *snf-10(RNAi)* is effective in suppressing the *swm-1* activated sperm phenotype. The indicated strains were fed bacteria containing *snf-10* dsRNA or the L4440 vector and scored for sperm activation (column graph) or fed bacteria expressing *unc-22* dsRNA and scored for the Twitching phenotype (% Unc). Graph shading as in Fig. 1E. n, 44-100.

**Supplementary Fig. 4. *snf-10* is expressed in germ cells undergoing spermatogenesis.** Paired (A) DIC and (B) mCherry fluorescence image of a 48 hr post L4 *jnSi74[Psnf-10::htas-1::mCh]; unc-119; him-5* male. In worms carrying this transcriptional reporter, chromatin-localized mCherry is expressed in cells undergoing spermatogenesis and retained in the posttranscriptional spermatids and sperm. Arrow indicates a karyosome-stage spermatocyte. Arrowheads indicate adjacent spermatids within the seminal vesicle. int, intestinal autofluorescence. Scale bar: 20 microns.

**Supplementary Fig. 5. SNF-10 localization to the plasma membrane is disrupted in *spe-17* mutant spermatids.** (A-D) SNF-10::mCh is localized to the cell periphery in nonactivated *jnSi96[Psnf-10::SNF-10::mCh]; jnSi192[Ppeel-1::PEEL-1::GFP]* spermatids. (E,F) In *jnSi96; spe-17* spermatids, SNF-10::mCh is present both at the plasma membrane and in asymmetrical cytoplasmic puncta. Images shown are live sperm visualized by (A,E) DIC, (B,F) SNF-10::mCh, (C) PEEL-1::GFP, and (D) merge of mCh and GFP fluorescence. All strains are mutant for *unc-119*, *him-5*, and *snf-10(hc194).* Scale bar is 5 microns and applies to all images.

**Supplementary References**

Ahringer, J., ed. 2006. Reverse genetics. The *C. elegans* Research Community, WormBook, doi/10.1895/wormbook.1.47.1, http://www.wormbook.org.

Cao, Y., Li, M., Mager, S., Lester, H. A., 1998. Amino acid residues that control pH modulation of transport-associated current in mammalian serotonin transporters. *J. Neurosci.* 18, 7739-49.

ClustalO, May 12, 2014. http://www.ebi.ac.uk/Tools/msa/clustalo/.

Goujon, M., McWilliam, H., Li, W., Valentin, F., Squizzato, S., Paern, J., Lopez, R., 2010. A new bioinformatics analysis tools framework at EMBL-EBI. *Nucleic Acids Res.* 38, W695-9.

Hobert, O., 2002. PCR fusion-based approach to create reporter gene constructs for expression analysis in transgenic *C. elegans*. *Biotechniques.* 32, 728-30.

Hofmann, K., Stoffel, W., 1993. TMbase - a database of membrane spanning protein segments. *Biol. Chem.* Hoppe-Seyler. 374.

Kamath, R. S., Fraser, A. G., Dong, Y., Poulin, G., Durbin, R., Gotta, M., Kanapin, A., Le Bot, N., Moreno, S., Sohrmann, M., Welchman, D. P., Zipperlen, P., Ahringer, J., 2003. Systematic functional analysis of the *Caenorhabditis elegans* genome using RNAi. *Nature*. 421, 231-7.

Loland, C. J., Granas, C., Javitch, J. A., Gether, U., 2004. Identification of intracellular residues in the dopamine transporter critical for regulation of transporter conformation and cocaine binding. *J. Biol. Chem.* 279, 3228-38.

Loland, C. J., Norregaard, L., Litman, T., Gether, U., 2002. Generation of an activating Zn(2+) switch in the dopamine transporter: mutation of an intracellular tyrosine constitutively alters the conformational equilibrium of the transport cycle. *Proc. Natl. Acad. Sci. U S A.* 99, 1683-8.

Pantanowitz, S., Bendahan, A., Kanner, B. I., 1993. Only one of the charged amino acids located in the transmembrane alpha-helices of the gamma-aminobutyric acid transporter (subtype A) is essential for its activity. *J. Biol. Chem.* 268, 3222-5.

Sievers, F., Wilm, A., Dineen, D., Gibson, T. J., Karplus, K., Li, W., Lopez, R., McWilliam, H., Remmert, M., Soding, J., Thompson, J. D., Higgins, D. G., 2011. Fast, scalable generation of high-quality protein multiple sequence alignments using Clustal Omega. *Mol. Syst. Biol.* 7, 539.

TMPred, May 12, 2014. http://www.ch.embnet.org/software/TMPRED_form.html.

WormBase, January 20, 2014. Release WS240. http://www.wormbase.org.

FigureS1

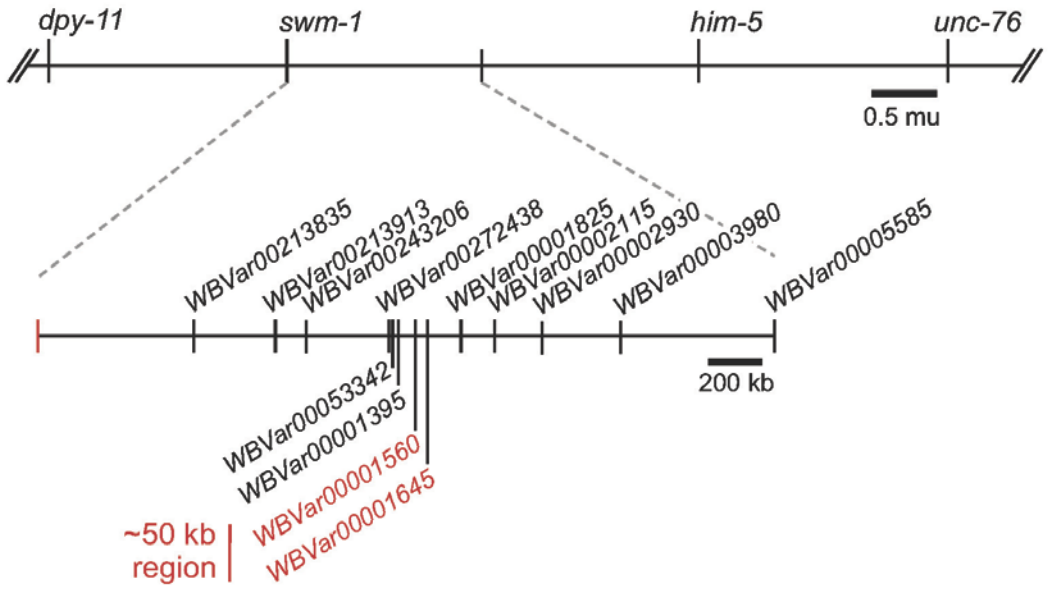
dpy-11
swm-1
him-5
unc-76
0.5 mu
WBVar00213835
WBVar00213913
WBVar00243206
WBVar00272438
WBVar00001825
WBVar00002115
WBVar00002930
WBVar00003980
WBVar00005585
200 kb
WBVar00053342
WBVar00001395
WBVar00001560
WBVar00001645
~50 kb
region

FigureS2

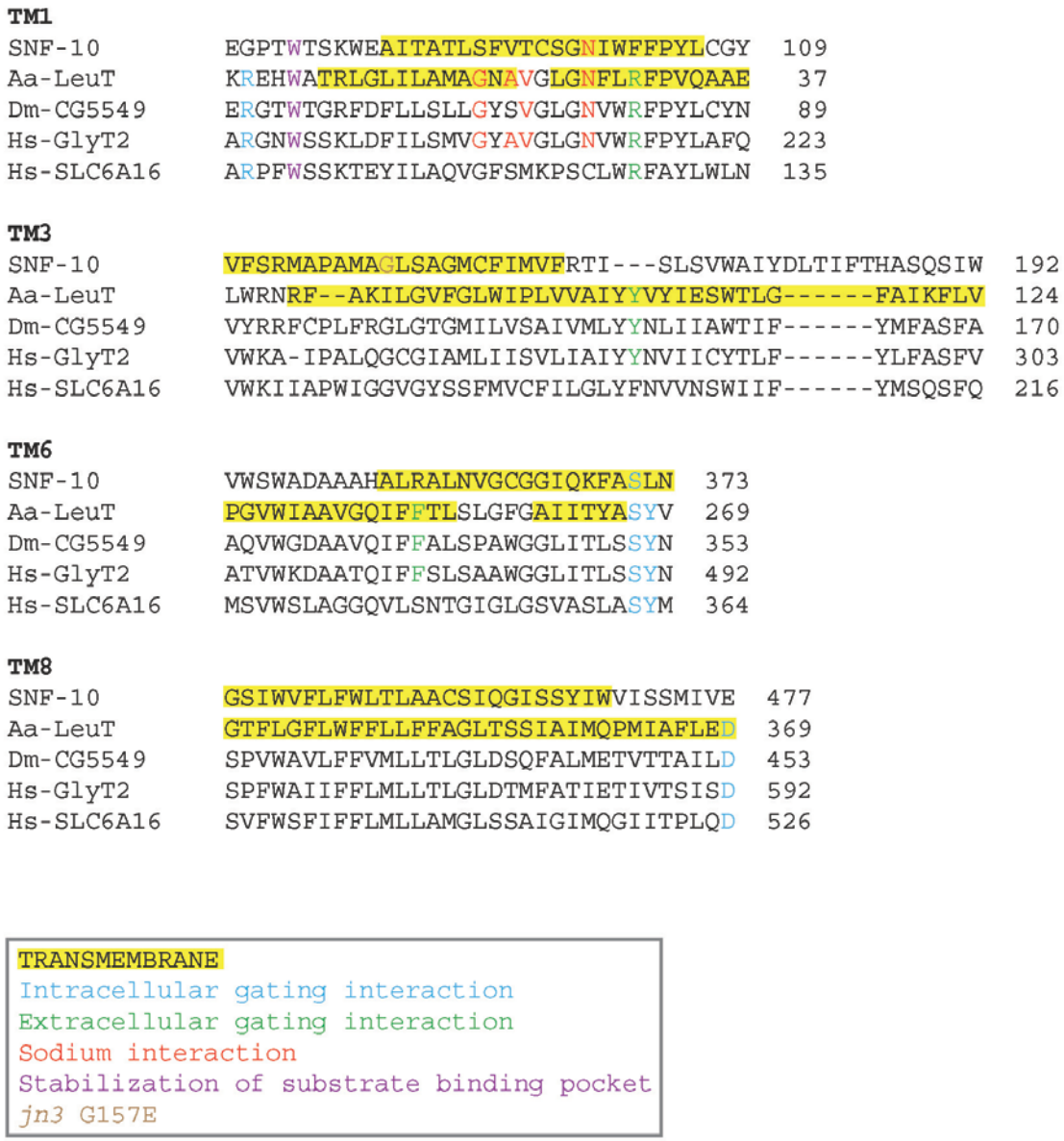
TM1
SNF-10 EGPTWTSKWEAITATLSFVTCSGNIWFFPYLCGY 109
Aa-LeuT KREHWATRLGLILAMAGNAVGLGNFLRFPVQAAE 37
Dm-CG5549 ERGTWTGRFDFLLSLLGYSVGLGNVWRFPYLCYN 89
Hs-GlyT2 ARGNWSSKLDFILSMVGYAVGLGNVWRFPYLAFQ 223
Hs-SLC6A16 ARPFWSSKTEYILAQVGFSMKPSCLWRFAYLWLN 135
TM3
SNF-10 VFSRMAPAMAGLSAGMCFIMVFRTI---SLSVWAIYDLTIFTHASQSIW 192
Aa-LeuT LWRNRF--AKILGVFGLWIPLVVAIYYVYIESWTLG------FAIKFLV 124
Dm-CG5549 VYRRFCPLFRGLGTGMILVSAIVMLYYNLIIAWTIF------YMFASFA 170
Hs-GlyT2 VWKA-IPALQGCGIAMLIISVLIAIYYNVIICYTLF------YLFASFV 303
Hs-SLC6A16 VWKIIAPWIGGVGYSSFMVCFILGLYFNVVNSWIIF------YMSQSFQ 216
TM6
SNF-10 VWSWADAAAHALRALNVGCGGIQKFASLN 373
Aa-LeuT PGVWIAAVGQIFFTLSLGFGAIITYASYV 269
Dm-CG5549 AQVWGDAAVQIFFALSPAWGGLITLSSYN 353
Hs-GlyT2 ATVWKDAATQIFFSLSAAWGGLITLSSYN 492
Hs-SLC6A16 MSVWSLAGGQVLSNTGIGLGSVASLASYM 364
TM8
SNF-10 GSIWVFLFWLTLAACSIQGISSYIWVISSMIVE 477
Aa-LeuT GTFLGFLWFFLLFFAGLTSSIAIMQPMIAFLED 369
Dm-CG5549 SPVWAVLFFVMLLTLGLDSQFALMETVTTAILD 453
Hs-GlyT2 SPFWAIIFFLMLLTLGLDTMFATIETIVTSISD 592
Hs-SLC6A16 SVFWSFIFFLMLLAMGLSSAIGIMQGIITPLQD 526
TRANSMEMBRANE
Intracellular gating interaction
Extracellular gating interaction
Sodium interaction
Stabilization of substrate binding pocket
jn3 G157E

FigureS3

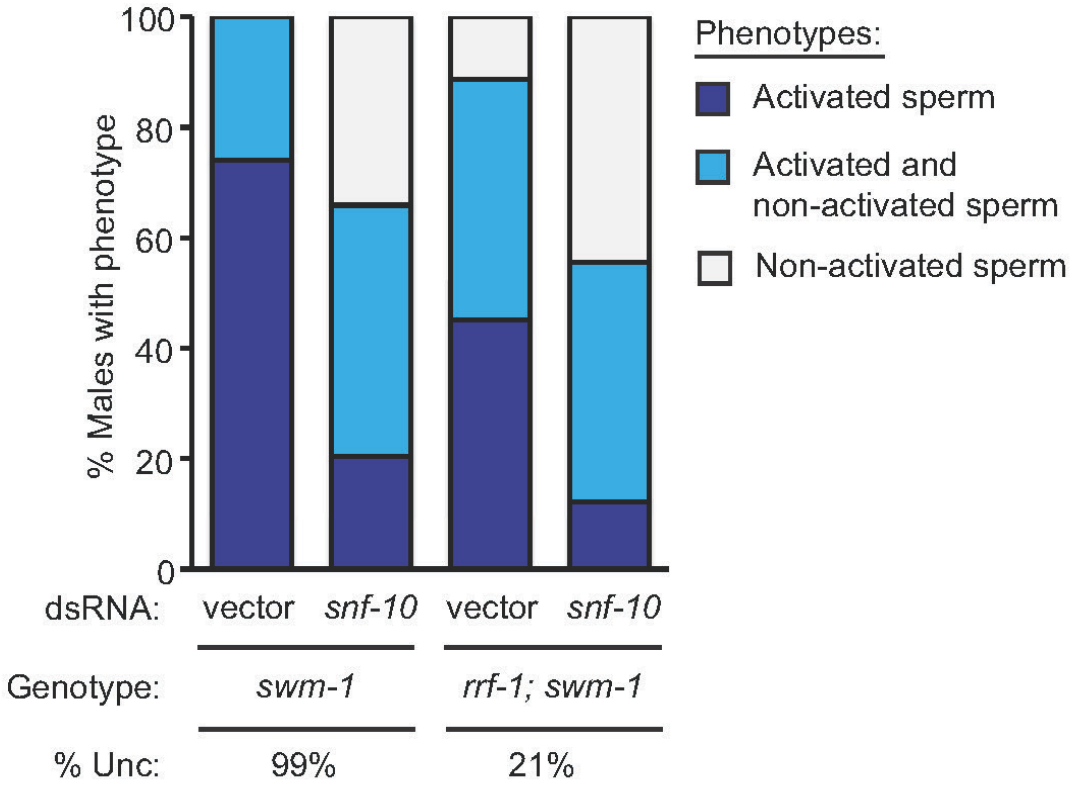
100
80
60
40
20
0
% Males with phenotype
Phenotypes:
Activated sperm
Activated and non-activated sperm
Non-activated sperm
dsRNA:
vector
snf-10
vector
snf-10
Genotype:
swm-1
rrf-1; swm-1
% Unc:
99%
21%

Figure S4

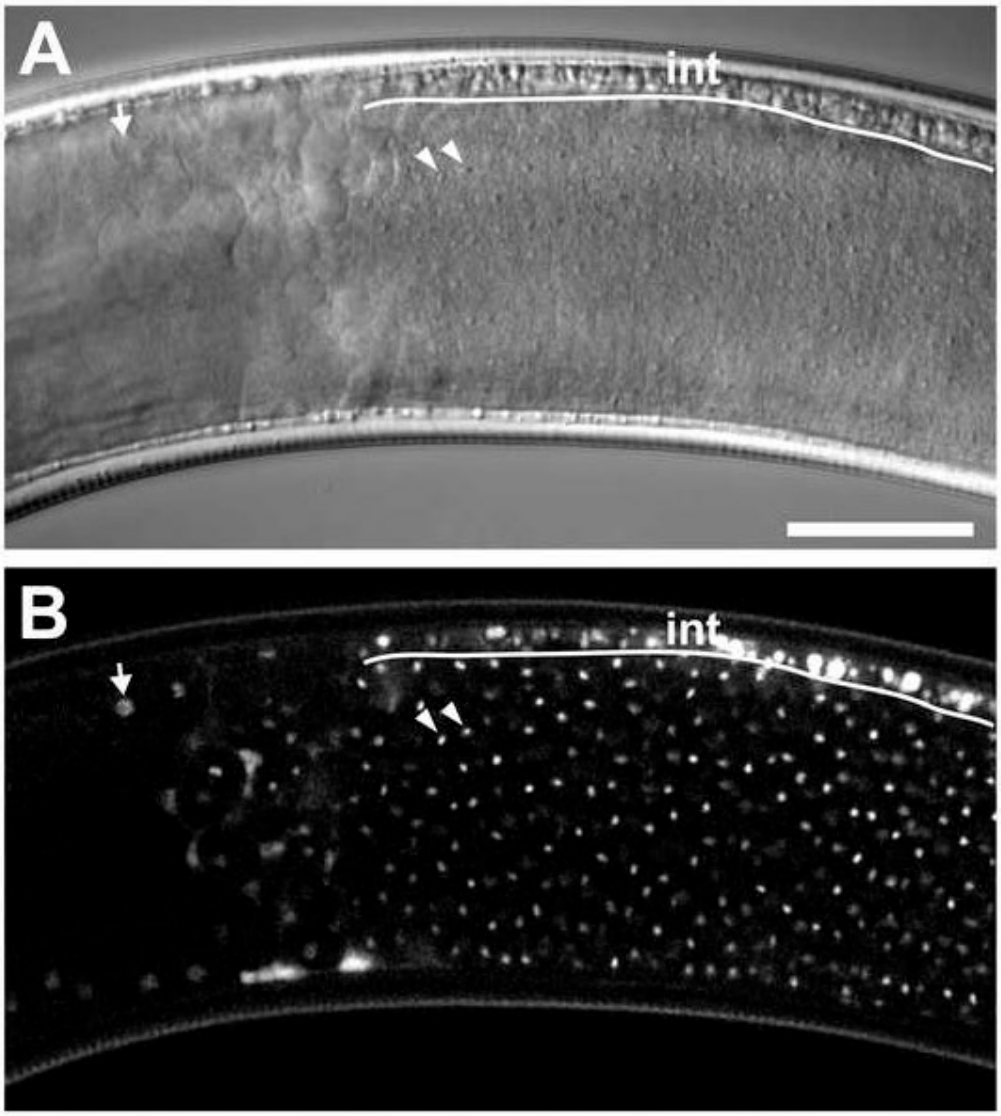

Figure S5

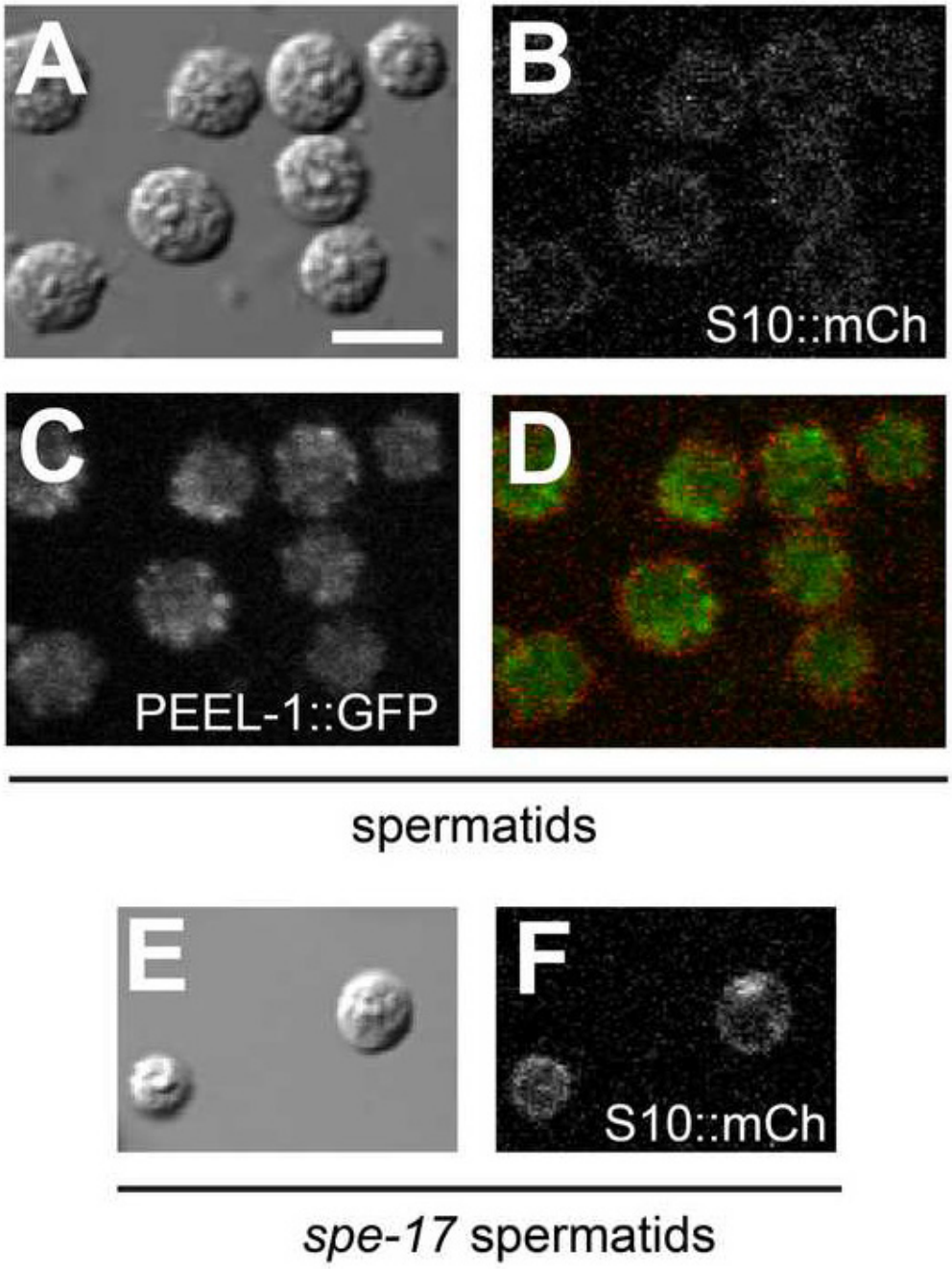
A
B
S10::mCh
C
PEEL-1::GFP
D
spermatids
E
F
S10::mCh
spe-17 spermatids

# CHAPTER 5

# SNF-10 CONNECTS MALE-DERIVED SIGNALS TO THE ONSET OF SPERM MOTILITY IN *C. ELEGANS*

Originally published as-Fenker, K.E. and Stanfield, G.M. (2015). SNF-10 connects male-derived signals to the onset of sperm motility in *C. elegans.* Worm 4(1), e1003002.

COMMENTARY

Worm 4:1, e1003002; January/February/March 2015; © 2015 Taylor & Francis Group, LLC

# SNF-10 connects male-derived signals to the onset of sperm motility in *C. elegans*

Kristin E Fenker and Gillian M Stanfield*

Department of Human Genetics; University of Utah; Salt Lake City, UT USA

**Sperm from the nematode *C. elegans* gain motility during a process termed activation, which they initiate in response to specific environmental signals. During this process, a number of subcellular rearrangements occur, culminating in an altered morphology that allows the cell to crawl toward and fertilize oocytes. Both hermaphrodites and males produce sperm, and redundant, sex-biased pathways regulate the sperm's activation. The male-derived signal for sperm activation involves TRY-5, a trypsin-like serine protease in seminal fluid, but until recently it was unknown what factors were active downstream of TRY-5. In our recent paper, we reported the discovery of SNF-10, a solute carrier 6 (SLC6) family protein that is expressed by sperm and connects the activation signal to changes in sperm morphology and, ultimately, the onset of motility. Here, we review our recent results, focusing on potential models for SNF-10's function in *C. elegans*, and additionally discuss the role SLC6 transporters may play in male reproductive biology from invertebrates to mammals.**

**Keywords:** sperm, cell motility, SLC6 transporter, protease signaling, reproduction

*Correspondence to: Gillian M Stanfield; Email: gillians@genetics.utah.edu

Submitted: 12/09/2014

Accepted: 12/22/2014

http://dx.doi.org/10.1080/21624054.2014.1003002

## Introduction: Environmental Cues Regulate Sperm Motility

For sexually reproducing animals, the production of offspring relies on 2 specialized gametes – the sperm and egg – coming together and developing into a zygote. While sperm-egg fusion is critical, its success relies on highly regulated processes that begin well before the 2 gametes encounter one another. For sperm, motility is a key facet of reproductive success, as they must both become motile and modulate their movements in response to environmental cues. Signals from the external environment influence the cells in 3 main ways: preventing motility until sperm enter the female reproductive tract, allowing motility once sperm have been transferred, and finally, guiding sperm toward oocytes.[1,2]

As in other animals, the motility of *C. elegans* sperm is tightly regulated, and worms have been an excellent system to study both the cell biology and genetics involved. In *C. elegans*, sperm become motile during a process termed activation, which is initiated when a signal acts on immature spermatids.[3] The spermatids respond by changing their morphology to become polarized spermatozoa, with pseudopods that are used for crawling.[4] In addition to cytoskeletal rearrangements, a number of other changes occur, including the fusion of lysosome-related vesicles called membranous organelles (MOs) with the plasma membrane and the relocalization of specific proteins.[5-7] Many of these processes are analogous to those that occur in other animals. For example, in mammalian sperm the cytoskeleton is restructured to form a flagellum, the membrane is altered through the acrosome reaction, and proteins required for fertilization such as Izumo are relocalized.[8,9]

Genetic analyses have revealed *C. elegans* sperm are regulated by 2 redundant pathways, a strategy that allows male and hermaphrodite sperm to activate at the time and place that is most advantageous for each sex. Hermaphrodite sperm, which are produced in limited quantities, activate rapidly after they are pushed into the sperm storage organ, the spermatheca, by the first ovulated oocyte.[10] This onset of

motility is regulated by the *spe-8* group of genes (*spe-8, 12, 19, 27,* and *29*), which encode a set of sperm proteins important for responding to zinc signals that promote activation in hermaphrodites (**Fig. 1A**).[10-13] Unlike hermaphrodites, males produce sperm throughout their adult lives and store it as nonactivated spermatids in their gonads (**Fig. 1B**). If sperm become activated while stored within a male, as occurs when a male loses the protease inhibitor *swm-1* (sperm activation without mating), they cannot be transferred to the hermaphrodite and the male is infertile.[14] Once mating occurs and sperm are transferred, they must quickly activate and gain motility, or risk being swept out of the reproductive tract as the hermaphrodite lays eggs.[15] Our lab previously demonstrated activation is achieved because male sperm respond to a protease signal in seminal fluid conferred by TRY-5 (trypsin-like protease).[16] TRY-5 is mixed with sperm during mating, coupling the male-derived activation signal to the entrance of male sperm into the hermaphrodite reproductive tract (**Fig. 1B**).[16]

While it is clear TRY-5 and SWM-1 provide an important, male-derived signal for sperm activation, how the signal is received and transduced by sperm remains unknown. We sought to address this question using a genetic screen to identify factors required for protease-mediated sperm activation. In our recent paper, we describe one such factor: *snf-10* (sodium:: neurotransmitter symporter family).[17] *snf-10* provides the first known link connecting the protease signal to changes in sperm cell motility, and is particularly interesting because it encodes a member of a well-conserved and well-studied family of proteins, the Solute Carrier 6 (SLC6) family. These proteins are sodium-dependent transporters best known for importing neurotransmitters, amino acids or osmolytes across the plasma membrane into cells, although they can have other roles.[18,19] In this commentary, we review what we have learned about *snf-10* so far, and discuss potential mechanisms for SNF-10's function in activating sperm. We hypothesize SNF-10 could have a function similar to other SLC6 proteins; alternatively, it may have been adapted by the nematode germ line to perform a novel cellular function, as either case could promote reproductive success.

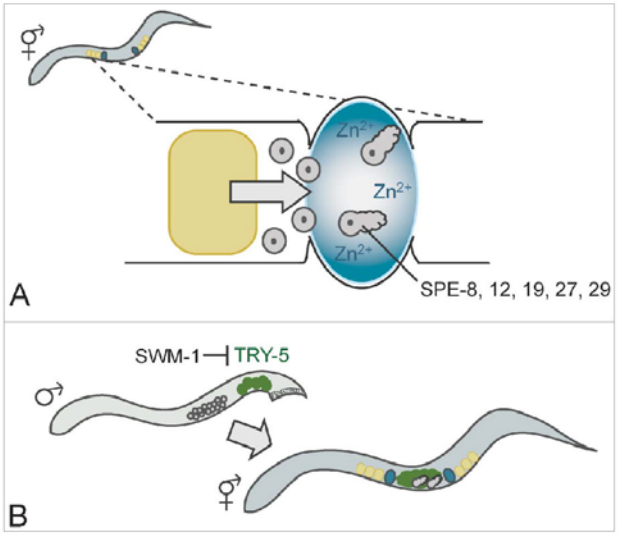


**Figure 1.** Genetic regulation and extracellular signals cooperate to ensure hermaphrodite and male sperm activate at the proper time and place. (**A**) In the hermaphrodite, spermatids are pushed into the spermatheca by a developing oocyte (yellow). There, they are exposed to zinc (blue), which triggers activation through the *spe-8* group of genes. This results in motile spermatozoa with pseudopods, which are stored in the spermatheca until they are used to fertilize oocytes. (**B**) In the male, sperm are stored as nonactivated spermatids, and maintaining this state requires the protease inhibitor SWM-1. During mating, the male transfers both sperm and seminal fluid containing the trypsin-like serine protease TRY-5 (green) to the hermaphrodite. This causes sperm to mix with TRY-5, which confers a cue to activate. Mature spermatozoa then crawl to the spermathecae to fertilize oocytes.

## Sperm Require SNF-10 to Respond to Extracellular Protease Signals

The screen that identified *snf-10* was done in a *swm-1* mutant background, as Swm males with activated sperm can be visually distinguished from wild-type males with nonactivated sperm. While *swm-1* mutant males are infertile because activated sperm are not transferred to hermaphrodites, we found that both fertility and the timing of activation were restored in males lacking both *swm-1* and *snf-10*. The fertility of these double mutant males led us to reason that *snf-10* would not be generally required for sperm activation, and when we tested this, we found that *snf-10* mutant males and hermaphrodites were both fertile.[17] This is likely because loss of *snf-10* causes a defect that can be circumvented by exposing sperm to hermaphrodite-derived activation signals, which trigger activation through the alternative *spe-8* group pathway.

Because of the design of the screen, we expected *snf-10* mutants to have defects in transducing or responding to the protease activation signal. Additionally, from tissue-specific rescue and inactivation experiments, we determined *snf-10* is both expressed in and functions cell autonomously in sperm. This led to the idea that *snf-10* may be required by sperm to respond to TRY-5 transferred in seminal fluid during mating. To test this hypothesis, we crossed males with defective sperm

but normal seminal fluid to *snf-10* mutant hermaphrodites. In this experiment, it was necessary to block activation through the hermaphrodite pathway.[3] Therefore, in addition to being mutant for *snf-10*, the hermaphrodites used were also mutant for *spe-27*, a member of the *spe-8* group. We found that *spe-27; snf-10* mutant hermaphrodites remained sterile in spite of exposure to male seminal fluid, indicating *snf-10* is required by sperm to respond to the male-derived protease signal. In a complementary experiment, we found *spe-27; snf-10* males are also sterile, as would be expected if both pathways to activation are blocked.[17] In addition to these *in vivo* defects, *snf-10* mutant sperm are also defective in their response to protease activation *in vitro*. When wild-type sperm are treated with protease, they develop cytoskeletal spikes, the MOs fuse with the plasma membrane, and finally, the cells extend a pseudopod and are fully activated.[3] *snf-10* mutant sperm, on the other hand, appear to be completely defective in their response to protease treatment.[17] Not only do the sperm fail to form pseudopods, they do not undergo cytoskeletal spiking or membranous organelle fusion, suggesting SNF-10 is active early in the activation process.

## How Does Localization Impact SNF-10's Function?

The fact that *snf-10* mutant sperm show no detectable response to protease is consistent with what would be expected if SNF-10 were a target of TRY-5 proteolysis. Additionally, when we examined SNF-10's localization, a rescuing SNF-10::mCherry reporter revealed that SNF-10 localizes to the plasma membrane of immature spermatids, which is also consistent with this model, although whether or not SNF-10 is cleaved during activation is still under investigation. Regardless if the interaction between TRY-5 and SNF-10 is direct or indirect, it is clear SNF-10 is key in transducing the protease signal into changes in cellular morphology.

The localization of SNF-10 during activation is dynamic. As spermatids transition into mature spermatozoa, SNF-10 also transitions from being localized across the entire plasma membrane to being polarized to the cell body plasma membrane.[17] This relocalization suggests 2 potential models. The first is that SNF-10 is actively functioning as the sperm respond to TRY-5 (**Fig. 2A**). In this case, SNF-10 could act to transduce the signal, to facilitate changes in sperm morphology, or to provide both of these functions. As a second model, SNF-10 may be acting earlier during sperm development to 'prime' sperm to respond to TRY-5 later on (**Fig. 2B**). For example, SNF-10 could function in spermatocytes to import a cargo that is packaged into spermatids and subsequently used to respond to the protease activation signal. In this second model, SNF-10's dynamic localization could be explained by an earlier interaction with a protein that functions during the activation process, rather than by direct involvement in cellular rearrangements.

SNF-10's polarized localization in spermatozoa represents a unique pattern compared to other sperm membrane proteins studied so far. The cell surface proteins SPE-9 and SPE-38 are restricted to the pseudopod, and other sperm membrane proteins are present on both the pseudopod and cell body.[20,21] There are cellular structures that, like SNF-10, are polarized to the cell body, including the MOs, mitochondria, and nucleus. However, the mechanisms by which this is achieved remain unknown, both at the

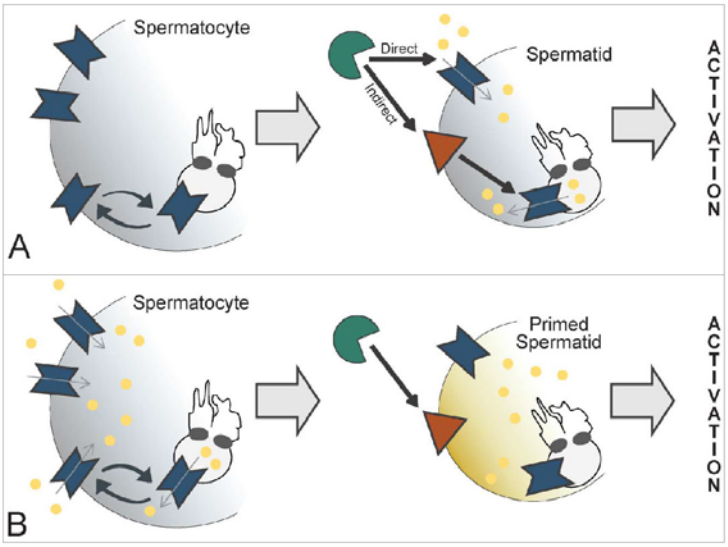


**Figure 2. Models for the regulation and function of SNF-10 in promoting sperm activation.** (**A**) SNF-10 functions in spermatids in response to TRY-5 signaling. TRY-5 (green) acts either directly on SNF-10 (blue) or through an intermediate protein (orange). This signal induces SNF-10's function, which may involve import of cargo or ions (yellow), or participation in protein-protein interactions (not shown). SNF-10 could function either on the cell surface or in MOs. (**B**) SNF-10 acts prior to activation by importing molecules (yellow) required for the activation process. Once primed, the spermatid can activate in response to a TRY-5-mediated signal. (A,B) The subcellular localization of SNF-10 may be regulated in developing spermatocytes.

level of proteins and organelles. Intriguingly, SNF-10's polarized localization in spermatozoa is disrupted in *fer-1* mutants, where the MOs do not fuse with the plasma membrane during activation.[17] This defect suggests that restricted localization of SNF-10 may be dependent on an interaction with either FER-1 or another MO protein that is sequestered when the MOs cannot fuse. It is possible that this protein could regulate the polarization of additional proteins as well, so SNF-10 potentially could be used as a tool to identify factors involved in sperm polarization. Alternatively, SNF-10 could play an active role in polarization. Another SLC6 protein, Bedraggled, plays a role in tissue polarity in *Drosophila*, possibly through protein-protein interactions.[22]

In addition to being localized to the plasma membrane, there is a subset of SNF-10 found on the MOs.[17] Our preliminary data suggests SNF-10 may be regulated at the level of trafficking to control the amount of protein localizing to the plasma membrane as compared to the MOs (**Fig. 2A, B**) (K. Fenker, unpublished results). Because SNF-10 is important in transducing the activation signal, sperm could use this type of regulation to control the amount of SNF-10 present on the plasma membrane, potentially as a means of regulating the strength and duration of downstream signaling cascades. There is precedent for this type of regulation in other signaling pathways.[23] However, this model implies SNF-10 functions from the plasma membrane rather than from the MO membrane, and the site of SNF-10's activity still needs to be tested.

## SNF-10 is a Member of the SLC6 Family

SNF-10 is part of the Solute Carrier 6 (SLC6) family of proteins, which are best-known for importing specific cargo coupled to the symport of sodium, although they can have other functions. SLC6 transporters have cargo such as neurotransmitters, amino acids, or osmolytes, and they are expressed in a wide number of tissue types, causing these proteins to have broad impacts on physiology.[18,19, 24] For example, in the nervous system SLC6 proteins are responsible for clearance of neurotransmitters after synaptic release, while in the intestine and kidney they mediate the absorption of amino acids. It is currently unclear if SNF-10 functions as a canonical SLC6 transporter, but if it does, there are several ways that import of a typical SLC6 substrate could affect sperm physiology. For example, amino acids and osmolytes can stimulate phosphorylation events, increase enzyme activity, or make certain protein conformations more favorable.[25] Any of these processes could promote activation. Additionally, while little is known about the amino acid content of *C. elegans* seminal fluid, the seminal fluid of *A. suum*, a related nematode, contains at least 16 types of free amino acids and is particularly enriched for lysine.[26] Amino acids may be present in *C. elegans* seminal fluid as well, and SNF-10 would have access to these molecules based on the protein's plasma membrane localization.

While import of specific cargo into the sperm cytoplasm could allow SNF-10 to promote sperm activation, based on amino acid sequence it is currently unclear if SNF-10 should actually be expected to function in this way. SNF-10 shares the greatest amount of homology with glycine transporters. However, residues involved in substrate and ion binding are not particularly well-conserved in SNF-10, as compared to either glycine transporters or other SLC6 transporters with known cargo. Additionally, no obvious cargo is present in the medium used to activate sperm *in vitro*. While it will be interesting to test if SNF-10 has specific cargo, some SLC6 family members exhibit ion channel activity in the absence of cargo movement,[27] and SNF-10 could reasonably promote activation through a role in ion flux as well.

Ion flux is well-studied in flagellate sperm and is involved in capacitation, the acrosome reaction, and initiation of intracellular signaling. None of the proteins implicated in these processes so far are SLC6 proteins; instead, they include the sperm-associated cation channels (CatSpers1, 2, 3, and 4), transient receptor potential (TRP) channels, proton, potassium, and sodium voltage-gated ion channels (Hv1, SLO3, and Nav1.1-1.9), and others.[28] In *C. elegans*, there is still much to be learned about how ion flux affects sperm, though activation does involve an elevation in $pH$[29] and the release of intracellular $Ca^{2+}$.[7] Additionally, nematode sperm appear to be sensitive to the type and concentration of ions present, as they activate *in vitro* when certain chloride channels are blocked,[30] in the presence of the weak base TEA,[29] or when sperm are treated with the ionophore monensin.[31] However, few ion channels have been identified in nematode sperm, and their roles in activation are not well understood. The main example is TRP-3/SPE-41, a calcium-permeable cation channel that relocalizes from the MOs to the plasma membrane during activation and mediates sperm-egg interactions.[6] Additionally, multiple channel activities have been detected in spermatocytes and residual bodies, and activity of an inward-rectifying chloride channel has been observed in spermatids, but the proteins themselves have not been identified yet.[30]

## Is There a Widespread Role for SLC6 Transporters in Male Reproduction?

Our recent identification of SNF-10 and its function in sperm, combined with other recent examples of SLC6 proteins expressed in sperm or the testis, indicates these transporters may be important for male fertility in a number of species. For example, spermatogenesis in *Drosophila* requires the SLC6 protein Neurotransmitter transporter-like (Ntl), which, like SNF-10, shares the greatest amount of its amino acid sequence with glycine transporters.[32] Additionally, *Anguilla japonica* (japanese eels) may use an SLC6 taurine transporter during spermatogenesis,[33] and human males express the orphan SLC6 protein NTT5[34] and the creatine transporter SLC6A10 in the testes.[35] In all of these cases, more exploration is needed to determine how the proteins are functioning. Therefore, it is possible that in addition to sharing roles in sperm physiology, the proteins may be acting through similar

mechanisms or in similar pathways as well. Alternatively, SNF-10 and some or all of the other transporters may have divergent functions, which would not be surprising due to their involvement in reproduction. In this case, it would be interesting to investigate if certain properties of SLC6 proteins have caused them to be repeatedly co-opted by reproductive processes. We were unable to identify a clear ortholog of SNF-10 from more distant species, such as *A. suum* or *P. pacificus*, but because SNF-10 is clearly conserved in closely related nematodes this suggests that even if the protein is divergent, it is important within *Caenorhabditis* for promoting reproductive success.

As far as we know, transducing a protease signal is a novel role for an SLC6 transporter. While we do not yet know if SNF-10 and TRY-5 directly interact or if they are simply part of the same signal transduction pathway, in either case it will be interesting to learn if SLC6 regulation by proteases could be more widespread, both in sperm development and elsewhere. Other SLC6 transporters expressed in the nervous system have been shown to be cleaved by calpain-family proteases, but this cleavage led to reduced activity or no functional change, although it was thought to disrupt protein-protein interactions.[36,37] The effect of protease activity in these experiments is thus different from the positive regulation protease signaling imparts on SNF-10, which based on our genetic experiments would likely induce or perhaps alter protein activity. In terms of protease regulation of sperm biology, proteomic studies have identified a large number of proteases in seminal fluid from insects to mammals, but few of these proteins have well-described functions.[38] Additionally, while a number of serine proteases and serine protease inhibitors are produced by the mouse testis,[39] little is known about the signaling cascades they are involved in and how they may impact sperm motility. Our identification of SNF-10 as a protein required for responding to an extracellular protease represents an opportunity to study a signaling cascade initiated by a protease, and importantly, to learn how an SLC6 protein can be used by cells to gain motility.

### Disclosure of Potential Conflicts of Interest

No potential conflicts of interest were disclosed.


### Funding

This work was supported by NIH R01-GM087705 to G.M.S. and by 5T32HD007491 to K.E.F.


### References


1. Suarez S. Regulation of sperm storage and movement in the mammalian oviduct. Int J Dev Biol 2008; 52:455-62; PMID:18649258; http://dx.doi.org/10.1387/ijdb.072527ss
2. Urner F, Sakkas D. Protein phosphorylation in mammalian spermatozoa. Reproduction 2003; 125:17-26; PMID:12622692; http://dx.doi.org/10.1530/rep.0.1250017
3. Shakes D, Ward S. Initiation of spermiogenesis in *C. elegans*: a pharmacological and genetic analysis. Dev Biol 1989; 134:189-200; PMID:2731646; http://dx.doi.org/10.1016/0012-1606(89)90088-2
4. Nelson G, Roberts T, Ward S. *C. elegans* spermatozoan locomotion: amoeboid movement with almost no actin. J Cell Biol 1982; 92:212-131; PMID:7199049; http://dx.doi.org/10.1083/jcb.92.1.121
5. Ward S, Argon Y, Nelson G. Sperm morphogenesis in wild-type and fertilization-defective mutants of *C. elegans*. J Cell Biol 1981; PMID:7298721
6. Xu X, Sternberg P. A *C. elegans* sperm TRP protein required for sperm-egg interactions during fertilization. Cell 2003; 114:285-97; PMID:12914694; http://dx.doi.org/10.1016/S0092-8674(03)00565-8
7. Washington N, Ward S. FER-1 regulates Ca2+-mediated membrane fusion during *C. elegans* spermatogenesis. J Cell Sci 2006; 119:2552-62; PMID:16735442; http://dx.doi.org/10.1242/jcs.02980
8. de Lamirande E, Leclerc, P, Gagnon C. Capacitation as a regulatory event that primes spermatozoa for the acrosome reaction and fertilization. Mol Hum Reprod 1997; 3:175-94; PMID:9237244; http://dx.doi.org/10.1093/molehr/3.3.175
9. Inoue N, Ikawa M, Isotani A, Okabe M. The immunoglobulin superfamily protein Izumo is required for sperm to fuse with eggs. Nature 2005; 434:234-8; PMID:15759005; http://dx.doi.org/10.1038/nature03362
10. L'Hernault, S. Spermatogenesis (February 20, 2006), *WormBook*, ed. The *C. elegans* Research Community, http://dx.doi.org/10.1895/wormbook.1.85.1, http://www.wormbook.org
11. L'Hernault S, Shakes D, Ward S. Developmental genetics of chromosome I spermatogenesis-defective mutants in the nematode *C. elegans*. Genetics 1988; 120:435-52; PMID:3197956
12. Geldziler B, Chatterjee I, Singson A. The genetic and molecular analysis of *spe-19*, a gene required for sperm activation in *C. elegans*. Dev Biol 2005; 283:424-36; PMID:15939418; http://dx.doi.org/10.1016/j.ydbio.2005.04.036
13. Liu Z, Chen L, Shang Y, Huang P, Miao L. The micronutrient element zinc modulates sperm activation through the SPE-8 pathway in *C. elegans*. Development 2013; 140:2103-7; PMID:23578924; http://dx.doi.org/10.1242/dev.091025
14. Stanfield G, Villeneuve A. Regulation of sperm activation by SWM-1 is required for reproductive success of *C. elegans* males. Curr Biol 2006; 16:252-63; PMID:16461278; http://dx.doi.org/10.1016/j.cub.2005.12.041
15. Argon Y, Ward S. *C. elegans* fertilization-defective mutants with abnormal sperm. Genetics 1980; 96:413-33; PMID:7196361
16. Smith J, Stanfield G. TRY-5 is a sperm-activating protease in *C. elegans* seminal fluid. PLoS Genetics 2011; 7:e1002375; PMID:22125495; http://dx.doi.org/10.1371/journal.pgen.1002375
17. Fenker K, Hansen A, Chong C, Jud M, Duffy B, Norton J, Hansen J, Stanfield G. SLC6 family transporter SNF-10 is required for protease-mediated activation of sperm motility in *C. elegans*. Dev Biol 2014; 393:171-82; PMID:24929237; http://dx.doi.org/10.1016/j.ydbio.2014.06.001
18. Bröer S, Gether U. The solute carrier 6 family of transporters. Br J Pharmacol 2012; 167:256-78; PMID:22519513; http://dx.doi.org/10.1111/j.1476-5381.2012.01975.x
19. Kristensen A, Andersen J, Jørgensen T, Sørensen L, Eriksen J, Loland C, Strømgaard K, Gether U. SLC6 neurotransmitter transporters: structure, function, and regulation. Pharmacol Rev 2011; 63:585-640; PMID:21752877; http://dx.doi.org/10.1124/pr.108.000869
20. Chatterjee I, Richmond A, Putiri E, Shakes DC, Singson A. The *C. elegans spe-38* gene encodes a novel four-pass integral membrane protein required for sperm function at fertilization. Development 2005; 132:2795-808; PMID:15930110; http://dx.doi.org/10.1242/dev.01868
21. Zannoni S, L'Hernault S, Singson A. Dynamic localization of SPE-9 in sperm: a protein required for sperm-oocyte interactions in *C. elegans*. BMC Dev Biol 2003; 3:10; PMID:14653860; http://dx.doi.org/10.1186/1471-213X-3-10
22. Rawls A, Schultz S, Mitra R, Wolff T. Bedraggled, a putative transporter, influences the tissue polarity complex during the R3/R4 fate decision in the Drosophila eye. Genetics 2007; 177:313-28; PMID:17890365; http://dx.doi.org/10.1534/genetics.107.075945
23. Golub T, Wacha S, Caroni P. Spatial and temporal control of signaling through lipid rafts. Curr Opin Neurobiol 2004; 14:542-50; PMID:15464886; http://dx.doi.org/10.1016/j.conb.2004.08.003
24. Rudnick G, Kramer R, Blakely R, Murphy D, Verrey F. The SLC6 transporters: perspectives on structure, functions, regulation, and models for transporter dysfunction. Eur J Physiol 2014; 466:25-42; http://dx.doi.org/10.1007/s00424-013-1410-1
25. Khan S, Ahmad N, Ahmad F, Kumar R. Naturally occurring organic osmolytes: from cell physiology to disease prevention. IUBMB Life 2010; 62:891-5; PMID:21190292; http://dx.doi.org/10.1002/iub.406
26. Abbas M, Foor W. *Ascaris suum*: free amino acids and proteins in the pseudocoelom, seminal vesicle, and glandular vas deferens. Exp Parasitol 1978; 45:263-73; PMID:680082; http://dx.doi.org/10.1016/0014-4894(78)90068-1
27. DeFelice L, Goswami T. Transporters as channels. Ann Rev Physiol 2007; 69:87-112; PMID:17059369; http://dx.doi.org/10.1146/annurev.physiol.69.031905.164816
28. Shukla K, Mahdi A, Rajender S. Ion channels in sperm physiology and male fertility and infertility. J Androl 2012; 33:777-88; PMID:22441763; http://dx.doi.org/10.2164/jandrol.111.015552
29. Ward S, Hogan, E, Nelson GA. The initiation of spermiogenesis in the nematode *C. elegans*. Dev Biol 1983; 98:70-9; PMID:6345236
30. Machaca K, DeFelice L, L'Hernault S. A novel chloride channel localizes to *C. elegans* spermatids and chloride channel blockers induce spermatid differentiation. Dev Biol 1996; 176:1-16; PMID:8654886; http://dx.doi.org/10.1006/dbio.1996.9999
31. Nelson G, Roberts T, Ward S. Vesicle fusion, pseudopod extension and amoeboid motility are induced in nematode spermatids by the ionophore monensin. Cell

1980; 19:457-64; PMID:7357613; http://dx.doi.org/10.1016/0092-8674(80)90520-6

32. Chatterjee N, Rolling J, Mahowald A, Bazinet C. Neurotransmitter transporter-like: a male germline-specific SLC6 transporter required for *Drosophila* spermiogenesis. PLoS One 2011; 6; e16275; PMID:21298005
33. Higuchi M, Miura C, Iwai T, Miura T. Trypsin regulates meiotic initiation in the Japanese eel (*Anguilla japonica*) by promoting the uptake of taurine into germ cells during spermatogenesis. Biol Rep 2013; 89:58; PMID:23926282; http://dx.doi.org/10.1095/biolreprod.113.109777
34. Farmer M, Robbins M, Medhurst A, Campbell D, Ellington K, Duckworth M, Brown A, Middlemiss D, Price G, Pangalos M. Cloning and characterization of human NTT5 and v7-3: two orphan transporters of the $Na^+/Cl^-$-dependent neurotransmitter transporter gene family. Genomics 2000; 70:241-52; PMID:11112352; http://dx.doi.org/10.1006/geno.2000.6387
35. Iyer G, Krahe R, Goodwin L, Doggett N, Siciliano M, Funanage V, Proujansky R. Identification of a testis-expressed creatine transporter gene at 16p11.2 and confirmation of the X-linked locus to Xq28. Genomics 1996; 34:143-6; PMID:8661037; http://dx.doi.org/10.1006/geno.1996.0254
36. Baliova M, Jursky F. Calcium dependent modification of distal C-terminal sequences of glycine transporter GlyT1. Neurochem Int 2010; 57:254-61; PMID:20542070; http://dx.doi.org/10.1016/j.neuint.2010.06.003
37. Baliova M, Knab A, Franekova V, Jursky F. Modification of the cytosolic regions of GABA transporter GAT1 by calpain. Neurochem Int 2009; 55:288-94; PMID:19576516; http://dx.doi.org/10.1016/j.neuint.2009.03.012
38. Laflamme B, Wolfner M. Identification and function of proteolysis regulators in seminal fluid. Mol Rep Dev 2013; 80:80-101; PMID:23109270; http://dx.doi.org/10.1002/mrd.22130
39. Odet F, Verot A, Le Magueresse-Battistoni B. The mouse testis is the source of various serine proteases and serine proteinase inhibitors (SERPINs): Serine proteases and SERPINs identified in Leydig cells are under gonadotropin regulation. Endocrinology 2006; 147:4374-83; PMID:16740973

# CHAPTER 6

# THE ROLE OF SNF-10 IN SIGNAL TRANSDUCTION

## Introduction

For most cell types, the ability to receive, interpret, and undergo an appropriate response to extracellular signals is critical for proper function. Sperm are particularly dependent on sensing their environment and responding to extracellular cues. They receive signals from their environment that regulate onset of motility, as well as cues from the female reproductive tract that guide migration toward oocytes. In many cell types, transduction of signals ultimately leads to changes in transcription and translation. However, sperm are unique in that their chromatin becomes very compact during development (Sassone-Corsi, 2002). This protects the DNA, but the cell can no longer produce new gene products, and therefore, sperm rely heavily on protein-protein interactions, ion balance, other biochemical interactions to regulate their response to environmental cues (discussed in Ellis and Stanfield, 2014).

In *C. elegans* sperm, a signaling pathway induces cell motility in response to a protease signal in seminal fluid (Stanfield and Villeneuve, 2006; Smith and Stanfield, 2011). This signal is transduced via the Solute Carrier 6 (SLC6) family protein, SNF-10, and SNF-10 provides the first known molecular link connecting the protease signal to changes in sperm motility (Fenker et al., 2014). When wild-type sperm receive the

protease signal, either through a mutation in the protease inhibitor *swm-1* in vivo or with Pronase treatment in vitro, they undergo a number of easily observed changes. In a process termed sperm activation, membrane fusion events, polarization, and cytoskeletal reorganization culminate to form a motile sperm cell with a pseudopod for crawling (Ward, 1983).

In Chapter 4, I demonstrate that while SNF-10 is downstream from the protease signal, it is also upstream of any detectable change in sperm physiology induced by protease exposure. *snf-10* mutant sperm showed no observable membrane fusion, polarization, or pseudopod formation upon either loss of *swm-1* or exposure to Pronase (Fenker et al., 2014). Based on these data, we hypothesize SNF-10 has an early role in transducing the protease signal. Additionally, I show via a C-terminal SNF-10::mCherry fusion that SNF-10 localizes to the sperm plasma membrane. Signals from a cell's environment can be transduced in a variety of ways, although typically, the signal is received by a receptor protein on the cell's plasma membrane and amplified by an intracellular network. Therefore, one hypothesis for SNF-10's function is that the protein could be directly responsible for receiving the sperm activation signal and propagating it into the cell to initiate activation (Fenker and Stanfield, 2015) (see Chapter 5 for more detail).

SLC6 proteins like SNF-10 are best known for importing neurotransmitters, amino acids, or osmolytes into cells, in a sodium- and sometimes chloride-dependent manner. They have well-established roles in synaptic transmission, neurotransmitter recycling, metabolic function, and fluid homeostasis (reviewed in Kristensen et al., 2011; Rudnick et al., 2014), but there may be roles for SLC6 transporters beyond their co-

transporter function as well. These additional roles include ion channel activity in the absence of substrate (DeFelice and Goswami, 2007), and perhaps establishing tissue polarity via protein-protein interactions (Rawls et al., 2007).

SNF-10 is a conserved SLC6 protein in that it shares the 12 transmembrane-domain structure characteristic to the family (Pramod et al., 2013), yet not all residues involved in substrate or ion binding are conserved in SNF-10 (Fenker et al., 2014). Therefore, it is difficult to predict if SNF-10 should be expected to have a typical SLC6 co-transport function or a different role during sperm development. Our identification of SNF-10 as part of a protease signaling cascade represents a novel means of regulation for an SLC6 protein, so a less-typical function would not be entirely unexpected.

In this chapter, I describe experiments designed to test several models SNF-10's function during the onset of sperm motility. I make an effort to address several outstanding questions regarding the mechanism of how SNF-10 transduces the protease activation signal to ultimately change sperm physiology. Is SNF-10 cleaved by a protease? Does SNF-10 function as a typical SLC6 co-transporter? In what other ways could SNF-10 transduce the protease signal into sperm? While none of the following experiments are entirely conclusive, I present the data obtained and discuss its potential indications, as well as how these experiments can be expanded in the future to better understand SNF-10.

## Materials and Methods

### Molecular biology

Standard procedures for molecular biology were used. Single-copy transgenic strains were generated using MosSCI (Frokjaer-Jensen et al., 2008; Frokjaer-Jensen et al., 2012). *Phsp16.2::snf-10::mCherry* was generated in the pCFJ150 vector using Gateway cloning (Life Technologies) and injected into *ttTi5605; unc-119* hermaphrodites. Heat-shock was performed at 34ºC for 2 hr, plates placed at 20ºC to recover for 6 hr, then worms were either used immediately in western blots or flash frozen and stored at -80ºC.

Constructs for *Xenopus laevis* injection were generated in the pCFJ240 vector using Gateway cloning. RNAs were prepared using the T7 mMessage mMachine kit (Ambion), according to kit instructions. Integrity of the final product was confirmed by gel electrophoresis.

### Western blots

Over 30 western blot procedures were performed in order to troubleshoot detection of SNF-10::mCherry. For the basic protocol, 400 virgin, 48 hr post L4 males were added to lysis buffer (100 mM Tris, pH 6.8, 2% SDS, 5% ß- mercaptoethanol, 15% glycerol, 8 M urea, and bromophenol blue), and run on a 6.5 or 7% gel using standard SDS-PAGE protocols. Brief sonication or passage through a syringe was often used to break up DNA and facilitate loading.

Variations included: overexpression of SNF-10::mCherry, use of alternative lysis buffers (Lamelli, RIPA, and NP-40), isolation of membrane fractions from worm lysates with the Mem-PER Plus Membrane Protein Extraction Kit (ThermoFisher), specialized

membrane protein protocols as in Abeyrathne and Lam (Abeyrathne and Lam, 2007), variation of transfer time and buffers, transfer to nitrocellulose and PVDF membranes, and alternative primary antibodies (Abcam anti-mCherry, Clontech anti-mCherry, and Rockland anti-RFP).

**In vitro sperm activation**

Sperm from 24-48 hr *jnSi96[snf-10::mCherry]; him-5(e1490)* males were dissected into Sperm Medium (5 mM HEPES pH 7.4, 50 mM NaCl, 25 mM KCl, 5 mM $CaCl_2$, 1 mM $MgSO_4$, and 10 mM dextrose) (Nelson et al., 1980). The sperm medium contained either 200 µg/ml Pronase or 60 mM triethanolamine (TEA) (Shakes and Ward, 1989). Sperm were imaged every 3 min for up to 21 min to observe activation.

**Electrophysiology**

The procedures for microinjection, superfusion, and voltage clamping of *Xenopus laevis* oocytes have been described previously (Fei et al., 1998; Jiang et al., 2005). Briefly, capped *snf-10* (50 ng), *snf-10::FLAG* (50 ng), or *snf-3* (5 ng) RNAs were injected into *Xenopus* oocytes. Oocytes were then stored at 18ºC in SuperBarth's (88 mM NaCl, 1 mM KCl, 0.41 mM $CaCl_2$, 0.33 mM $Ca(NO_3)_2$, 1 mM $MgSO_4$, 2.4 mM $NaHCO_3$, 10 mM HEPES, 1 mM pyruvate, 100 units/ml penicillin, 100 µg/ml streptomycin, 0.25 µg/ml amphotericin B, pH 7.2). Recordings were performed 3-4 days after injection, using the two-electrode voltage clamp method with the voltage clamped at -60 mV. The standard bath solution was Ringer's (115 mM NaCl, 2.5 mM KCl, 1.8 mM $CaCl_2$, 10 mM Hepes, pH 7.2). Each oocyte was subjected to 20 s application of plain

Ringer's, 60 s substrate (in Ringer's) followed by a 40 s Ringer's wash. Candidate SNF-10 substrates were purchased from Sigma and used at 10 mM. When Pronase was used, oocytes were incubated in 200 µg/ml Pronase in Ringer's for 5 min just prior to perfusion. Each candidate substrate for SNF-10 was tested on 2-7 different oocytes. For the positive control, *snf-3*-injected oocytes were perfused with 2.5 mM betaine.

## Results

### SNF-10 cleavage by the protease activation signal is unclear

SNF-10 localizes to the sperm plasma membrane downstream of the protease activation signal (Fenker et al., 2014). Therefore, one model is that cleavage of SNF-10 may take place during the process of sperm activation. To test this idea, I used strains expressing a *SNF-10::mCherry* transgene in either a wild-type background or a *swm-1(me87)* background, in which sperm are exposed to the protease activation signal (Stanfield and Villeneuve, 2006; Smith and Stanfield, 2011). I then performed western blots and probed for SNF-10::mCherry. If SNF-10 were a direct target of the activation signal, I expected to observe full length SNF-10::mCherry in the wild-type background, with a smaller band resulting from cleavage in the *swm-1* mutant background.

Unfortunately, after many attempts at probing for SNF-10::mCherry, I was unable to detect the protein via western blot for either genotype, although an alternative sperm protein with the same tag, COMP-1::mCherry, was detected. An example of a typical western blot is shown in Figure 6.1A. Along with testing a variety of lysis buffers, transfer conditions, membrane types, and antibodies, I also generated strains that overexpressed SNF-10::mCherry via a heat-shock inducible promoter, and isolated and

probed membrane fractions (see Materials and Methods). However, SNF-10::mCherry remained undetectable, and thus, it remains unclear if SNF-10 is cleaved during sperm activation.

**SNF-10 localization does not change in response to different in vitro activators**

*C. elegans* sperm can be activated in vitro by a number of compounds that alter cell physiology in ways that are thought to tie into the in vivo activation pathway. Two examples of such compounds include Pronase and triethanolamine (TEA). Pronase is a commercially available mixture of proteases thought to mimic the activation signal in seminal fluid (Smith and Stanfield, 2011), while TEA leads to alkalization of the sperm cytoplasm and is thought to bypass the requirement for an activation signal (Ward, 1983). Because *snf-10* mutant sperm activate at wild-type levels in response to TEA, but show no response to Pronase (Fenker et al., 2014) (Chapter 4), I hypothesized the dynamic localization of SNF-10::mCherry during sperm activation may be different in response to TEA compared to Pronase, and would lend insight as to the mechanism of SNF-10's function. Therefore, I dissected sperm from SNF-10::mCherry males into media containing either TEA or Pronase, and performed time-lapse imaging to track the localization of SNF-10::mCherry during sperm activation.

The localization pattern of SNF-10::mCherry remained dynamic yet consistent as sperm activated, regardless of whether TEA or Pronase was used to trigger activation. Representative time-points from the experiments are shown in Figure 6.2A-F. Shortly after exposure to activator, most SNF-10::mCherry localized to the cell periphery (Figure

6.2A,D). By 3-6 min after dissection, membrane fusion events were visible as puncta near the cell periphery (Figure 6.2B,E), and at later time-points, these puncta took on a polarized localization and were present in a "C" shaped pattern along the periphery of the sperm cell body and absent from the pseudopod (Figure 6.2C,F). As SNF-10::mCherry has faint fluorescence and is prone to photobleaching, I also performed antibody staining with fixation at several time-points after dissecting sperm into TEA or Pronase, and confirmed the same localization patterns (data not shown). Thus, the dynamic localization of SNF-10 during sperm activation is not dependent on receiving the protease signal.

**A specific cargo for SNF-10 is not yet identified**

The best-studied function for SLC6 family proteins is their role as co-transporters, and many members of the family transport a specific substrate (or small set of substrates) into cells in a sodium-dependent manner (Wang and Lewis, 2010). To test if SNF-10 functions as a transporter, I expressed SNF-10 in *Xenopus laevis* oocytes and used the two microelectrode voltage clamp method to assay if exposure to candidate cargo was electrogenic, as would be expected if ion-coupled transport occurs (Fei et al., 1998).

A list of candidate cargo for SNF-10 is shown in Figure 6.3A. Candidates comprise both substrates common to SLC6 transporters as well as free amino acids present in the seminal fluid of *Ascaris suum*, a nematode closely related to *C. elegans* (Abbas and Foor, 1978). I tested these initial candidates in oocytes injected with *snf-10* cRNA, and observed no generation of current above baseline. An example recording is shown in 6.3B, where glycine was tested as a potential substrate. SNF-10 shares the

greatest amount of sequence similarity to the human glycine transporter SLC6A5/GlyT2; however, the substrate binding residues are somewhat divergent in SNF-10 (Fenker et al., 2014). Because it remains a possibility that SNF-10 must be cleaved in order to function, I next tested the same candidate substrates on oocytes that were incubated with Pronase for 5 min just prior to recording. As before, no transport of a SNF-10-specific cargo was observed. There were two candidate substrates, lysine and arginine, that produced small currents under the Pronase-treatment conditions, but the same current was produced by both *snf-10*-injected oocytes and water-injected controls, suggesting this was due to Pronase and not a SNF-10-specific event (data not shown).

To confirm the electrophysiology was being performed appropriately, I expressed SNF-3, a previously characterized *C. elegans* SLC6 betaine transporter, in *Xenopus* oocytes and confirmed perfusion with betaine was electrogenic (Peden et al., 2013), (Figure 6.3C). The *snf-3*-injected oocytes appeared much less healthy compared to either *snf-10*-injected oocytes or water-injected controls. To test if SNF-10 was being expressed by the *Xenopus* oocytes, I injected oocytes with a C-terminal *snf-10*::3xFLAG fusion, and performed western blots. I was unable to detect SNF-10::FLAG via western blot (Figure 6.3D); however, no western blot for SNF-10 has ever worked, thus leaving the expression of SNF-10 by oocytes uncertain. Injection of a SNF-10::GFP fusion did produce oocytes with faint fluorescence on a dissecting microscope (data not shown), but further analysis is needed to determine whether or not the protein localizes to the surface of the oocytes. For all electrophysiology experiments, I performed electrophoresis to analyze the RNA produced prior to oocyte injection, to confirm it was the appropriate size and not degraded. From these experiments, I was unable to identify a specific substrate for SNF-

10, and further analysis with expanded substrates and confirmed surface expression of SNF-10 should be considered.

## Discussion

During sperm development, the timing of sperm activation is very important. If sperm are activated too early, they cannot be transferred from males to hermaphrodites and males are sterile (Stanfield and Villeneuve, 2006). Our lab identified a protease signal that regulates this important event (Smith and Stanfield, 2011), and signals via the SLC6 protein SNF-10 to initiate a number of physiological changes to allow sperm to become motile and fertilization competent. The mechanism of SNF-10's function and how the protein affects sperm physiology remains unknown. In this chapter, I tested several models for SNF-10's function.

Is SNF-10 cleaved during activation? While I attempted to clarify this question with western blots to visualize the size of the SNF-10 protein under normal and protease-exposed conditions, these experiments were inconclusive. The question of SNF-10 cleavage is an important one; if SNF-10 cleavage is necessary and sufficient for sperm activation, this would strengthen the model that it is a direct target of the protease signal. Our identification of SNF-10 functioning within a protease signaling cascade is novel, and identification of direct cleavage by a protease would allow for this mechanism of SLC6 transporter regulation to be easily tested in other contexts and tissues as well.

The structure of SNF-10 contains 12 transmembrane domains connected by intra and extracellular loops, based on predictions made by the transmembrane prediction software TMpred, and consistent with the crystal structure of another SLC6 family

member (Yamashita et al., 2005). While predicted trypsin cleavage sites occur across the protein, over half of them are concentrated together on one specific extracellular loop, while the rest are predominantly intracellular (predicted by ExPASy PeptideCutter). Therefore, I hypothesize that if SNF-10 is cleaved during activation, it is likely to occur to this extracellular loop. Experiments to engineer a cleavage site at this predicted location, for example an Tobacco Etch Virus (TEV) site, combined with experiments to remove the endogenous trypsin sites would be informative in understanding the role of cleavage on SNF-10's function.

Does SNF-10 transport a specific cargo into sperm? Using electrophysiology, I have thus far been unable to detect a specific cargo for SNF-10. While it cannot be ruled out that this is how SNF-10 functions, it would not be my first prediction. While SNF-10 is clearly in the SLC6 family (Fenker et al., 2014), many of the residues involved in sodium or substrate binding that are highly conserved in other SLC6 proteins are divergent in SNF-10. Additionally, sperm activation in response to Pronase can be triggered in vitro, in media containing sodium, potassium, calcium, and magnesium, but no obvious cargo molecules for an SLC6 protein. If SNF-10 does function through cargo transport, the cargo must come from sperm during activation. This also seems unlikely, as the main exocytosis event during sperm activation (MO fusion) occurs after receiving the protease signal and is dependent on the presence of SNF-10 (Fenker 2014), although we cannot rule out at this point that cargo could be delivered to the sperm surface in another manner. I hypothesize it is more likely for SNF-10 to function through channel activity or protein-protein interactions, rather than amino acid transport. This function of SNF-10 could be assayed using radiometric dyes that indicate ion concentrations within cells (as

in Tsien, 1989 or Rong et al., 2017), and by using CRISPR-directed modifications to SNF-10 to probe candidate protein-protein interaction sites that can be predicted based on SNF-10's amino acid sequence.

The identification of SNF-10 provides the first link between the environmental protease signal and sperm themselves, and future work on how SNF-10 functions will answer interesting questions about how sperm maturation is regulated. Genetic screens performed by others in the lab have obtained many more mutants with defects in sperm activation in response to protease signaling. Identifying the genes disrupted by these mutations will also be important to further clarify transduction of the protease signaling pathway, including the specific contribution of SNF-10 during the onset of sperm motility.

## Acknowledgements

I would like to thank the many people who gave me advice on western blotting, especially Jon Nelson for sharing equipment, and members of the Thummel and Elde labs for advice and lending me various reagents to try. I would also like to thank the Jorgensen lab for reagents and allowing me to use electrophysiology equipment, especially Patrick Mac for training me on how to perform experiments, including oocyte injections and using the electrophysiology rig, sharing reagents, and answering my many questions.

## References

Abbas, M., Foor, W., 1978. *Ascaris suum*: free amino acids and proteins in the pseudocoelom, seminal vesicle, and glandular vas deferens. Exp. Parasitol. 45, 263-273.

Abeyrathne, P.D., Lam, J.S., 2007. Conditions that allow for effective transfer of membrane proteins onto nitrocellulose membrane in western blots. Can. J. Microbiol. 53, 526-532.

DeFelice, L., Goswami, T., 2007. Transporters as channels. Annu. Rev. Physiol. 69, 87-112.

Ellis, R.E., Stanfield, G.M., 2014. The regulation of spermatogenesis and sperm function in nematodes. Semin. Cell Dev. Biol. 29, 17-30.

Fei, Y., Fujita, T., Lapp, D., Ganapathy, V., Leibach, F., 1998. Two oligopeptide transporters from *C. elegans*: molecular cloning and functional expression. Biochem. J. 332 565-572.

Fenker, K.E., Hansen, A.A., Chong, C.A., Jud, M.C., Duffy, B.A., Paul Norton, J., Hansen, J.M., Stanfield, G.M., 2014. SLC6 family transporter SNF-10 is required for protease-mediated activation of sperm motility in *C. elegans*. Dev. Biol. 393, 171-182.

Fenker, K.E., Stanfield, G.M., 2015. SNF-10 connects male-derived signals to the onset of sperm motility in C. elegans. Worm 4, e1003002.

Frokjaer-Jensen, C., Davis, M.W., Ailion, M., Jorgensen, E.M., 2012. Improved Mos1-mediated transgenesis in *C. elegans*. Nat. Methods 9, 117-118.

Frokjaer-Jensen, C., Davis, M.W., Hopkins, C.E., Newman, B.J., Thummel, J.M., Olesen, S.P., Grunnet, M., Jorgensen, E.M., 2008. Single-copy insertion of transgenes in *Caenorhabditis elegans*. Nat. Genet. 40, 1375-1383.

Jiang, G., Zhuang, L., Miyauchi, S., Miyake, K., Fei, Y.J., Ganapathy, V., 2005. A Na+/Cl- -coupled GABA transporter, GAT-1, from Caenorhabditis elegans: structural and functional features, specific expression in GABA-ergic neurons, and involvement in muscle function. J. Biol. Chem. 280, 2065-2077.

Kristensen, A., Andersen, J., Jørgensen, T., Sørensen, L., Eriksen, J., Loland, C., Strømgaard, K., Gether, U., 2011. SLC6 neurotransmitter transporters: structure, function, and regulation. Pharmacol. Rev. 63, 585-640.

Nelson, G., Roberts, T., Ward, S., 1980. Vesicle fusion, pseudopod extension and amoeboid motility are induced in nematode spermatids by the ionophore monensin. Cell 19, 457-464.

Peden, A., Mac, P., Fei, Y.-J., Castro, C., Jiang, G., Murfitt, K., Miska, E., Griffin, J., Ganapathy, V., Jorgensen, E., 2013. Betaine acts on a ligand-gated ion channel in the nervous system of the nematode *C. elegans*. Nat. Neurosci. 16, 1794-1801.

Pramod, A., Foster, J., Carvelli, L., Henry, L., 2013. SLC6 transporters: structure, function, regulation, disease association and therapeutics. Mol. Aspects Med. 34, 197-219.

Rawls, A.S., Schultz, S.A., Mitra, R.D., Wolff, T., 2007. Bedraggled, a putative transporter, influences the tissue polarity complex during the R3/R4 fate decision in the *Drosophila* eye. Genetics 177, 313-328.

Rong, G., Kim, E.H., Poskanzer, K.E., Clark, H.A., 2017. A method for estimating intracellular ion concentration using optical nanosensors and ratiometric imaging. Sci. Rep. 7, 10819.

Rudnick, G., Kramer, R., Blakely, R., Murphy, D., Verrey, F., 2014. The SLC6 transporters: perspectives on structure, functions, regulation, and models for transporter dysfunction. European J. Physiol. 466, 25-42.

Sassone-Corsi, P., 2002. Unique chromatin remodeling and transcriptional regulation in spermatogenesis. Science 296, 2176-2178.

Shakes, D.C., Ward, S., 1989. Initiation of spermiogenesis in *C. elegans*: a pharmacological and genetic analysis. Dev. Biol. 134, 189-200.

Smith, J., Stanfield, G., 2011. TRY-5 is a sperm-activating protease in *C. elegans* seminal fluid. PLoS Genetics 7.

Stanfield, G., Villeneuve, A., 2006. Regulation of sperm activation by SWM-1 is required for reproductive success of *C. elegans* males. Curr. Biol. 16, 252-263.

Tsien, R.Y., 1989. Fluorescent indicators of ion concentrations. Methods Cell Biol. 30, 127-156.

Wang, C.-I.A., Lewis, R., 2010. Emerging structure-function relationships defining monoamine NSS transporter substrate and ligand affinity. Biochem. Pharmacol. 79, 1083-1091.

Ward, S., Hogan, E., Nelson, G., 1983. The initiation of spermiogenesis in the nematode *C. elegans*. Dev. Biol. 98, 70-79.

Yamashita, A., Singh, S., Kawate, T., Jin, Y., Gouaux, E., 2005. Crystal structure of a bacterial homologue of Na+/Cl--dependent neurotransmitter transporters. Nature 437, 215-223.

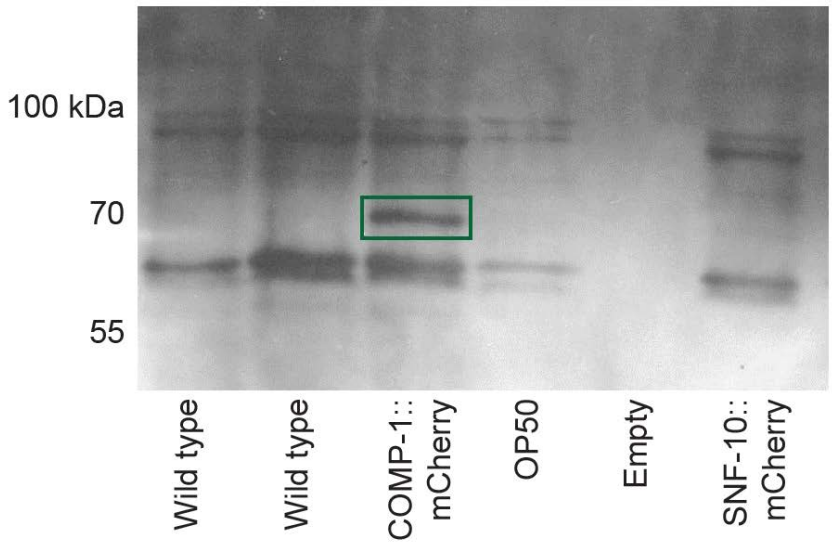


**Figure 6.1. Example of a western blot for SNF-10::mCherry, showing detection of the positive control.**
In each lane, 400 adult males were loaded, except for the OP50 lane, in which only bacteria were loaded. Wild-type and OP50 lanes are background controls with no mCherry. SNF-10::mCherry is absent from the blot, but has a predicted size of 100 kDa. COMP-1::mCherry is a positive control, and is approximately 75 kDa (green box). Primary antibody was anti-RFP (Rockland) at 1:5000. Secondary antibody was goat anti-rabbit (HRP (BioRad) at 1:5000.

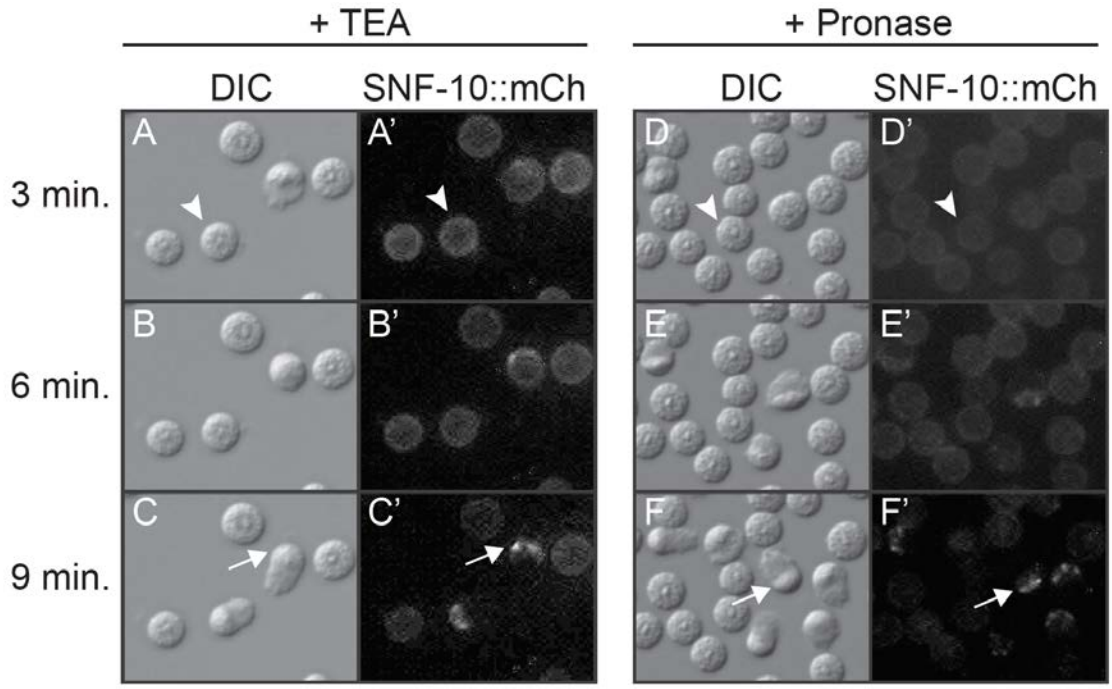


**Figure 6.2. SNF-10's dynamic localization is not dependent on receiving the protease signal.**
Sperm was dissected into media containing either TEA (A-C') or Pronase (D-F') and imaged every 3 min during activation. Regardless of activator, early SNF-10::mCherry initially localized to the cell periphery (arrowhead) and was polarized to the cell body in activated spermatozoa (arrows).

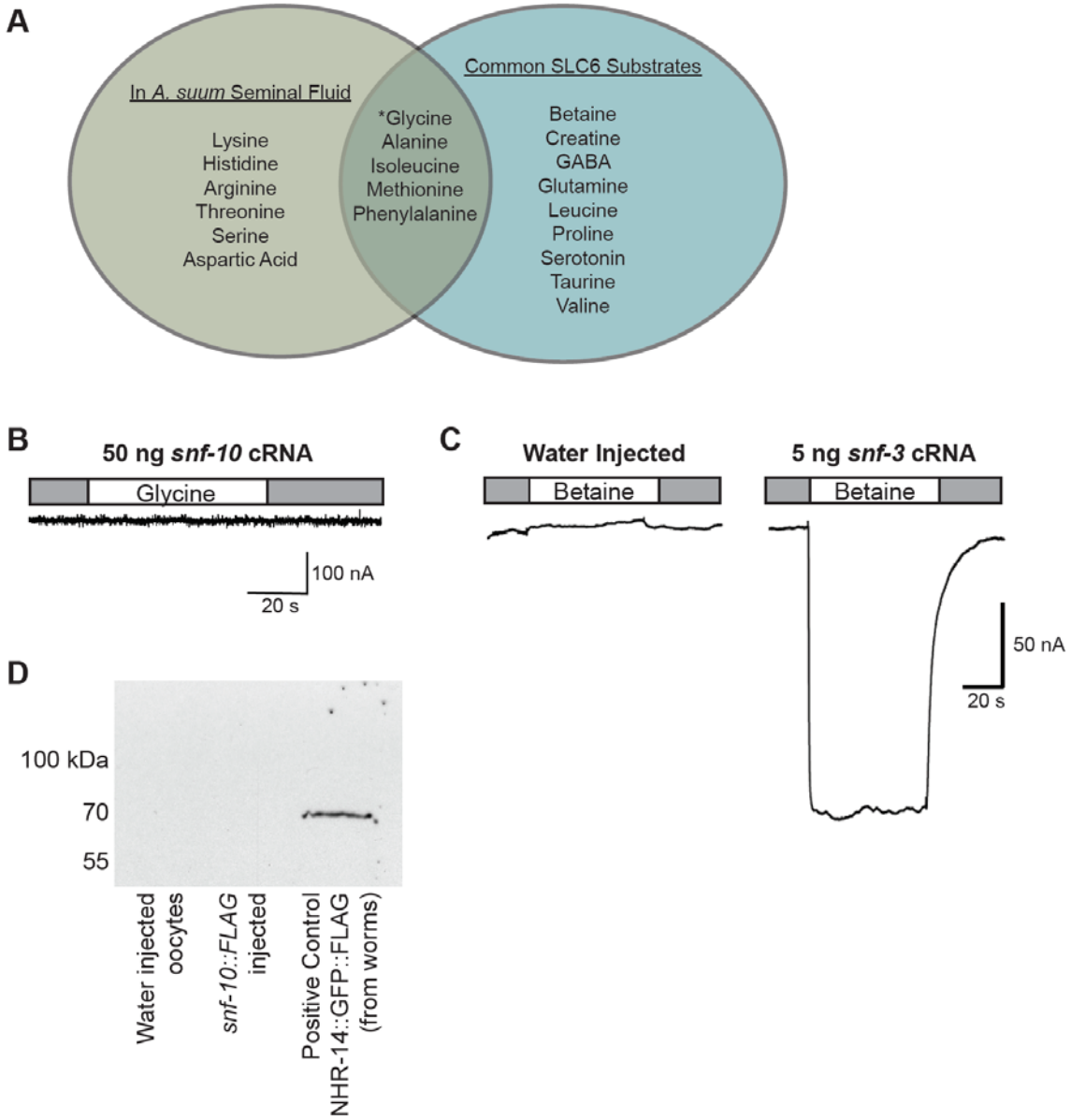


**Figure 6.3. A specific cargo has not been identified for SNF-10.**
(A) List of candidate cargo for SNF-10. By sequence, SNF-10 is most similar to the human glycine transporter GlyT2. (B) A *snf-10*-injected oocyte was perfused for 20s with plain Ringer's, 60s with 10 mM glycine, and finally 40s with plain Ringer's. No current was detected using the two-electrode voltage clamp method. All candidate cargo were tested using this setup, in conditions with and without Pronase treatment. (C) Positive control recording; *snf-3*-injected oocytes are electrogenic upon exposure to their known substrate, betaine. (D) SNF-10 expression by *Xenopus* oocytes could not be confirmed by western blot.

# CHAPTER 7

# SUMMARY AND FUTURE DIRECTIONS

The goal of my dissertation was to advance understanding of the question: How do highly specialized sperm cells develop? Work on *syx-7* and *snf-10* has described how these two well-conserved genes function during sperm development and sheds light on how cell division and differentiation can occur. For SYX-7, I described a new role for the t-SNARE in cell division, and added to existing evidence that it is important for normal function of lysosome-like organelles. For SNF-10, I described a new role for an SLC6 family protein in sperm differentiation as well as a new means of regulation for a protein in this family. Both syntaxins and SLC6 family genes have broad expression in many cell and tissue types (Linial, 1997; Broer, 2013; Pramod et al., 2013; Han et al., 2017). Therefore, further characterization of the mechanisms of SYX-7 and SNF-10 function will continue informing our understanding of these proteins, the ways they can function, and how this fits into a broader biological context.

## *syx-7* in Cytokinesis and Lysosome-related Organelle Biogenesis

In Chapters 2 and 3 of this dissertation, I focus on cell division, and report the discovery and characterization of the t-SNARE *syx-7* in sperm development. Prior to the discovery of *syx-7*, much of our knowledge regarding SNARE function in sperm was in

the context of the acrosome reaction, a specialized exocytosis event required for fertilization to occur (Kierszenbaum, 2000). Only two other SNAREs have been identified that function in sperm cytokinesis (Xu et al., 2002; Fujiwara et al., 2013). However, these other SNAREs are not completely understood, and it is likely that the role they serve is very different from *syx-7*'s. This underscores that *syx-7* and related genes are important in many stages of sperm development, and we have much to understand about how they function, as well as how these functions are modulated.

My findings for *syx-7* describe a role for the gene during meiotic cell division. *syx-7* is required to complete cytokinesis following meiosis II, demonstrating it is required not for general meiotic or cell division, but for a specific, specialized cytokinesis to occur. For sperm, asymmetric partitioning of cellular components is a key event during cytokinesis. Sperm without *syx-7* achieve much of this asymmetric partitioning and appear poised for division. However, the final abscission to separate spermatids fails. *syx-7* sperm have two major defects that may contribute to the incomplete cytokinesis. First, actin is mislocalized in sperm that do not complete division, suggesting models in which missing forces at the division plane or inappropriate connection of sperm to the residual body could prevent abscission in the *syx-7* mutant. It is an interesting finding that a trafficking protein like SYX-7 functions upstream of actin localization, as few other examples of this have been identified and the cooperation between trafficking events and actin remains an unclear aspect of cell division.

The second major defect in sperm lacking *syx-7* is the presence of abnormalities in organelles of the secretory system: membranous organelles (MOs). It is intriguing to think MO function could be required for cell division in sperm, although this remains

unclear. One model that ties abnormal MOs and actin together is that MOs could be responsible for trafficking necessary machinery, including actin regulatory proteins, to the proper subcellular location. An intriguing paradigm is that membranous organelles could serve as a streamlined “trafficking hub” in sperm, a cell type that undergoes specialized development to leave behind many typical cellular components in order to improve motility (Ward et al., 1981; Xu et al., 2013). As with previous data (Wolf et al., 1978), our electron micrographs (Chapters 2 and 3) revealed there are no other obvious organelles of the secretory system present in sperm, consistent with the model that perhaps a single, generalized secretory organelle is all sperm can afford. This model predicts other proteins would mislocalize in *syx-7* sperm. While most of the markers for sperm partitioning I assayed in Chapter 2 localized appropriately, it would be interesting to focus on MO proteins as well as proteins known to have dynamic localization during sperm development.

In Chapter 2, I show SYX-7 moves to the MOs as sperm develop, suggesting the protein may play a role in membrane reorganization or cargo delivery to the organelle. Perhaps SYX-7 has a key role in forming functional MOs, and it is solely due to these abnormal MOs that further defects occur, ultimately resulting in mislocalized actin. In support of this model, sperm cytokinesis is disrupted in three other *C. elegans* mutants that affect the biogenesis or function of MOs (L'Hernault and Arduengo, 1992; Machaca and L'Hernault, 1997; Arduengo et al., 1998; Zhu and L'Hernault, 2003; Gleason et al., 2012). However, in contrast to what the above model would predict, two of the other MO mutants have normal actin localization, and data for the third does not yet exist (Machaca and L'Hernault, 1997; Arduengo et al., 1998). This suggests instead of solely disrupting

MOs, *syx-7* likely has a second function in trafficking and cargo delivery as sperm divide. Alternatively, *syx-7* function could be required once for MO function, but it disrupts them in a way that specifically affects actin. Either of these cases are consistent with current data. Actin localization in MO mutants beyond *syx-7* was probed using an antibody for total actin, rather than our live marker for F-actin (Machaca and L'Hernault, 1997; Arduengo et al., 1998). It would be interesting to view live F-actin in other MO mutant strains, to better understand if it is affected by MO function. Another means to test the current model is to perform a combination of experiments to determine if abnormal FB-MOs can ever be uncoupled from cell division defects. For example, while sperm and fertility appeared normal in *vti-1* and *syx-6* mutants, I did not look directly at MOs and it remains possible these mutants contain abnormal MOs that do not affect sperm division. Additionally, screens for MO mutants, as well as using drugs to block MO function and aspects of membrane trafficking in sperm, may also support current models or suggest alternatives.

Large, multinucleated germ cells like those found in *syx-7* mutants are also found in human pathological conditions that occur within the testes (Holstein and Eckmann, 1986). These conditions often develop in men older than 65 years, but can also occur in younger men and cause fertility problems. How these conditions arise remains unclear, although it is proposed that it is through improper maintenance of intercellular bridges, a feature of sperm development that relies heavily on cytokinesis machinery (Greenbaum et al., 2011). Notably, the arrested human sperm, often referred to as “giant” sperm, share a number of features with the large terminal sperm in our *syx-7* mutants. Electron microscopy of both the giant human sperm and *C. elegans syx-7* mutant sperm reveal

cytoplasmic disorganization and severe degradation of cellular structures, as well as numerous small vesicles and abnormal membrane structures present throughout the sperm cytoplasm (Holstein and Eckmann, 1986; Miething, 2005) (Chapters 2-3). Thus, further understanding of *syx-7* may shed light on the mechanisms of sperm pathologies that occur in other organisms, including humans, and may have important implications for improving fertility. Using *syx-7* to answer questions about why cellular components break down after division fails may be particularly interesting in this context.

SYX-7 is an ortholog of mammalian STX12 (sometimes called STX13), a protein with functions beyond reproductive biology. STX12 localizes predominantly to early endosomes in a number of cell and tissue types (Tang et al., 1998). The protein is less studied compared to some other t-SNARES; however, it is known to mediate fusion of endosomal membranes by participating in homotypic fusion events, as well as in targeting vesicles during endosome-mediated recycling of surface proteins (Prekeris et al., 1998; Brandhorst et al., 2006). In a few cases, a role for STX12 is apparent in the biogenesis of lysosome-related organelles (LROs) such as melanosomes, the pigment-producing organelles in melanocytes. During melanosome biogenesis, enzymes required for synthesizing melanin must be transported from endosomes to maturing melanosomes (Wasmeier et al., 2008). When STX12 is depleted using shRNAs, several enzymes that should be routed to melanosomes are instead routed to lysosomes and degraded (Jani et al., 2015). Additionally, STX12 interacts with pallidin (PLDN), a component of the biogenesis of LRO complex-1 (BLOC-1), and it is proposed the two function together in vesicle fusion during the formation of several types of LROs (Huang et al., 1999). These data, combined with our own observation that a similar type of organelle is disrupted in

the *C. elegans* mutant, suggests the role of SYX-7/STX12 in LRO biogenesis may be widespread. Also notable is that in the LRO-related disorder Chediak-Higashi Syndrome, one of the many problems for patients is inappropriate white blood cell division (Introne et al., 1993), representing another possible connection between LROs and cell division, this time in the context of human disease.

In humans and model organisms alike, disrupting genes involved in melanosome maturation causes a reduction in pigmentation, but this is very often accompanied by other defects that at first seem unrelated, such as abnormal bleeding, respiratory disorders, and immunodeficiencies (Spritz et al., 2003; Hornyak, 2006). These defects, however, are connected and result from generalized LRO defects, as other examples of LROs include platelet-dense granules, lamellar bodies, basophil granules, and lytic granules (Dell'Angelica et al., 2000; Huizing et al., 2008; Marks et al., 2013). Using tools like our *syx-7* mutants to understand how specific trafficking events are exploited to generate cell-type specific organelles will help us understand the plasticity of the endosomal and secretory systems, and in the long term may inform treatments for a number of human disorders that result from abnormal LROs, including Chediak-Higashi Syndrome, Hermansky-Pudlak Syndrome, and Griscelli Syndrome (Huizing et al., 2008; Cullinane et al., 2011). Study of *syx-7* in *C. elegans* has unique advantages for helping us understand LROs, as loss of *syx-7* appears to cause a sperm-specific defect rather than the organism-wide defects seen when LROs are disrupted in other organisms. Therefore, use of *syx-7* will complement studies done in current mouse models of LRO-related disorders. While these are excellent models of disease, analysis is often complicated due to widespread abnormalities and short life spans (McGarry et al., 1999; Bonifacino,

2004). With this combined toolkit, we can answer interesting questions about how LROs form and function, as well as pursue the important question of whether or not LROs play an active role in cell division.

## *snf-10* in Protease Signaling

In Chapters 4-6 of this dissertation, I focus on cellular differentiation, probing how sperm can respond to extracellular cues to undergo large changes in physiology and become motile. I report the discovery and characterization of *snf-10*, a member of the Solute Carrier 6 family of genes, and demonstrate *snf-10* is required to transduce a signal from the extracellular environment (seminal fluid) into sperm cells to trigger cell polarization and the onset of motility. The discussion of my work on *snf-10* in this chapter is brief, as Chapter 5 is the reprint of a Commentary Article in which I provide an in-depth discussion of my findings and future directions regarding *snf-10*.

Through previous work, our lab identified a signaling pathway that induces sperm to become polarized and motile, a process termed sperm activation, in response to an extracellular protease signal. This signal comprises the protease inhibitor, SWM-1, and the trypsin-like serine protease, TRY-5. Both SWM-1 and TRY-5 are components of seminal fluid (Stanfield and Villeneuve, 2006; Smith and Stanfield, 2011). However, prior to our identification of SNF-10, it was unknown how the signal from seminal fluid was transduced into sperm to induce activation. A genetic screen identified SNF-10 as a factor downstream of the protease signal, and I investigated the protein's role in signal transduction and sperm activation.

In Chapter 4, I demonstrate both in vivo and in vitro that SNF-10 is downstream of the protease activation signal. However, SNF-10 is also upstream from a number of cellular events that must occur in sperm cells as they become motile. When wild-type sperm are exposed to the protease signal, the membranous organelles fuse with the plasma membrane, specific proteins move to new domains, and cytoskeletal proteins form a pseudopod to facilitate crawling (Ward, 1983). When sperm lacking *snf-10* are exposed to proteases, there are no noticeable morphological changes to the cells. This suggests that SNF-10 functions very early during the onset of sperm motility, perhaps even in receiving the protease signal and propagating it into sperm to initiate changes in intracellular physiology. In further support of this model, we would predict the target of the extracellular protease would localize to the plasma membrane; this is, in fact, the main cellular compartment in which SNF-10 resides.

While current data are consistent with a model in which SNF-10 is a direct target of the extracellular sperm activation signal, important questions remain. Notably, is SNF-10 cleaved during activation, and is this cleavage sufficient to induce sperm motility? This is an important question and will be key to understanding both SNF-10's function in sperm, and that of SLC6 proteins in other biological contexts. Positive regulation by a protease signaling pathway is a novel means of regulation for an SLC6 family protein. Cleavage of SLC6 proteins does occur; for example, the GABA transporter GAT1 and the glycine transporter GlyT1 are cleaved by calpain-family proteases (Baliova et al., 2004; Baliova et al., 2009), but this cleavage either reduced or had no effect on transporter function. Widespread positive regulation by protease signaling remains a possibility, and could apply to a subset of transporters in specific cell-types or tissues.

Knowing if SNF-10 is directly cleaved during sperm activation will lead to a better understanding and perhaps identification of a similar means of regulation in other contexts. Although the western blots I performed to determine if SNF-10 undergoes direct cleavage by proteases were inconclusive (Chapter 6), there are other ways to address this question. For example, tools could be created to induce or block cleavage of the protein (for details, see Chapter 6). Additionally, there is evidence SNF-10's localization is regulated during activation, and a candidate approach is currently underway, using CRISPR to disrupt genes that may be involved in regulating SNF-10's localization. If a mutant could be identified that prevents SNF-10 from localizing to the plasma membrane, this could further support or disprove our model, depending on whether or not sperm can respond to protease signals.

SLC6 proteins like SNF-10 have many roles in human physiology. There are 20 SLC6 family members in the human genome (Chen et al., 2004; Bröer, 2006). They can be found in the central nervous system and peripheral neurons, as well as in the intestine, kidneys, lungs, and testis (Bröer and Gether, 2012). Disruptions to these proteins are implicated in a variety of disorders, including neuropsychiatric disorders (Grunhage et al., 2000; Kim et al., 2006; Kohli et al., 2011), nutrient uptake disorders (Kleta et al., 2004; Seow et al., 2004), blood pressure abnormalities (Halushka et al., 1999), and orthostatic intolerance (Shannon et al., 2000). In the SLC6 field, much work has explored how the transporters function within the context of the nervous system. This is very important, but it provides a perhaps limited view of the variety and complexity of SLC6 protein function. Additionally, many of the SLC6 proteins have been implicated in human disorders by genome-wide association studies (Lee et al., 2013; Scharf et al.,

2013), and functional validation is needed. Study of proteins like SNF-10 will help the field expand to consider transporters in many biological contexts, as well as identify new means of regulation for this important family, and thus better understand amino acid homeostasis across the entire body.

## Conclusions

In conclusion, sperm development in *C. elegans* provides the opportunity to study many different aspects of cell division and differentiation. Many of the genes identified as important for *C. elegans* sperm development are conserved or function in analogous processes that take place during the development of other cell types (reviewed in L'Hernault, 2006; Lesch and Page, 2012; Ellis and Stanfield, 2014). Continuing to identify and investigate the genes involved will continue to improve our understanding of both germ cell development and general cellular processes. For example, the work presented here on *syx-7* and *snf-10* identified a new role for each gene during sperm development. Interesting questions remain about these genes and the mechanisms of their function, and it will also be interesting to determine how widespread these mechanisms are, both in sperm biology and beyond.

## References

Arduengo, P., Appleberry, O., Chuang, P., L'Hernault, S., 1998. The presenilin protein family member SPE-4 localizes to an ER/Golgi derived organelle and is required for proper cytoplasmic partitioning during *C. elegans* spermatogenesis. J. Cell Sci. 111, 3645-3654.

Baliova, M., Betz, H., Jursky, F., 2004. Calpain-mediated proteolytic cleavage of the neuronal glycine transporter, GlyT2. J. Neurochem. 88, 227-232.

Baliova, M., Knab, A., Franekova, V., Jursky, F., 2009. Modification of the cytosolic regions of GABA transporter GAT1 by calpain. Neurochem. Int. 55, 288-294.

Bonifacino, J.S., 2004. Insights into the biogenesis of lysosome-related organelles from the study of the Hermansky-Pudlak Syndrome. Ann. N. Y. Acad. Sci. 1038, 103-114.

Brandhorst, D., Zwilling, D., Rizzoli, S.O., Lippert, U., Lang, T., Jahn, R., 2006. Homotypic fusion of early endosomes: SNAREs do not determine fusion specificity. Proc. Natl. Acad. Sci. 103, 2701-2706.

Broer, S., 2013. Diseases associated with general amino acid transporters of the solute carrier 6 family (SLC6). Curr. Mol. Pharmacol. 6, 74-87.

Bröer, S., 2006. The SLC6 orphans are forming a family of amino acid transporters. Neurochem. Int. 48, 559-567.

Bröer, S., Gether, U., 2012. The solute carrier 6 family of transporters. Br. J. Pharmacol. 167, 256-278.

Chen, N.H., Reith, M.E., Quick, M.W., 2004. Synaptic uptake and beyond: the sodium- and chloride-dependent neurotransmitter transporter family SLC6. Pflugers. Arch. 447, 519-531.

Cross-Disorder Group of the Psychiatric Genomics, C., Lee, S.H., Ripke, S., Neale, B.M., Faraone, S.V., Purcell, S.M., Perlis, R.H., Mowry, B.J., Thapar, A., Goddard, M.E., Witte, J.S., Absher, D., Agartz, I., Akil, H., Amin, F., Andreassen, O.A…..International Inflammatory Bowel Disease Genetics, C., 2013. Genetic relationship between five psychiatric disorders estimated from genome-wide SNPs. Nat. Genet. 45, 984-994.

Cullinane, A.R., Curry, J.A., Carmona-Rivera, C., Summers, G.C., Ciccone, C., Cardillo, N.D., Dorward, H., Hess, R.A., White, J.G., Adams, D., Huizing, M., Gahl, W.A., 2011. A BLOC-1 mutation screen reveals that PLDN is mutated in Hermansky-Pudlak Syndrome type 9. Am. J. Hum. Genet. 88, 778-787.

Dell'Angelica, E.C., Mullins, C., Caplan, S., Bonifacino, J.S., 2000. Lysosome-related organelles. FASEB J 14, 1265-1278.

Ellis, R.E., Stanfield, G.M., 2014. The regulation of spermatogenesis and sperm function in nematodes. Semin. Cell Dev. Biol. 29, 17-30.

Fujiwara, Y., Ogonuki, N., Inoue, K., Ogura, A., Handel, M., Noguchi, J., Kunieda, T., 2013. t-SNARE Syntaxin2 (STX2) is implicated in intracellular transport of sulfoglycolipids during meiotic prophase in mouse spermatogenesis. Biol. Reprod. 88, 141-141.

Gleason, E., Hartley, P., Henderson, M., Hill-Harfe, K., Price, P., Weimer, R., Kroft, T., Zhu, G.-D., Cordovado, S., L'Hernault, S., 2012. Developmental genetics of secretory vesicle acidification during *C. elegans* spermatogenesis. Genetics 191, 477-491.

Greenbaum, M.P., Iwamori, T., Buchold, G.M., Matzuk, M.M., 2011. Germ cell intercellular bridges. Cold Spring Harb. Perspect. Biol. 3, a005850.

Grunhage, F., Schulze, T.G., Muller, D.J., Lanczik, M., Franzek, E., Albus, M., Borrmann-Hassenbach, M., Knapp, M., Cichon, S., Maier, W., Rietschel, M., Propping, P., Nothen, M.M., 2000. Systematic screening for DNA sequence variation in the coding region of the human dopamine transporter gene (DAT1). Mol. Psychiatry 5, 275-282.

Halushka, M.K., Fan, J.B., Bentley, K., Hsie, L., Shen, N., Weder, A., Cooper, R., Lipshutz, R., Chakravarti, A., 1999. Patterns of single-nucleotide polymorphisms in candidate genes for blood-pressure homeostasis. Nat. Genet. 22, 239-247.

Han, J., Pluhackova, K., Bockmann, R.A., 2017. The multifaceted role of SNARE proteins in membrane fusion. Front. Physiol. 8, 5.

Holstein, A.F., Eckmann, C., 1986. Multinucleated spermatocytes and spermatids in human seminiferous tubules. Andrologia 18, 5-16.

Hornyak, T.J., 2006. The developmental biology of melanocytes and its application to understanding human congenital disorders of pigmentation. Adv Dermatol 22, 201-218.
Huang, L., Kuo, Y.M., Gitschier, J., 1999. The pallid gene encodes a novel, syntaxin 13-interacting protein involved in platelet storage pool deficiency. Nat. Genet. 23, 329-332.

Huizing, M., Helip-Wooley, A., Westbroek, W., Gunay-Aygun, M., Gahl, W.A., 2008. Disorders of lysosome-related organelle biogenesis: clinical and molecular genetics. Annu. Rev. Genomics Hum. Genet. 9, 359-386.

Introne, W.J., Westbroek, W., Golas, G.A., Adams, D., 1993. Chediak-Higashi Syndrome, in: Adam, M.P., Ardinger, H.H., Pagon, R.A., Wallace, S.E., Bean, L.J.H., Mefford, H.C., Stephens, K., Amemiya, A., Ledbetter, N. (Eds.), GeneReviews((R)), Seattle (WA).

Jani, R., Purushothaman, L., Rani, S., Bergam, P., Setty, S., 2015. STX13 regulates cargo delivery from recycling endosomes during melanosome biogenesis. J. Cell. Sci. 128, 3263-3276.

Kierszenbaum, A.L., 2000. Fusion of membranes during the acrosome reaction: a tale of two SNAREs. Mol. Reprod. Dev. 57, 309-310.

Kim, C.H., Hahn, M.K., Joung, Y., Anderson, S.L., Steele, A.H., Mazei-Robinson, M.S., Gizer, I., Teicher, M.H., Cohen, B.M., Robertson, D., Waldman, I.D., Blakely, R.D., Kim, K.S., 2006. A polymorphism in the norepinephrine transporter gene alters promoter

activity and is associated with attention-deficit hyperactivity disorder. Proc. Natl. Acad. Sci. 103, 19164-19169.

Kleta, R., Romeo, E., Ristic, Z., Ohura, T., Stuart, C., Arcos-Burgos, M., Dave, M.H., Wagner, C.A., Camargo, S.R., Inoue, S., Matsuura, N., Helip-Wooley, A., Bockenhauer, D., Warth, R., Bernardini, I., Visser, G., Eggermann, T., Lee, P., Chairoungdua, A., Jutabha, P., Babu, E., Nilwarangkoon, S., Anzai, N., Kanai, Y., Verrey, F., Gahl, W.A., Koizumi, A., 2004. Mutations in SLC6A19, encoding B0AT1, cause Hartnup disorder. Nat. Genet. 36, 999-1002.

Kohli, M.A., Lucae, S., Saemann, P.G., Schmidt, M.V., Demirkan, A., Hek, K., Czamara, D., Alexander, M., Salyakina, D., Ripke, S., Hoehn, D., Specht, M., Menke, A., Hennings, J., Heck, A., Wolf, C., Ising, M., Schreiber, S., Czisch, M., Muller, M.B., Uhr, M., Bettecken, T., Becker, A., Schramm, J., Rietschel, M., Maier, W., Bradley, B., Ressler, K.J., Nothen, M.M., Cichon, S., Craig, I.W., Breen, G., Lewis, C.M., Hofman, A., Tiemeier, H., van Duijn, C.M., Holsboer, F., Muller-Myhsok, B., Binder, E.B., 2011. The neuronal transporter gene SLC6A15 confers risk to major depression. Neuron 70, 252-265.

L'Hernault, S., 2006. Spermatogenesis. WormBook, ed.

L'Hernault, S.W., Arduengo, P.M., 1992. Mutation of a putative sperm membrane protein in Caenorhabditis elegans prevents sperm differentiation but not its associated meiotic divisions. J. Cell Biol. 119, 55-68.

Lesch, B.J., Page, D.C., 2012. Genetics of germ cell development. Nat. Rev. Genet. 13, 781-794.

Linial, M., 1997. SNARE proteins--why so many, why so few? J Neurochem. 69, 1781-1792.

Machaca, K., L'Hernault, S.W., 1997. The *Caenorhabditis elegans spe-5* gene is required for morphogenesis of a sperm-specific organelle and is associated with an inherent cold-sensitive phenotype. Genetics 146, 567-581.

Marks, M.S., Heijnen, H.F., Raposo, G., 2013. Lysosome-related organelles: unusual compartments become mainstream. Curr. Opin. Cell Biol. 25, 495-505.

McGarry, M.P., Reddington, M., Novak, E.K., Swank, R.T., 1999. Survival and lung pathology of mouse models of Hermansky-Pudlak Syndrome and Chediak-Higashi Syndrome. Proc. Soc. Exp. Biol. Med. 220, 162-168.

Miething, A., 2005. Arrested germ cell divisions in the ageing human testis. Andrologia 37, 10-16.

Pramod, A., Foster, J., Carvelli, L., Henry, L., 2013. SLC6 transporters: structure, function, regulation, disease association and therapeutics. Mol. Aspects Med. 34, 197-219.

Prekeris, R., Klumperman, J., Chen, Y.A., Scheller, R.H., 1998. Syntaxin 13 mediates cycling of plasma membrane proteins via tubulovesicular recycling endosomes. J. Cell Biol. 143, 957-971.

Scharf, J.M., Yu, D., Mathews, C.A., Neale, B.M., Stewart, S.E., Fagerness, J.A., Evans, P., Gamazon, E., Edlund, C.K., Service, S.K., Tikhomirov, A., Osiecki, L., Illmann, C., Pluzhnikov, A., Konkashbaev, A., Davis, L.K., ….. 2004. Hartnup disorder is caused by mutations in the gene encoding the neutral amino acid transporter SLC6A19. Nat. Genet. 36, 1003-1007.

Shannon, J.R., Flattem, N.L., Jordan, J., Jacob, G., Black, B.K., Biaggioni, I., Blakely, R.D., Robertson, D., 2000. Orthostatic intolerance and tachycardia associated with norepinephrine-transporter deficiency. N. Engl. J. Med. 342, 541-549.

Smith, J., Stanfield, G., 2011. TRY-5 is a sperm-activating protease in *C. elegans* seminal fluid. PLoS Genetics 7.

Spritz, R.A., Chiang, P.W., Oiso, N., Alkhateeb, A., 2003. Human and mouse disorders of pigmentation. Curr. Opin. Genet. Dev. 13, 284-289.

Stanfield, G., Villeneuve, A., 2006. Regulation of sperm activation by SWM-1 is required for reproductive success of *C. elegans* males. Current Biology 16, 252-263.
Tang, B.L., Tan, A.E., Lim, L.K., Lee, S.S., Low, D.Y., Hong, W., 1998. Syntaxin 12, a member of the syntaxin family localized to the endosome. J. Biol. Chem. 273, 6944-6950.

Ward, S., Argon, Y., Nelson, G., 1981. Sperm morphogenesis in wild-type and fertilization-defective mutants of *C. elegans*. The Journal of Cell Biology.
Ward, S., Hogan, E., Nelson, G., 1983. The initiation of spermiogenesis in the nematode *C. elegans*. Dev. Biol. 98, 70-79.

Wasmeier, C., Hume, A.N., Bolasco, G., Seabra, M.C., 2008. Melanosomes at a glance. J. Cell Sci. 121, 3995-3999.

Wolf, N., Hirsh, D., McIntosh, J., 1978. Spermatogenesis in males of the free-living nematode, *C. elegans.* J. Ultrastruct. Res., 63, 155-169.

Xu, H., Brill, J.A., Hsien, J., McBride, R., Boulianne, G.L., Trimble, W.S., 2002. Syntaxin 5 is required for cytokinesis and spermatid differentiation in *Drosophila*. Dev. Biol. 251, 294-306.

Xu, H., Yuan, S.Q., Zheng, Z.H., Yan, W., 2013. The cytoplasmic droplet may be indicative of sperm motility and normal spermiogenesis. Asian J Androl 15, 799-805.
Zhu, G., L'Hernault, S., 2003. The *C. elegans spe-39* gene is required for intracellular membrane reorganization during spermatogenesis. Genetics 165, 145-157.